TECHNISCHE UNIVERSITÄT MÜNCHEN

TUM School of Medicine and Health

Migration of mamma carcinoma cell lines after irradiation

Jessica Sandra Ott

Vollständiger Abdruck der von der TUM School of Medicine and Health der Technischen Universität München zur Erlangung einer

Doktorin der Medizin (Dr. med.)

genehmigten Dissertation.

Vorsitz: apl. Prof. Dr. Lutz Renders

Prüfende der Dissertation:

1. Prof. Dr.Stephanie E. Combs
2. apl. Prof. Dr. Thomas E. Schmid

Die Dissertation wurde am 09.10.2023 bei der Technischen Universität München eingereicht und durch die TUM School of Medicine and Health am 05.06.2024 angenommen.

FACULTY OF MEDICINE

TECHNISCHE UNIVERSITÄT MÜNCHEN

Klinik für RadioOnkologie und Strahlentherapie am Klinikum Rechts der Isar, TU München

Migration of mamma carcinoma cell lines after irradiation

Jessica Sandra Ott

FACULTY OF MEDICINE

TECHNISCHE UNIVERSITÄT MÜNCHEN

Klinik für RadioOnkologie und Strahlentherapie am Klinikum Rechts der Isar, TU München

Migration of mamma carcinoma cell lines after irradiation

Author:	Jessica Sandra Ott
Supervisor:	Prof. Dr. Stephanie E. Combs
Advisor:	Prof. Dr. Thomas Schmid

Ich, Jessica Ott, geboren am 25.06.1991 in Erlangen, erkläre hiermit, dass ich die vorliegende Arbeit ohne unzulässige Hilfe Dritter und ohne Benutzung anderer als der angegebenen Hilfsmittel angefertigt habe. Die aus anderen Quellen direkt oder indirekt übernommenen Daten und Konzepte sind unter Angabe der Quelle gekennzeichnet. Insbesondere habe ich nicht die entgeltliche Hilfe von Vermittlungs- bzw. Beratungsdiensten (Promotionsberater oder andere Personen) in Anspruch genommen. Niemand hat von mir unmittelbar oder mittelbar geldwerte Leistungen für Arbeit erhalten, die im Zusammenhang mit dem Inhalt der vorgelegten Dissertation stehen. Die Arbeit wurde bisher weder im In- noch im Ausland in gleicher oder ähnlicher Form einer anderen Prüfungsbehörde vorgelegt. Ich versichere, dass ich diese Arbeit selbstständig verfasst und nur die angegebenen Quellen und Hilfsmittel verwendet habe.

Erlangen, 07.09.2023 Jessica Sandra Ott

Abstract

Breast cancer affects every eighth to tenth woman in Germany, increasing tendency. With surgical resection, chemotherapy, anti-hormonal therapy, and radiotherapy, the majority of women are treated successfully. Current questions are the extent of adjuvant therapies in early breast cancer and treatment options for metastatic disease. Research already led to improved diagnostics with predictable testing such as the Endopredict-Test. This is already used in the clinical setting, providing a first step of personalized medicine in breast cancer. Another major challenge is the distant metastasis rate of up to 20%, which is particularly unsettling for patients. In these cases, distant metastases often occur years after initial curation, mainly as single bone metastases in the spinal column. Today, radiotherapy plays a major role in treating breast cancer patients in all UICC-stages of the disease. In invasive breast cancer, adjuvant radiotherapy prolongs overall survival and reduces the local recurrence rate. In a metastatic setting, it is analgetic and leads to remineralization of the bone, hence stability improvement. Metastasis is an ongoing problem in this otherwise well controllable disease. Migration and invasion contribute to a large extent to metastization.

This work aims at evaluating migration in breast cancer cell lines using an improved gap closure assay, which, in future could be applied in vitro before the start of radiotherapy as a part of a personalized treatment concept. The migratory potential of four different breast cancer cell lines (T47D, MDA-MB 361, MCF-7 and SkBr3) was evaluated in a first step. MCF-7 and SkBr3 cell lines were selected due to their morphology and migratory behavior for the main experiments. Cells were irradiated using doses of 0, 2, 4 and 8 Gy and migration was analyzed at different time points. Both cell lines showed increasing migratory potential in the irradiated groups. The cell line SkBr3 showed a statistically significant increase in migration in the 4 Gy and 8 Gy groups compared to sham irradiation. MCF-7 cells showed no statistically significant effect, however a tendency was observed using the gap closure assays. Additionally, cell viability and apoptosis assays were performed to detect possible effects of proliferation and apoptosis induction.

Zusammenfassung

Brustkrebs betrifft jede achte bis zehnte Frau in Deutschland mit steigender Tendenz. Mit chirurgischer Resektion, Chemotherapie, antihormoneller Therapie sowie Strahlentherapie kann die Mehrzahl der Patientinnen gut therapiert werden. Aktuelle Forschungsfragen sind der Umfang der adjuvanten Therapien bei Brustkrebs im Frühstadium und die Behandlungsmöglichkeiten bei metastasierter Erkrankung. Die Forschung hat bereits zu einer verbesserten Diagnostik mit prognostischen Tests wie dem Endopredict-Test geführt. Dieser wird bereits im klinischen Umfeld eingesetzt und stellt einen ersten Schritt der personalisierten Medizin bei Brustkrebs dar. Eine weitere große Herausforderung ist die Fernmetastasierungsrate von bis zu 20 %, die für die Patientinnen besonders verunsichernd ist. In diesen Fällen treten die Fernmetastasen oft erst Jahre nach initialer Heilung auf, hauptsächlich als singuläre Knochenmetastasen der Wirbelsäule. Die Strahlentherapie spielt heute eine wichtige Rolle in der Behandlung von Brustkrebspatientinnen aller UICC-Stadien. Bei invasivem Brustkrebs verlängert die adjuvante Strahlentherapie das Gesamtüberleben und verringert die Lokalrezidivrate. Bei metastasiertem Brustkrebs wirkt sie analgetisch und führt durch eine Remineralisierung des Knochens zu einer Verbesserung der Stabilität. Metastasierung ist ein bedeutendes Problem bei dieser ansonsten gut beherrschbaren Erkrankung. Migration und Invasion tragen in großem Umfang zur Metastasierung bei.

Ziel dieser Arbeit ist, die Migration in Mammakarzinom-Zelllinien zu beobachten und zudem zu prüfen, ob ein verbesserter Wundheilungsassay in vitro vor Beginn der Strahlentherapie als Teil eines personalisierten Behandlungskonzepts angewandt werden kann. In einem ersten Schritt wurde das Migrationspotential von vier verschiedenen Brustkrebszelllinien (T47D, MDA-MB 361, MCF-7 und SkBr3) untersucht. Die MCF-7- und SkBr3-Zelllinien wurden aufgrund ihrer Morphologie und ihres Migrationsverhaltens für die Hauptexperimente ausgewählt. Die Zellen wurden mit Energiedosen von 0 Gy, 2 Gy, 4 Gy und 8 Gy bestrahlt, und die Migration zu verschiedenen Zeitpunkten analysiert. Beide Zelllinien zeigten ein zunehmendes Migrationspotenzial in den bestrahlten Gruppen. Die Zelllinie SkBr3 zeigte eine statistisch signifikante Zunahme der Migration in den 4 Gy- und 8 Gy-Gruppen im Vergleich zur Schein-Bestrahlung. MCF-7-Zellen zeigten keinen statistisch signifikanten Effekt, aber eine Tendenz wurde im Migrations-Assays beobachtet. Zusätzlich wurden Zellviabilitäts- und Apoptose-Assays durchgeführt um mögliche Effekte von Proliferation sowie Apoptose zu detektieren.

Contents

1 Introduction

1.1 Incidence of breast cancer

Breast cancer affects every eighth to tenth woman in Germany, increasing tendency [1], [2]. An estimation of the Robert-Koch-Institute for 2016 estimated a number as high as 68 900 women newly diagnosed with breast cancer in Germany in 2016 [3]. Reported deaths rise up to 18 570 per year (report 2016).

The UICC-stages are distributed among breast cancer diagnosed women as follows in percentage: UICC I: 41 UICC II: 39 UICC III: 13 UICC IV: 7 stage at point of diagnosis [4].

survival rates as follows: 5 year overall survival rates in percentage UICC I: 100 UICC II: 94 UICC III: 73 UICC IV: 29 stage at point of diagnosis [4].

Figure 1.1: The UICC-stages are distributed among breast cancer diagnosed women as follows in percentage:

Stage		Percentage
UICC I	:	41
UICC II	:	39
UICC III	:	13
UICC IV	:	7

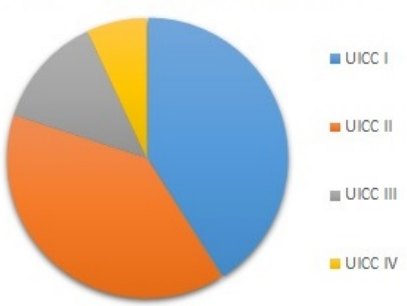

Figure 1.2: Survival rates as follows: 5 year overall survival rates in percentage

Stage		Percentage
UICC I	:	100
UICC II	:	94
UICC III	:	73
UICC IV	:	29

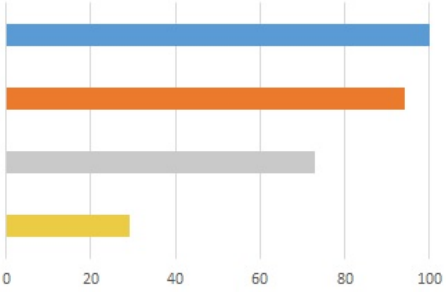

Men can also suffer from breast cancer, at a lower incidence rate than women of 1.43 cases in 100 000 or 1% in all men and all breast cancer diagnoses [5]. Often, they have a poorer

prognosis as women. Three main arguments are mainly presented here such as the shorter life expectancy in men than in women, the more advanced stages at point of diagnosis and the older age at diagnosis [5].

With it being the largest cancer entity in women, it has a high impact on women's health physically and psychologically. Another aspect is the widespread impact on the health system, health providers, and the economy. With it being the most frequent entity in women, the economical impact has interesting sides, the following sentences will give a short insight. French researchers calculated a total cost of about 12 000 Euros for the first year after diagnosis for women with early breast cancer and another additional 8800 euros for sick leave due to work leave in the year 2019 [6]. This number might be higher among working women, and will have further reaching impact, because of the usual diagnosis at an early age on their working life and earnings. In Europe treatment of breast cancer is the largest post among available funds in health care, being allocated to this, with the cost per patient being at an average, appropriate reason [7].

Metastatic breast cancer costs are more difficult to calculate. A review from 2019 estimated a cost of about 20 000 euros and more for a standard chemotherapy for metastatic breast cancer patients, with numbers of over 50 000 euros to 100 000 euros per year for targeted therapies [8], [9], [10].

1.2 Current treatment options

With multi modality treatment containing surgical resection, chemotherapy, anti-hormonal therapy, and radiotherapy, most cases can be treated well. Depending on the TNM-UICC-tumor stage, cure can be reached with the above-mentioned treatment options, especially in early breast cancer. Intermediate and advanced stages involve further treatment and lead to shorter overall survival and progression free survival rates.

UICC I In early breast cancer current standard is the breast conserving surgery, followed by radiation therapy and according to the hormonal status - her2neu targeted therapy or antihormonal therapy. Antihormonal treatment can be applied with different substances such as aromatase inhitors or selective estogene receptor modulators. It depends on the monopausal status of the patient. A possible option is also neoadjuvant chemotherapy prior to resection. Resection standard is now resection of subsections - aiming at resecting as little as possible while still providing a R0/free margins resection.

UICC II UICC stages II to III are treated according to stage I breast cancer, but involve larger tumor sizes and/ or nodal involvement. In radiotherapy, axillary irradiation may be included in therapy.

UICC III After completing the standard therapy, patients in these UICC-stages have a 5 year overall survival, that is relevantly lower than in early breast cancer. The nodal status is a huge factor as well as hormonal status and rarely but important mutations for prognosis. Nodal status correlates with relapse and metastasis [11].

UICC IV Metastatic disease is a non-localized stage. It requires systemic therapy as well as local options. Metastatic disease is an individual situation. It can be divided up to substages, such as oligometastasis. The following chapters will give deeper insights to metastatic breast cancer and the role of radiation oncology.

1.3 The role of radiation oncology in breast cancer

The intentional role of radiation oncology in breast cancer is to prevent local relapse and prolong overall survival in a curative setting, and to reduce pain and increase stability of bones in a palliative setting.

The majority of patients with breast cancer will get in contact with radiation oncology as part of their therapy. In the primary setting, after breast conserving surgery, there will be an adjuvant radiotherapy. In distinct cases a boost is applied to the former tumor site, and different fractionation models are available. A boost is recommended for patients with a tumor size of T2 and larger, age under 50 years, Her2neu positivity, G3-histology and triple negative tumors. An EORTC study showed in 2017 that it improves local control also in patients, that do not fulfill the above mentioned requirements. It leads to an improved local control without an advantage in overall survival [12]. A usual fractionation model is a normofractionation of 50,4 Gy total dose in 1,8 Gy of single fraction dose or hypofractionation of 2,67 Gy singular dose up to 40,05 Gy of cumulative dose. Usually irradiation is applied in form of external beam therapy. In case of mastectomy, RT is applied when a T4 situation is prevailing or lymphnodes are involved [11]. Radiation oncology can be performed as intraoperative as a forwarded boost. Other possibilities involve brachytherapy boost. For very early breast cancer options such as a accelerated partial breast irradiation exist, this can be performed as a brachytherapy treatment or delivered percutaneously [13], [14]. First, I will give a short summary of treatment of the primary tumor and second the metastatic therapy will be discussed.

According to the tumor status, most patients with early breast cancer receive breast-conserving therapy followed by adjuvant radiation therapy of the chest wall. In most cases, the tumor has positive estrogen and progesterone receptor-expression. In such cases, an antihormonal therapy is advised for two to five years [11]. About 90% percent of all breast cancer patients receive radiation therapy to improve the local control and the overall survival of these patients (5% improvement in negative nodal cases and 7% improvement in positive nodal patients) [15]. The current standard of therapy in breast-conserving surgery is reducing the resection preparation to the smallest reasonably achievable volume. As a first step toward personalized medicine, many women receive the opportunity to stratify the risk and benefit of adjuvant chemotherapy through genetic testing of the resection specimen (commercial providers of these tests: Oncotype, Endopredict, Mammaprint). Developments in radiation oncology have been gating-techniques to spare the heart during left-sided treatment, comparing different planning techniques (IMRT vs 3D) for the lowest heart dose (Dmean) and lung-sparing (V20). Further options for dosimetry of organs at risk are dose constraints to the left ventricle and LAD-artery. Additional IGRT secures safe administration of therapy and

constant online and offline imaging resulting in adaption. Long term data for heart sparing have shown different results but a general decline in heart dose measured as Dmean over time with radiation oncology developments and image guided radiation therapy [16].

Radiation therapy is performed either to increase local tumor control - such as in the case of DCIS and mamma carcinoma or to additionally increase the overall survival - in the case of mamma carcinoma and distant metastasis. It is also used for pain relief and to stabilize bone in metastasis. Sadly, the rate of distant metastasis in breast cancer patients is as high as 20 %. Usually, bone metastasis of the vertebral column represents the most frequent localization among those. In the majority of cases, distant metastases occur years after initial cure, as late as 10 to 12 years after initial treatment [17]. Patients then usually receive biphosphonates, radiation therapy of the involved bone and systemic therapy.

Current challenges in radiation oncology involve irradiation of nodes, improvement of techniques, heart dose reduction, and motion management.

Metastatic Mamma carcinoma mainly occurs in the sites of bones, lung, liver and brain. Bones of the spine and pelvis are the most frequent localization. Different fractionation regimes are possible and lead to an initial reduction of pain. Usually, single doses of 3 Gy up to a cumulative dose of 30 to 36 Gy are the standard. Extreme hypofractionation is a palliative option with single doses of up to 8 Gy, but might not lead to equally lasting results in pain relief [18]. Other sources state, that single doses of 8 Gy are a good option for terminally ill patients for pain relief, in addition to analgetics [19]. An emergency in radiation oncology is spinal cord compression. If not treated, it will lead to paralysis. Neurosurgical decompression is favourable for the outcome, but not always possible with all patients [20]. An option for treatment for these patients is radiation therapy. These patients need an urgent start of the treatment and an adaption of the plan in the course of it. Here, serveral fractionation options are available [21], [22], [23].

Metastasis occurs in up to 20% of patients, but who is at major risk? It is yet circumstance of research, but some hints are available: Metastasis is more likely to occur in certain more aggressive tumors, such as triple negative or with BCRA-mutations, in highly proliferative tumors, in young patients [24], [25], [26], [27]. Nodal positivity is also a risk factor for metastasis. It also occurs in larger numbers eight to twelve years after initial curative treatment. Bone metastasis is most likely to happen and mostly it is in the region of the spine and pelvis. Other localizations for metastasis are the lung, liver and brain. In case of cerebral metastasis, chemotherapy is required and whole brain irradiation. In case of singular and oligometastasis, stereotactic radiosurgery is a beneficial concept. Current research is performed on sparing the hippocampus in whole brain irradiation and therefore reducing side effects such as loss of cognitive functions [28], [29], [30].

Radiotherapy is used as a therapy that leads to excellent treatment results such as local control. But can only work locally - set aside of recurrently discussed immune effects [31]. A systemic treatment is in most cases needed.

Metastasis is always linked to migration. Without motility of cells, no cell could leave their origin in the breast tissue and later reappear in the vertebral column, pelvis or brain. Targeting migration and motility of cancer cells and examining these is a step towards a

better understanding and better possible treatment options for the huge number of metastatic mamma carcinoma patients. Today, the major challenge in treating breast cancer is facing the rate of women suffering from distant metastasis arising 8 to 12 years after the initial diagnosis and treatment. Mainly this occurs as bone metastasis in the vertebral column and pelvis. The treatment for it is currently symptomatic and includes radiation therapy, antihormonal treatment, biphosphonates, and in case of danger of instability, neurosurgery. Systemic therapy options are multiple and underly constant development.

1.4 Metastatic breast cancer

After treatment of early-stage mamma carcinoma (UICC-stages I and II), most patients remain free of local and distant recurrence [11].

However, patients with higher UICC-tumor stages III and IV have a higher risk of recurrence or are already metastatic. Metastasis can occur synchronously or metachronously. Main sites are bones (mainly vertebral column and pelvis), lung, liver and brain. Metastasis can be classified as singular, multiple or oligometastasis. The later refers to an intermediate status of 3 to 5 or 7 metastasis, that can be treated differently and proved to have a more beneficial outcome [32], [33], [34]. The aim in therapy for oligometastasis is leading the patient to a stable disease status over a longer period of time. This involves not only systemic but also high precision local ablative procedures - such as provided by radiosurgery for instance.

Prognosis in general is poor for stage IV breast cancer, and ranges from months to years. However, there is substantial heterogeneity within the overall survival, depending on metastatic load and location and hence available treatment options.

Risk factors include mutations in tumors that can be either somatic, only expressed in tumor cells or a genetic mutation of the person beholding it. Another risk factor is the inflammatory disease - a rare subtype involving the skin and characterised as UICC stage IV. It is generally linked with poorer outcome [35]. Nodal status and tumor size alongside tumor biology have a high impact on the estimation of risk of recurrence and metastasis. More aggressive tumor subtypes such as in individuals with the BRCA-mutations and the absence of receptor positivity (triple negative type) are also linked to poorer outcomes. A subgroup of young patients with triple-negative breast cancers is at special risk of recurrence and metastasis, as it limits survival rates [36], [37]. Current research aims at discovering therapy options for these subgroups who sadly have meager survival rates despite the seemingly success of treatment in the first place. Mutations such as in TP53, PIK3CA, and ERBB2 [24] occur in the tumor itself (somatic) or all cells of the bearer of the mutation as a germline mutation: Such as BRCA1, BRCA2, and more rarely TP53, ATM, PTEN, CHEK2, PALB2 [25]. A clinical approach to detecting these is by using a multi-gene-panel test. Some therapies have been developed such as PARP-inhibitors for germline BRCA-mutations.

Current treatment options for those patients being metastatic at first diagnosis involve using an aromatase inhibitor, biphosphonates, and systemic therapy (for instance, as the EC-scheme, followed by paclitaxel or CDK-4/6 inhibitors or fulvestrant). This is done in coordination to treating acute damage such as unstable and painful bone metastasis or cutaneous metastasis

involving osteosynthesis, surgery and radiation therapy [11].

Oligometastatic cancer can be targeted by treating the lesions locally and by offering a systemic treatment option as well.

In more generalized metastasis with higher metastatic burden, it is generally offered to receive systemic therapy and treat singular metastases that cause pain or instability.

The following figure, taken from Kroigaard et al. depicts an example of the tumor burden of a patient with metastatic disease over a time span [38].

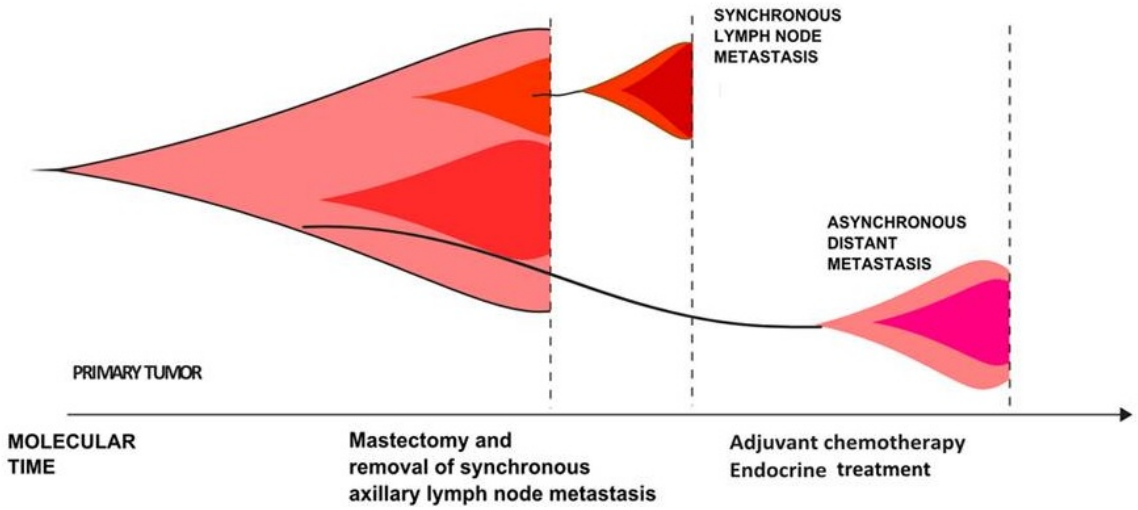

Figure 1.3: Diverse patterns of progression within patients, excerpt from figure 2 in [38]: "Phylogenetic trees depict the clonal evolution through cancer progression. An increase in color intensity reflects the acquisition additional somatic mutations."

1.4.1 Metastasis

In principle metastasis is the process of cancer progression and formation of secondary tumors at distant organs. Despite being a complex process [39], it involves some similar and common steps for all cancer entities. These encompass the tumor dissemination, colonization and metastatic progression. The separation from the primary tumor is the first step. The invasion then follows through tissues with the penetration of the basal membrane. Later, the cell enters into the blood flow (or other spaces and fluids such as the lymphatic flow or peritoneal and pleural spaces). After their journey through the blood flow the involved cells come to an arrest and stop in a distant organ, becoming hence the target organ [39]. It is widely accepted, that metastasis requires progression of the disease. Other theories about the sequence of metastasis exist and will be further elaborated.

At first, several mutations take place in the cancer cells. These may be mutations in proto-oncogenes or tumor-suppressor-genes. In the previous chapter, some of these were mentioned for metastatic breast cancer. Only after the acquisition of these mutations, cells gain the ability to detach from the primary tumor, perform epithelial-mesenchymal transition

(EMT), travel with the blood flow and enter other target organs to finally grow firm there. Then, cells transfer back to their epithelial phenotype via mesenchymal-epithelial-transition (MET). The first physical step of metastization requires motility of the cell among further qualities acquired through mutations. The timing of these steps is still under discussion. In the remainder of this chapter, I will make a brief digression on the timing of metastasis in breast cancer. When mentioning metastasis, it is necessary to emphasize that it is itself a selection process. It involves several steps of mutations accumulating and processes running successfully in order to enter a distant organ. From a distinct number of cells starting to gain mutations to a cell homing at a distant organ, there is a huge amount of unsuccessful cells failing the process [39]. Due to these reasons, metastasis is an inefficient process. Tumors shed millions of tumor cells into the blood flow but only few successful metastasis are in fact formed [39], [40].

Important contributors to metastasis formation as an overall process are EMT, the pre-metastatic niche, hypoxia, cancer stem cells, angiogenesis and many more. Of huge significance is the tumor microenvironment. This notion describes a complex network of extracellular matrix components, signaling molecules, soluble factors and different types of cells. Among these are fibroblasts and macrophages, which are activated by oxidative stress and contribute to the tumor stroma. Endothelial and perivascular cells are also recruited via signalling. The tumor microenvironment remodels the extracellular matrix in its favour. In conclusion: the surroundings prepare and contribute with its conditions to the tumor progression, they build a "favourable nest" [41]. Other components of the tumor microenvironment are cancer cells, such as circulating tumor cells and later also cancer stem cells [42]. Circulating tumor cells have the unique ability of maintaining tumor mass in the primary tumor but also the ability to survive outside of the primary location. Common cancer cells are able to develop into cancer stem cells (CSC). This process requires pressure with influence from the microenvironment, such as hypoxia, previously described external and internal influences and EMT. At the end of this process, CSC remain, that are more chemoresistant and thus difficult to target [43], [41], [44]. Later, Cancer stem cells circulate in the blood flow and have the ability to fight off reactive oxygen species (ROS) [45], [46]. They form therefore a malignant phenotype and are resistant to many forms of currently available therapy. Cancer stem cells feature other major commonalities with normal stem cells, such as dormancy, active DNA-repair, expression of ABC-drug transporters, and intrinsic resistance to apoptosis. They may reside in niches, that protect them from being targeted by current common treatment options. Thus they may remain in the body even after primary tumor and lymph nodes have been successfully treated.

With increasing size, angiogenesis is vital for supplying oxygen and nutrients to the tumor, otherwise parts of it become necrotic. Only then, after these meticulous preparations, conditions are favourable for metastization. It ensures the tumors oxygen supply and nutrients vital for persistence and growth. At the same time it's blood vessels - even though of minor quality than in normal organs (due to time, pressure etc.), provide access for cancer cells to disseminate. When cells metastasize, metastasis from the same primary tumor may be highly heterogeneous. Their heterogeneity lies in their biology, that leads to the expression of differ-

ent surface receptors and the presence of different mutations. In vitro experiments showed that cancer cell lines show an organ tropism [47], [48]. In breast cancer, the preference of metastatic sites, are for instance mainly bones, but also lung metastasis, with lesser frequency hepatic metastasis and lastly brain metastasis.

In the second part of this chapter, I would like to discuss timing and sequence of the process of metastasis. Among other references, my main sources here are the reviews of Hunter [39], Dong [49], and Fares [47]. Current models intend to find an explanation to the grand questions when tumors metastasize, when mutations take place and how the difference in metastatic potential of tumor cells is shaped. Is the metastatic disease already defined within the genotype? Questions from a clinicians point of view are, for instance, why metastization occurs years after an initially successful treatment of a primary tumor.

Metastasis was historically seen as resembling the rather linear process of carcinogenesis (as in the progression model and linear carcinogenesis model)[50]. Today we know, this is not a requirement [49]. Historic models could not determine several frequently occurring situations, such as nodal only relapse and metastasis after initial cure. It also failed to explain cancer of unknown primary-Syndrome (CUP) - usually emerging as affected lymph nodes without a primary being found. In this situation, it is assumed, that the initial tumor, that later receded, shed circulating tumor cells into the blood flow, that formed dormant tumor cells in special niches - such as the bone marrow. After the immune system successfully eliminated the primary tumor, the initially dormant tumor cells succeeded in forming a metastasis [51].

To highlight a specific situation in treating cancer patient, especially women with breast cancer, I would like to elaborate on this particular situation: A relevant percentage of these women develop bone metastasis up to 12 and more years after initial cure. There have been publications about bone metastasis in mamma carcinoma claiming that at the stage of the first diagnosis, already 60 to 70 % of patients have microscopic metastasis [17]. Those were located in the vertebral column and pelvic bones. In the following, I would like to take a closer look at this particular publication. Schmidt-Kittler at al. isolated cancer cells and performed single cell comparative genomic hybridization. Their findings were that up to 60% of patients have these cells already at the non-metastatic stage of disease. That counteracts to the historic paradigm of sequential mutations (genetic and epigenetic). In this group of about 300 non-metastatic breast cancer patients the progenitors sat in the bone marrow. It is presumed they were present there from the beginning of the disease on. The group stained for cytokeratin antibodies, that are on the surface of epithelial malignancies only. These occur very rarely (10^{-5} to 10^{-6} only), they seem to disseminate early in genomic development. This might explain why non-metastatic patients with complete remission of their primary site relapse as metastatic years later. It is presumed, that the dissemination must have taken place before the diagnosis of metastasis, probably even at the same time as the tumor formation. The progenitor cells the group analysed had not yet undergone the complete cascade of metastasis. This stands in contrast to the presumed historic model. This outstanding publication by Schmidt-Kittler et al. is of high importance for my work: it contributed to the understanding of metastatic breast cancer. Today, we have further knowledge on cancer stem cells, often

showing radioresistance and dormant tumor cells [52]. Both cell populations share some properties, such as therapy resistance and rareness, associated with poor prognosis. Today, we estimate, that cancer stem cells circulate with the blood flow and dormant tumor cells might reside in the bone marrow and other sites. More evidence for the theory of dormant tumor cells in breast cancer patients is available [53]. Meng et al. examined cured breast cancer patients who had undergone mastectomy. They found circulating tumor cells in 13 of the examined 36 patients, in one case even 22 years after treatment.

Historic models of metastasis have contributed to our present understanding of the subject. Scientific approaches to metastasis date back as soon as 1889 with Stephen Paget's seed and soil hypothesis [54]. Especially since the 1970s, there have been great advances in this field.

The progression model (later also called dynamic heterogeneity model) dates back to 1976 [55]. It states that serial somatic mutations take place in cancer cells (in the primary or circulating tumor cells)[39], [55]. Finally, few cells complete this process and develop their full metastatic potential. All steps on a metastatic cascade need to be acquired according to this model. As this is an immensely complex process, only a minor share of cells reaches this level. A contradiction to this model is that it could not explain cancers of unknown primary (overall 5% of all cancers). The second point of critique is why some cells loose the high metastatic capacity later on.

IN 1990, Weiss et al. proposed the transient compartment model. This model states that all tumor cells in the primary tumor can reach a metastatic capacity. But only a small fraction of these will do so on time complete the process on time and in the correct moment. This might be due to different positions of the cells within the tumor, due to random epigenetic events, or physical factors such as a lack of blood supply for growth [39], [56]. In 2002, new discoveries led to the idea of the early oncogenesis model. It claims that all cells and tumors are established early. A source supporting parts of this theoretical model is the above mentioned paper by Schmidt-kittler et al. [17].

The fusion model states that proliferational, migrational and invasional properties of cancer cells results from a nuclear transduction from lymphoid cells. The cancer cells fuse with either myloid cells or take up circulating DNA [57], [58]. In the result, the cancer cell gains favorable abilities. Although cellular fusion was witnessed in experiments before, no lasting evidence in vivo was finally reached. Today, this model is considered of minor importance. A slightly different model is the gene transfer model. This model is based on the theory of horizontal gene transfer, as stem cells taking up circulating tumor DNA and forming metastasis at a distant organ. Similarly to the fusion model, this one has it's weaknesses and deviates from in vitro findings [39].

The microenvironment is vital in metastasis. Despite not being a model nor theory, I would like to reemphasize the vital and large role in the tumor surroundings in many aspects. The microenvironment creates the conditions, that enable a last step of detachment from a primary tumor or arranging homeostasis as a metastasis at a distant site. They create a climate that enables survival and progression. Among its many contributors are immune cells. For instance macrophages contribute to the tumor motility. The bone marrow as such is also a possible environment for a pre-metastatic niche. Source 90. Source 91: lyden: bone marrow

cells, pre-metastatic niche. On a non-cellular basis, just a singular example of influences of the microenvironment would be microRNA (possible also inside exosomes) [59]. Further discussion of its role follows in the next subchapter. Source 89: Condelis, Pollard: motility and migration, macrophages. Metastasis needs motility and mechanisms of this. The intrinsic properties of a tumor plus the selective mechanism and the correct microenvironment leads to a successful metastasis. The microenvironment enables necessary phenotypic, such as EMT and MET.

For some of the questions about the timing of metastasis, an answer has been found. There are risk factors for recurrence of certain cancer types, within the tumor size, nodal affection and molecular markers. In a short conclusion: With many contributors to metastasis, it is a large and complex research field. Fortunately, it offers multiple targets for treatment.

1.4.2 Invasion and Migration

The microenvironment contributes to metastization as it sets off migration due to EMT, among other effects. The tumor microenvironment is an important component contributing to a favourable environment that enables tumor cells to detach and migrate to other target organs and then to harbor there and form distant metastasis. Understanding the microenvironment and the tumor stroma, will lead to gains in optimized therapy and prevention of metastatic spread.

Migratory mechanisms in cells are important for multiple purposes. They play a vital role in embryo-genesis, development and cell maturation, wound healing, organ fibrosis and metastization. For instance the directed movement of cells in embryonic development is determined by migration. One mechanisms involves EMT. It begins with mesenchymal stem cells losing their cell polarity and cell-cell contacts. By removing the adhesion to the neighboring cell they loose junctions, polarity and polarization and adhesion to their previous surface. Epithelial cells loose expression of E-cadherine when transforming to mesenchymal cells (only focal junctions). This leads to change of morphology and phenotype, thus function of the cell.

Migration is part of the stages of metastization. These include the invasion, circulation and colonization at a distant site. Invasion is usually classified in three steps. The extracellular matrix needs to be degraded and deformed, to be passed by the tumor cells. This is done with the help of proteases and other degrading enzymes. After that, cell migration is possible. Invasion is considered as the most difficult step on the cells' way to a distant organ.

Invasion and migration can be analyzed using different assays in cell culture. For measuring invasion, a coating is included, which needs to be penetrated by the cells. Whereas measuring migration focuses on cells covering a distance, that will be measured. The assays can be performed in 2D cell cultures or 3D spheroids. Options for observing underly constant improvement in microscopy. In vivo models usually encompass tumor migration models in immunocompromised mice.

Recent works on advances in microscopy emphasize the impact of observing migration in vivo. It enables the observation of migration tracks in the ECM. Previously used 2D-assays might not fully represent locomotion of cancer cells and the microenvironment as it is in

vivo [60]. Migratory tracks may follow anatomical structures like blood vessels, lymph vessels,nerves. They may also follow a leading cancer cell or a cancer-associated stromal cell that opens up paths for migration in the ECM. They only then need to degrade the ECM if pores within are smaller than 7 micrometres in square.

Another aspect of invasion is the consideration of confinement as a physical cue in order to modulate intracellular signalling and therefore then afterwards changing tumor cell migration mechanism. The extracellular matrix is also perforated by cells of the immune system such as mast cells, macrophages, as well as fibroblast. They all contribute to its remodelling and shaping. The extracellular matrix is also shaped by the use of proteinase and collagen cross-linking. This way tracks and migratory niches are created. This is also important for the building of the pre-metastatic niche. Though invasion and migration here is mostly restricted to a cancer environment, it has several other functions, such as a regular shaping of the ECM in healthy tissues (in muscles and nerve fibres as well, blood vessels, lymph vessels).

Among examples for use of anatomical structures for invasion and migration, the white matter tracts in the brain are mentioned as highways for gliomal cell migration. and one source is cited that melanoma cells use the outer surface of blood vessels as a guidance structure for migration and proliferation in order to form brain metastases [61], [62].

Many other cancer cell lines have also been reported to migrate along anatomic structures. It is also noted that tumor cell movement does not destroy the pre-existing tracks, they are not modified in diameter, as long as they are larger than 7 square micrometers. Konstantinoupolos at al. express the hypothesis that this might be the reason why the use of matrix metalloproteinases inhibitors as single agents do not result in the expected effect in vivo [60]. For the correct representation of the ECM in research, 3D-assays with a special gel simulating the ECM are needed. They represent the fibres and channels in the exact dimensions and stiffness in order to study migration and also 3D confined migration realistically. 2D-assays are easier to perform and analyse. They are a good method for examining singular factors.

1.5 Overview of migration in different cancer cell lines

Migration following a previous irradiation has been observed in a variety of cancer cell lines in vitro, especially in primary brain tumors, lung, liver and breast cancer [63], [64]. Ionizing irradiation is therapeutically used for treating cancer, aiming at creating single- and double strand breaks in the DNA, enabled by reactive oxygen species (ROS). Simultaneously, irradiation can lead to migration via EMT-inducing pathways [63], [65]. These include the induction of migration, but also a metabolic change towards cancer stem cell like properties [63]. Irradiation can induce the expression of transcription factors, such as snail, HIF-1, ZEB1 and Stat3, which lead to EMT. With the activation of the TGF-beta, Wnt, Hedgehog, Notch, G-CSF, EGFR/PIK3/Akt and MAPK-pathways, the metabolic changes are also induced. The following adapted figure gives an illustrative presentation of these links: [63].

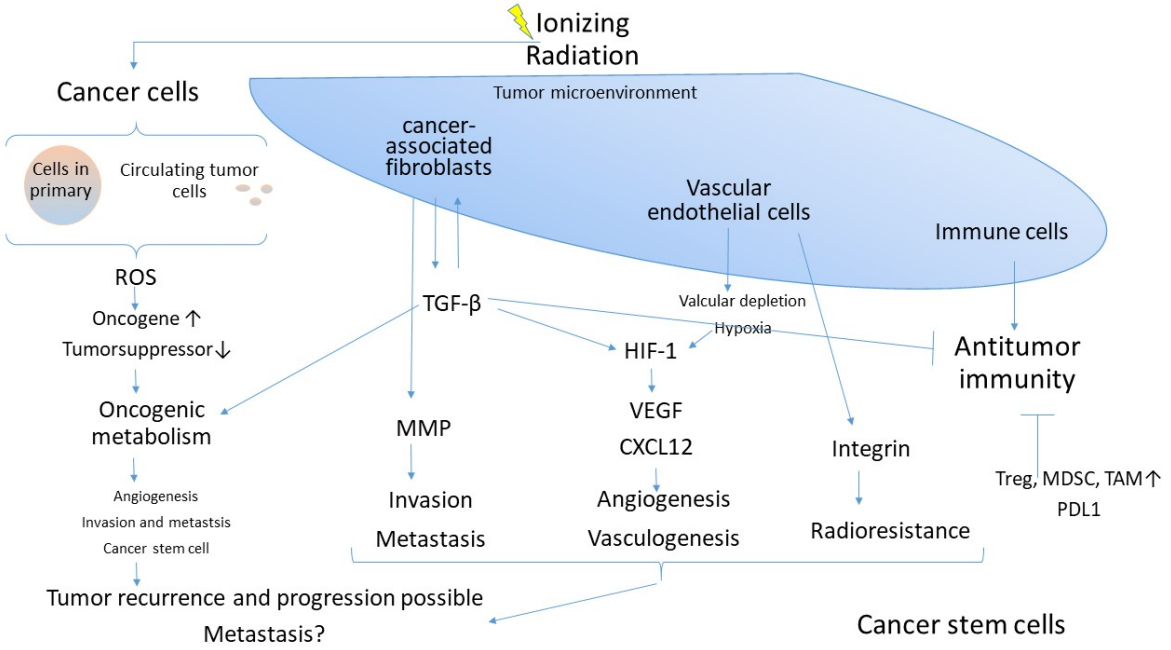

Figure 1.4: Side effects of irradiation on tumor cells and the tumor microenvironment, adapted from [63]

In the figure above, links are shown, that occur as paradox side effects of irradiation. These are described as follows, adapted from Lee's legend to the figure [63]: it may in conclusion increase tumor aggressiveness. Irradiation promotes ROS-production. This leads to two effects: one effect is that it targets DNA and leads to single- and double-strand breaks. Another effect is that it may activate oncogenes and inactivate tumor-suppressor genes. If this aspect prevails, then it increases the oncogenic metabolic activities. It promotes tumor activity and proliferation. Irradiation may also induce EMT and cancer stem cell like properties in the cancer cells irradiated. Irradiation can also lead to alterations in the tumor microenvironment: the extracellular matrix is remodeled, fibroblasts are activated. This results in fibrosis, hypoxia

and a following inflammatory response. Fibroblasts then release growth factors, among them the transforming growth factor beta (TGF-beta) and extracellular matrix modulators such as matrix metalloproteinases. These facilitate metastasis and invasion by degrading the ECM. TGF-beta plays a huge role and activates HIF-1. Irradiation may also damage vascular endothelial cells, it then results in hypoxia. Hypoxia further promotes HIF-1 activation. This induces angio- and vasculogenesis through VEGF and Chemokine ligand 12 expression.
First, I would like to focus on brain cancer-related cell lines. Glioma cell lines have been largely investigated concerning invasiveness due to the aggressive nature of the disease. Sadly, in 2022 the prognosis for the most frequent malign brain tumor, glioblastoma, is still very poor. Potential options for treatment including surgery, radiochemotherapy with Temozolomide and adjuvant administration of Temozolomide, Bevazizumab and CCNU as well as TTF-Therapy. Despite all efforts, there has been no great improvement in OS largely since the publication on improved OS with adjuvant chemo-irradiation by Stupp et al. in 2005 [66].

Examples of these brain cancer-related cell lines are for instance medulloblastoma cell lines, such as D425 and Med8A, that showed to be less motile after irradiation with photons and carbon ions using the transmigration assay [67]. Findings on primary cultures and established cell lines in glioblastoma by Wank, Baulch, Park, Cordes and Rieken et. al. showed among others that high-LET irradiation introduced less invasive behavior than low-LET and a heterogeneity in between the aggressiveness of cell lines [68], [69], [70], [71], [67].

Among the previously mentioned publication, I would like to focus on [68]. Wank et al. set up a primary culture of glioblastoma cell lines and examined these among three established cell lines on invasiveness [68]. Using low LET irradiation (X-ray) and high LET irradiation (alpha-particles) on these cell lines, 6 of the 7 primary cultures showed higher invasiveness after low-LET irradiation as well as 2 of the 3 established cell lines. However although there is suspicion that photon irradiation alters migratory behavior in cancer cell lines, this is not always the case. A study conducted by Rieken showed that medulloblastoma cell lines reduced transmigration after irradiation with photons and carbon ions [67]. They observed that matrix metallo proteases- (in this case MMP9) and integrin-alteration that are vital for cell adhesion, lead to changes in migratory potential. Migration is widely accepted as a vital part of the forming of metastasis in cancer [72]. So motility seems to be dependent on irradiation type, mutations and influences such as messenger RNA, cytokines and others. Migratory experiments tend to vary between their biological replicates [67].

The following table gives a abbreviated overview of the above mentioned studies:

Table 1.1 Overview of above mentioned cell lines and migration

Author	Cell lines	Findings on migration	Source
Wank, M et al. 2018	Glioblastoma	Low LET irradiation leads to higher levels of invasiveness than high LET irradiation	[68]
Simon, F et al. 2015	Meningioma	Carbon-ion irradiation: no migration; photon irradiation: promotes migration	[73]
Rieken, S et al. 2011	U87 and Ln229 glioma cells	Photon irradiation: promotes migration	[74]
Rieken, S et al. 2012	Glioblastoma	Carbon ion irradiation: inhibits migration	[75]
Rieken, S et al. 2015	Medulloblastoma D425 and Med8A	Carbon ion and photon irradiation: inhibit migration	[67]
Rieken, S et al. 2014	Isogenic W12 (intact E2 gene status) and S12 (disrupted E2 gene status) keratinocytes	E2-disrupted keratinocytes showed increased migration after irradiation	[76]
Ogata, T et al. 2005	HT1080 human fibrosarcoma cells, mouse osteosarcoma	Particle irradiation: lower levels of migration; photon irradiation: promotes migration	[77]
Merrick, M. et al. 2021	HCN2 neurons and T98G glioblastoma	X-ray irradiation: promotes migration	[78]
Park, C M et al. 2006	Glioblastoma: U87, U251, U373, LN18, LN428,C6 (rat)	Ionizing radiation enhances invasion	[70]
Baulch, J E et al. 2016	Glioblastoma: primary culture	Irradiation of primary human gliomas triggers dynamic and aggressive survival responses involving microvesicle signaling	[69]
Cordes, N et al. 2003	Glioblastoma: A172, U138, LN229, LN18	Irradiation differently affects substratum-dependent survival, adhesion, and invasion of glioblastoma cell lines	[71]
Wild-Bode, C et al. 2001	Glioblastoma: U138MG, U87MG, D247MG, T98G, LN319, U251MG, U373MG, LN308, LN229, LN308, LN18	Sublethal Irradiation Promotes Migration and Invasiveness of Glioma Cells	[79]
Nguemgo Kouam, P et al. 2018	Glioblastoma: U373MG, U87MG	Robo1 and vimentin regulate radiation-induced motility of human glioblastoma cells	[80]
Stahler, C et al. 2013	Glioblastoma: U87, LN229	Impact of carbon ion irradiation on epidermal growth factor receptor signaling and glioma cell migration in comparison to conventional photon irradiation	[81]
Eke, I et al. 2012	Glioblastoma: U87MG, U138MG, A172, LN229, DD-T4 (primary culture), DD-HT7606 (primary culture)	Three-dimensional Invasion of Human Glioblastoma Cells Remains Unchanged by X-ray and Carbon Ion Irradiation In Vitro	[82]
Steinle, M et al. 2011	Glioblastoma: T98G, U87MG	Ionizing radiation induces migration of glioblastoma cells by activating BK K+ channels	[83]

1.6 Overview on other cancer cell lines previously examined

Migration in MCF-7 cells was studied in many publications, as it is a cell line with a migratory phenotype that can be suitably used for observing inhibitors.

SkBr3 is HER2 positive and a migrating breast cancer cell line, that is frequently used in evaluation of trastuzumab therapy in vitro. Further details about the used cell lines will be discussed in chapter 2.

An overview on current literature on migratory behavior after irradiation of cell lines usually refers to an examination of a specific protein or an overexpression/ knock-down model. Commonly examined pathways and topics include ERK, HIF-1α, EMT - migration, NF-κbeta-pathway and stat3 signalling in case of SkBr3 [64].

The following tabular will give a short insight of current research on Skbr3 and MCF-7 concerning migration. Often this aims at examining the impact of a molecule or pathway rather than simply examining the impact of migration and irradiation.

Among the displayed sources, I would like to outline two among these. Ferraro et al. published in 2019 that epithelial exosomes and supernatant influence migration in SkBr3 cells, depending on the status of the epithelial cells. They examined the STAT3-signalling and mentioned the influence of the microenvironment on migration [84]. Schmucker et al. examined in 2018 that AREG promotes migration and invasion in SkBr3. They used a scratch migration assay [85]. Do et al. published in 2021 about XCL1 and how this downregulates E-Cadherin in MDA-MB-231 cells and upregulates N-cadherin and vimentin, and β-catenin nucleus translocation, leading to more EMT, hence migration. In a second part of the publication, they state that XCL1 introduces migration through EMT induction, HIF-1α accumulation, and ERK phosphorylation in SK-BR-3 cells, MMP 2 and 9 expression in SkBr3 is enhanced here [86].

Many of these publication focus on targeting a single inhibiting substance and using it on the cell line rather than examining effects of irradiation. The above mentioned papers put an additional emphasize on migratory research.

Table 1.2: Overview of further cell lines and migration

Author	Cell lines	Findings on migration	Source
Acharyya, S et al. 2012	Breast cancer: MDA-MB-231	A CXCL1 paracrine network links cancer chemoresistance and metastasis	[35]
Mutschelknaus, L et al. 2018	Head and neck: BHY	Functional analysis of head and neck cancer exosomes released in response to ionizing radiation	[59]
Liu, H et al. 2018	Breast cancer: MCF-7	MiR-22 down-regulates the proto-oncogene ATP citrate lyase to inhibit the growth and metastasis of breast cancer	[87]
Radulovic, V 2017	Breast cancer: MDA-MB-361, MCF-10A (mammary epithelial)	Role of miR-21 in determining sensitivity of mammary epithelial cells to radiation treatment	[88]
Tsai, Pei-W et al. 2003	Breast cancer: MCF-7, SkBr3, and T47D	Up-regulation of vascular endothelial growth factor C in breast cancer cells by heregulin-β1 a critical role of p38/nuclear factor-κb signaling pathway	[89]
Gest, C et al. 2013	Breast cancer: MDA-MB-231 and MCF-7	Rac3 induces a molecular pathway triggering breast cancer cell aggressiveness: differences in MDA-MB-231 and MCF-7 breast cancer cell lines	[90]
Mattila, M et al. 2002	Breast cancer: MCF-7	VEGF-C induced lymphangiogenesis is associated with lymph node metastasis in orthotopic MCF-7 tumors	[1]
Pérez-Yépez, E A et al. 2012	Breast cancer: MCF-7	Selection of a MCF-7 breast cancer cell subpopulation: morphological and molecular changes leading to increased invasiveness	[91]
Schmucker et al. 2018	Breast cancer: SkBr3	AREG promotes migration and invasion	[85]
Ferraro et al. 2019	Breast cancer: SkBr3	Epithelial exosomes and supernatant influence migration in SkBr3 cells, depending on the status of the epithelial cells. They examined the STAT3-signalling and mentioned the influence of the microenvironment on migration	[84]
De Bacco et al. 2011	Breast cancer: MDA-MB-231, MDA-MB-435S, U251	Irradiation actived EMT expression (here called MET)	[92]
Kawamoto et al. 2011	Colorectal cancer: CaR1 and DLD1	Irradiation induced EMT	[93]
Zhang X et al. 2011	Breast cancer: MCF-7	Low dose ionizing irradiation induced EMT	[94]
Park J K et al. 2012	Cholangio carcinoma: C6L in nude mice	Irradiation induced EMT and MMP-expression	[95]

1.7 Research aim and hypothesis

The main aim of this work was to analyze migration in mamma carcinoma cell lines using an improved migration assay. A second aim was to validate the migratory assay which was used here. The larger context is to drive forward the development of personalized therapies in radiation oncology.

2 Material and Methods

2.1 Material

2.1.1 Consumables and supplies

	Consumables and supplies	Manufacturer
	Culture insert 12 Well, 5 mm gap	Ibidi GmbH, Planegg, Germany
	Culture insert 2 Well, 500 micrometer gap	Ibidi GmbH, Planegg, Germany
	Petri dish 9 cm diameter	Sarstedt, Nümbrecht, Germany
	Petri dish 5 cm diameter	Sarstedt, Nümbrecht, Germany
	Cell culture flask, 75 cm2	Sarstedt, Nümbrecht, Germany
	Cell culture flask, 25 cm2	Sarstedt, Nümbrecht, Germany
	Positioning help for culture insert positioning	Self made
	24 Well plate	Sarstedt, Nümbrecht, Germany
	12 Well plate	Sarstedt, Nümbrecht, Germany
	6 Well plate	Sarstedt, Nümbrecht, Germany
	Tubes 5 ml, 2 ml, 1 ml	Eppendorf, Hamburg, Germany
	Pipette tips (various)	Eppendorf, Hamburg, Germany
	CellTiter-Glo, luminescent cell viability assay	Promega, Mannheim, Germany
	Caspase-Glo, luminescent apoptosis assay	Promega, Mannheim, Germany
	96 well plate	BD Bioscience
	Cell culture medium supplies	
	RPMI 1640 Medium	Gibco, Fisher scientific
	DMEM, high glucose, GlutaMAX™ Supplement	Gibco, Fisher scientific, Karlsruhe, Germany
	DMSO (Dimethylsulfoxide)	Sigma-Aldrich, Steinheim, Germany
	Ethanol absolute	Merck, Darmstadt, Germany
	NEACC amino acids 5 % (non essential amino acids)	Sigma Aldrich, Taufkirchen, Germany
	Puromycin dihydrochloride solution	Sigma-Aldrich, Steinheim, Germany
	Fetal Calf Serum Gold (FCS)	PAA Laboratories GmbH, Cölbe, Germany
	Insulin from bovine pancreas	Sigma-Aldrich, Steinheim, Germany
	Trypsin	Invitrogen, Darmstadt, Germany
	Transduction	
	HEK293T cells	N. Anastasov
	10 cm petri dish	Sarstedt, Nümbrecht, Germany
	Lipofectamine 2000	Life Technologies, USA
	Puromycin dihydrochloride	Sigma-Aldrich, Steinheim, Germany
	Soybean Trypsin Inhibitor	Thermo Fisher Scientific, Darmstadt, Germany
	pGreenPuro (pGP) expressing copGFP	System Biosciences, USA
	packaging plasmids pMDLg/pRRE, pRSV.Rev and pMD2.G	D. Trono, Ecole Polytechnique federale de Lausanne, Switzerland

Table 2.1: Consumables and supplies

2.1.2 Breast cancer cell lines

The following cell lines were used: T47D-GFP, MDA-MB 361-GFP, SkBr3-GFP, MCF-7-GFP. The transfection using stable green fluorescent protein (GFP) was performed by Natasa Anastasov[96] (ISB, Helmholtz Zentrum München). The pilot experiments were performed using all four cell lines. After further selection, the main experiments were performed using the remaining cell lines SkBr3-GFP and MCF-7-GFP.

T47D-GFP

The human cell line T47-D was first identified from a ductal mammacarcinoma in 1979 at the metastatic site of a 54 year old Caucasian woman and retrieved from pleural punction material[97] [98]. It expresses progesterone, estrogen and her2neu (Source ATCC: HTB-133, date:03/2021).

It was used in the preselection in 1mm migration grids. Due to its poor migratory behavior, as well as lack of confluency, it did not qualify for futher trials and was excluded from the experiments.

MDA-MB 361-GFP

The human mammacarcinoma cell line MDA-MB 361 was first identified in the year 1973 after being isolated from a brain metastasis of a 40 year old Caucasian woman suffering from adenocarcinoma of the breast [99] [100]. It expresses the oncogene wnt7h, it is a ER-positive/Progesterone receptor (PgR) negative, luminal mammary carcinoma cell line [101]. The her2neu-oncogene is highly amplified in this cell line [102]. It was excluded from the trial due to the same reasons as cell line T47D. It lacked migratory behavior, but showed better confluency in cell culture.

SkBr3-GFP

SkBr3 cells derive from an adenocarcinoma that is receptor negative (ER -, PR -) and Her2neu positive. (ATCC®HTB-30TM). It is named after the Sloan Kettering-Cancer Center and was retrieved in 1970 from a Caucasian woman with metastatized breast cancer from a pleural effusion [103]. SkBr3 cells are known for a high invasive and migratory potential, possibly due to the lack of receptor positivity for Estrogenes. They are often used for research on her2/neu targeting.

MCF-7-GFP

MCF-7 cells are derived from the pleural effusion of a 69 year old Caucasian woman with metastatic breast cancer in 1973 at the Michigan Cancer Foundation [104]. Herbert Soule et al. were the first to stable cultivate a breast cancer cell line in 1973. It was then named as the Michigan Cancer Foundation 7-Cell line. MCF-7 is described as a Hormone receptor positive cell line with the Luminal A molecular subtype (ER +, PR +). The MCF-7 cell line is one of

the most important cell lines in research for breast cancer. In the 1970ies it lead to the central discovery that Estrogen provokes tumor growth in Estrogen receptor positive breast cancer. Reviews state that MCF-7 is the most sought after cell line in breast cancer in vitro research. Shirazi et al. describe MCF-7 as poorly aggressive and non-invasive [105]. The epithelial like structures of this cell line survived in parts and are estrogen sensitive, although concerns about the expression of different evolving receptors are expressed in the literature [106]. There is controversy upon the migratory potential of MCF-7 cell lines. Parental cell lines are described as non invasive and non migratory in literature [90]. Certain factors contribute to a migratory and invasive phenotype in passaging of cells in vitro. Such as VEGF, especially VEGF-C [89]. Higher levels of VEGF, such as in the cell line MDA-MB 361 lead to a higher capacity of invasion and migration. [1] Estrogenes are discribed as inducing metastasis in mice with a low capacity of in vitro migration [107]. The subpopulation MCF-7A3 expresses an invasive and migratory phenotype under the influence of IL-1beta, thus delocalizing E-cadherin from the cell membrane to inner cell compartments [91].

2.1.3 Culture media and supplements

According to the requirements of the cell lines published in ATCC [98] [99] T47D-GFP, MDA-MB 361-GFP, SkBr3-GFP, MCF-7-GFP cells received the recommended culture media and supplements.

- T47D-GFP: RPMI 1640 + bovine/human insulin 10 µg/ml as 0.2 U/ml + 10% FBS + Puromycin if GFP-labelled
- MDA-MB 361-GFP: DMEM Glutamax + 10 % FCS + 0.25 % Puromycin if GFP-labelled
- SkBr3-GFP: DMEM Glutamax + 10 % FCS + 0.25 % Puromycin if GFP-labelled
- MCF-7-GFP: RPMI 1640 + 10 % FCS + 1 Aliquot (5ml) Insulin + 5 ml Neacc (100)

2.1.4 Additional substances and solutions

The following agents were used for cell culture media:

- RPMI 1640 Medium
- DMEM Glutamax Medium
- NEACC amino acids 5 % (non essential amino acids)
- Puromycin solution
- FCS 10 % and 1 %
- Insulin

Further on for experiments were used: Keyence Fluorescence Microscope, Coulter Counter Cell Counting Machine, manual glass counting chamber, Adobe Photoshop Software, For the cell viability experiments: CellTiter-Glo, luminescent cell viability assay- Kit. For the apoptosis induced effect measuring: Caspase-Glo, luminescent apoptosis assay- Kit.

2.1.5 Equipment

Purpose	Equipment	manufacturer
Centrifugation	Centrifuge Biofuge pico	Heraeus Instruments, Osterode, Germany
	Centrifuge Eppendorf 5424R	Eppendorf, Hamburg, Germany
	Centrifuge Rotina 420R	Andreas Hettich, Tuttlingen, Germany
	Centrifuge tubes (15 ml and 50 ml)	Greiner BioOne GmbH, Frickenhausen, Germany
	Centrifuge/vortex combi-spin FVL 2400	PeqLab, Erlangen, Germany
Source	Cs137-γ-source	HWM-D 2000 machine, Wälischmiller Engineering, Markdorf, Germany
Cell culture	Dispenser Multipette® plus	Eppendorf, Hamburg, Germany
	Freezer -20°C	Liebherr, Ehingen(Donau), Germany
	Freezer -80 °C	New Brunswick, Nurtingen, Germany
	Incubator	Sanyo, Bad Nenndorf, Germany
	LSR II flow cytometer BD	BD Biosciences, Heidelberg, Germany
	Microplate reader Infinite® M200	Tecan, Switzerland
	Microscope Axiovert 25	Carl Zeiss, Jena, Germany
	Microscope KEYENCE BZ-9000 series	Keyence, Frankfurt, Germany
	Multiple plate reader	TECAN Infinity M200, Tecan, Crailsheim, Germany
	Nalgene Cryo Freezing Container	Sigma-Aldrich, Steinheim, Germany
	Pipette tips Graduated Filter Tips	TipOne Starlab, Ahrensburg, Germany
	Pipettes 10, 20, 100, 200, 1000μl	Eppendorf, Hamburg, Germany
	Reaction tubes 1.5 ml, 2.0ml	Eppendorf, Hamburg, Germany
	Reaction tubes 15ml, 50ml	Falcon Blue Max BD Biosciences, Heidelberg, Germany
	Sterile laminar flow work bench	BDK Luft und Reinraumtechnik, Sonnenbühl-Genkingen,Germany
	Z1 Coulter Particle counter	Beckman Coulter, Fullerton, USA

Table 2.2: Equipment

2.1.6 Software

Statistical analyzis was performed using Excel and SPSS. Adobe Photoshop was used for image processing and the images were analyzed by the software written by Marcus Vetter.

Adobe photoshop was used for defining the excerpt that forms the gap between the two sides of cell layers. Marcus Vetters program counts the amount of green pixels above a pre-defined threshold.

Purpose	Software	Source
Preparation of images	Adobe Photoshop Version CC 15.5	Adobe, Dublin, Ireland
Analyzing	Software calculating green pixels	Marcus Vetter, Munich, Germany
Statistics	Microsoft Excel for Office 365 Version 16.0	Microsoft Germany, Munich, Germany
	IBM SPSS Statistics for Windows, Version 26.0.	IBM Corporation, Armonk, NY, USA

Table 2.3: Software

2.2 Methods

2.2.1 Cell culture

Cell culture was performed according to the guidelines available on ATCC for each cell line. Cells were cultivated at 37°C using 5 % CO^2 concentration in the incubators. Incubators were regularly cleaned and temperature as well as CO^2 concentration was supervised. Cell culture was performed in an S2-lab according to the German regulations on work with genetically modified cells. Regular testing on mycoplasma was performed and negative at all times.

2.2.2 Cell viability assays

Cell viability was at first measured using Trypan blue staining and a Beckman Coulter ViCell Counter for measuring viable cells or by the cell titer glo viability kit.

2.2.3 Cell viability assay using luminescence

Cell viability was measured for determination of viable cells after irradiation. Its second contribution to this work was to rule out proliferation effects on the migration assays, a possible bias in the results. The cell viability kit quantifies ATP through the metabolic activity of cells emitting the later. A luminescent signal is detected by the luminometer and emitted in relative light units (RLU). The cell number is then directly proportional to the signal in the luminescence output.

Materials used in this protocol were: a 96 well plate with an opaque bottom, in this case white bottom for avoiding scattered luminescence, the buffer and substrate, medium used in the experiments, cells at different time points and irradiation doses. (FCS 10 vs 1%).

Experiments were performed according to the user's instruction manual. Probes of each arm of the experiment were taken as 100 µl of the cells and examined according to the general design. Preparation of the assay was as follows. The substrate provided in the kit was dissolved in the provided buffer and it was either directly used after dissolution or stored at -20°C for further usage. 100 µl of the solution were added to 100 µl of medium with cells. After shaking program of two minutes duration, the luminescence was recorded directly using the luminometer. The principle behind the Cell titer glo kit is that it is using the amount of ATP produced in living cells but not emitted by dead ones. The output from the luminometer is then directly proportional to the amount of living cells.

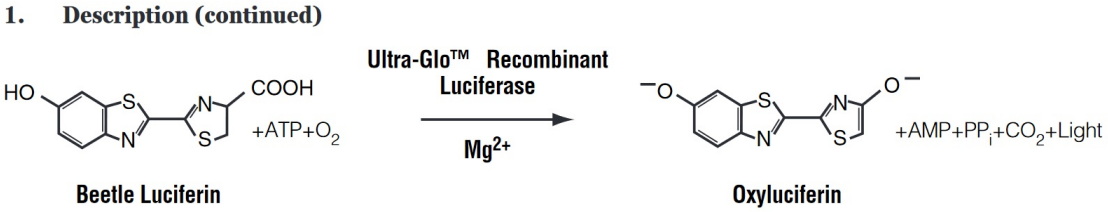

Figure 3. The luciferase reaction. Mono-oxygenation of luciferin is catalyzed by luciferase in the presence of Mg^{2+}, ATP and molecular oxygen.

Figure 2.1: Linear registration of RLU, figure from [108]

The buffer contains the luciferase in a stable form, that oxygenates luciferin with ATP in a reaction in the cells to AMP and oxyluciferin and subsequently emits luminescence. This can then be measured using the luminometer.

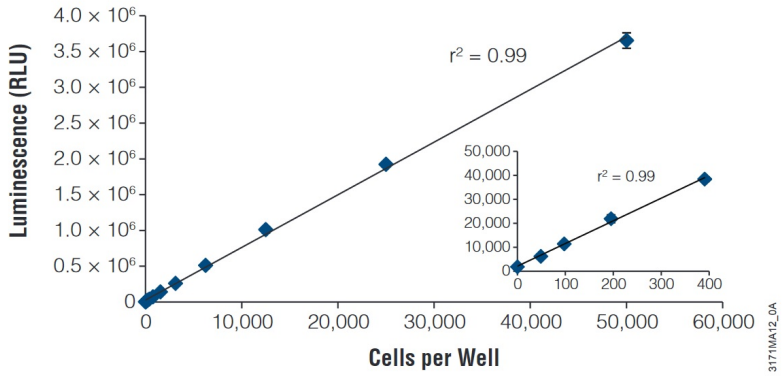

Figure 2. Cell number correlates with luminescent output. A direct relationship exists between luminescence measured with the CellTiter-Glo® Assay and the number of cells in culture over three orders of magnitude. Serial twofold dilutions of HEK293 cells were made in a 96-well plate in DMEM with 10% FBS, and assays were performed as described in Section 3.B. Luminescence was recorded 10 minutes after reagent addition using a GloMax®-Multi+ Detection System. Values represent the mean ± S.D. of four replicates for each cell number. The luminescent signal from 50 HEK293 cells is greater than three times the background signal from serum-supplemented medium without cells. There is a linear relationship ($r^2 = 0.99$) between the luminescent signal and the number of cells from 0 to 50,000 cells per well.

Figure 2.2: Luciferase reaction, figure from [108]

The Cell titer glo kit was used in all further gap closure experiments: Using the same time points of the wound healing assay, six plates of seeded and irradiated cells each were used for the cell viability and apoptosis assays. Five biological replicates with each three technical replicates were performed at each time point. For cell lines MCF-7 and SKBr3, I took off each replicates containing the required 100 µl of medium with cells that were dissolved from the bottom of the plate after irradiation with 0, 2, 4, 8 Gy. The buffer was added to the 100 µl of

cells with medium. After incubation in an opaque special 96 well plate with a white bottom, it was transferred into the luminometer for measuring. The program consists of 2 min of shaking, then registration of the luminescence. The output was further analyzed using Excel sheets. Several wells were used as control group containing medium and the buffer-substrate mixture as a reference for background luminescence.

Reasons for choosing this assay were the fast performance (as all experiments had to be done within 2 hours), and the high output/input of samples and provide robust and sensitive data [108].

2.2.4 Apoptosis Experiments

Apoptosis was measured through use of the Caspase Glo 3/7 assay. This assay measures Caspase 3 and 7 activity through luminescence. The kit contains a substrate which is being metabolized by caspase 3 and 7. The target cells are being lysed, then the caspase cleaves the substrate, and emits a "glow type"-signal which is being detected by the luminometer [109]. The emitted signal is directly proportional to the caspase activity, hence here our marker for apoptosis.

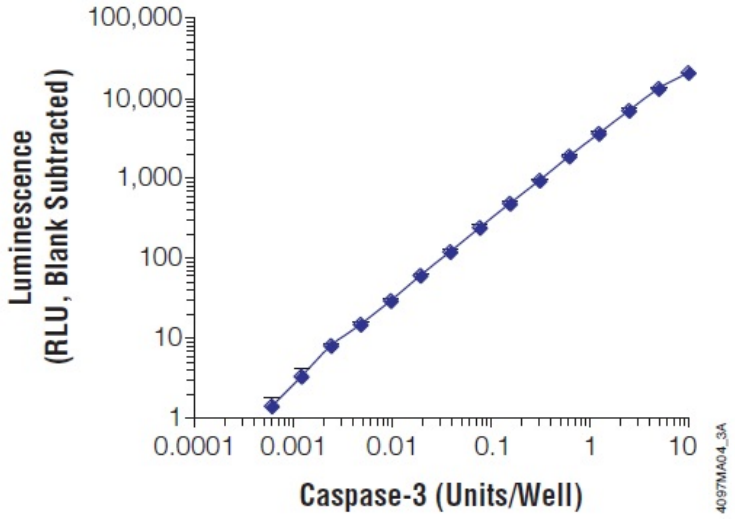

Figure 2.3: Luminescence is proportional to caspase-3 activity, figure from [109] "Purified caspase-3 was titrated and assayed in a total volume of 200μl per well in a 96-well plate. Luminometer readings were taken 1 hour after adding the Caspase-Glo®3/7 Reagent. The assay is linear over 4 orders of magnitude of caspase concentration ($R^2 = 0.998, slope = 0.989$)[1]. One unit caspase (0.07ng protein) is the amount of enzyme required to cleave 1pmol of substrate at(Ac-DEVD-pNA) hydrolyzed/minute at 30°CC per the manufacturer's unit definition[2]. Each point represents the average of 4 wells. Values are blank-substrated *(blank=no caspase)*. Notes:1) Due to the extended dynamic range of the Caspase-Glo 3/7 Assay, data were graphed on a log scale. For this reason, and because unit definitions may vary, your results may differ" [109].

For the performing of the assay, the buffer is mixed with the substrate to form the reagent. Then an equal volume of the reagent is added to the samples. The 96 well plate is then shaked and incubated. AIn the next step, the luminescence is recorded. In this case 100 µl of sample and the equal volume of reagent was used. For measuring the control group 100 µl of substrate was added to 100 µl of PBS. One of the used cell lines, MCF-7, naturally lacks expression of caspase 3. Further details will be discussed in the results chapter.

2.2.5 Gap closure assays

Five biological replicates with three technical replicates each were used for each trial. Cell culture inserts with 2 wells were firmly placed into 6 well plates. Cells were seeded at an exact number into each wellof the size of 0.22 cm². (Numbers for each cell line: T47 D: 51 000, MDA-MB 361:65 000, MCF-7: 27 000, SkBr3: 60 000) According to the trial medium containing 1 % FCS or 10 % FCS was used to produce a constant volume of 70 microliters in each well of the two-well-Ibidi version. After 24 h of cultivation in an incubator at a constant temperature

of 37 °C and 5 % of CO^2, the plates were irradiated at a cesium source with dosis of 0 G y, 2 Gy, 4 Gy and 8 Gy. The cell culture medium was carefully removed without damaging the cell layer. Two triangular shaped marks were printed into the surface of each well of the 6 well plate serving as a positioning help for further photo documentation. This was done with a syringe tip. Pictures at the 0 h time-point- were taken using a fluorescent microscope using the triangular shaped marks as a recognition helper. As the cells were GFP-labelled, phase contrast and fluorescent pictures were recorded. At each time point specific for each cell line, the plates were taken out of the incubator and pictures were taken. (0 h, 16 h, 18 h, 24 h, 48 h).

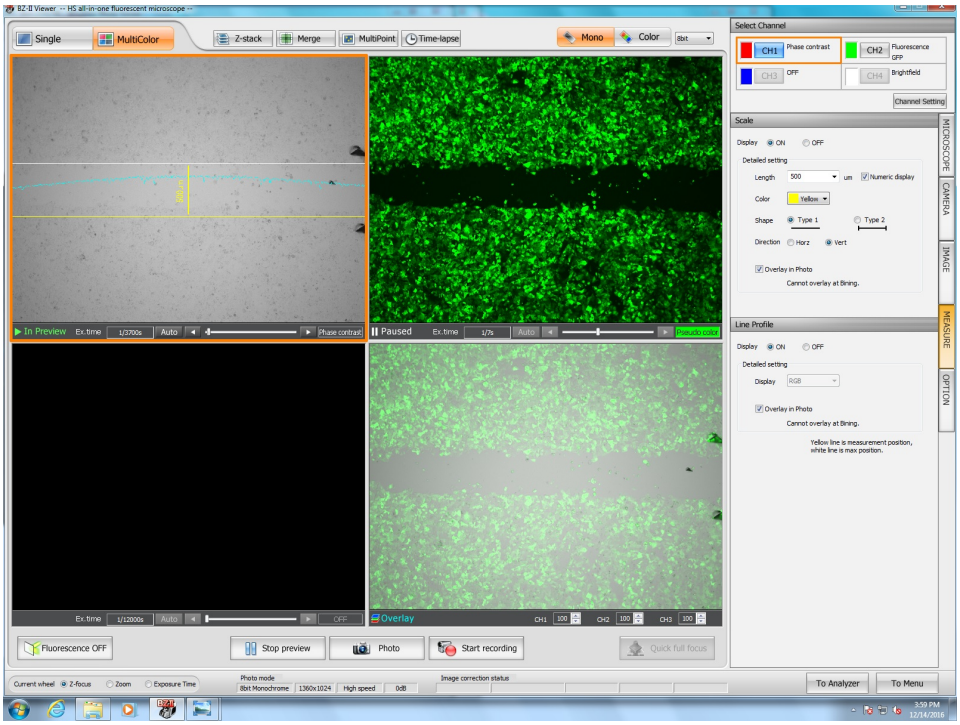

Figure 2.4: Fluorescence microscopy: MCF-7 cells showed complete confluency after 16 hours of observation

This slide shows the general overview displayed on the fluorescence microscope. Top left is the phase contrast, top right shows the fluorescence display, bottom right is a overlay. A fourth channel (bottom left) is not in use. Adjustments to channel settings can be made on the panel on the right hand side. Photographs taken, are then output in tif format.

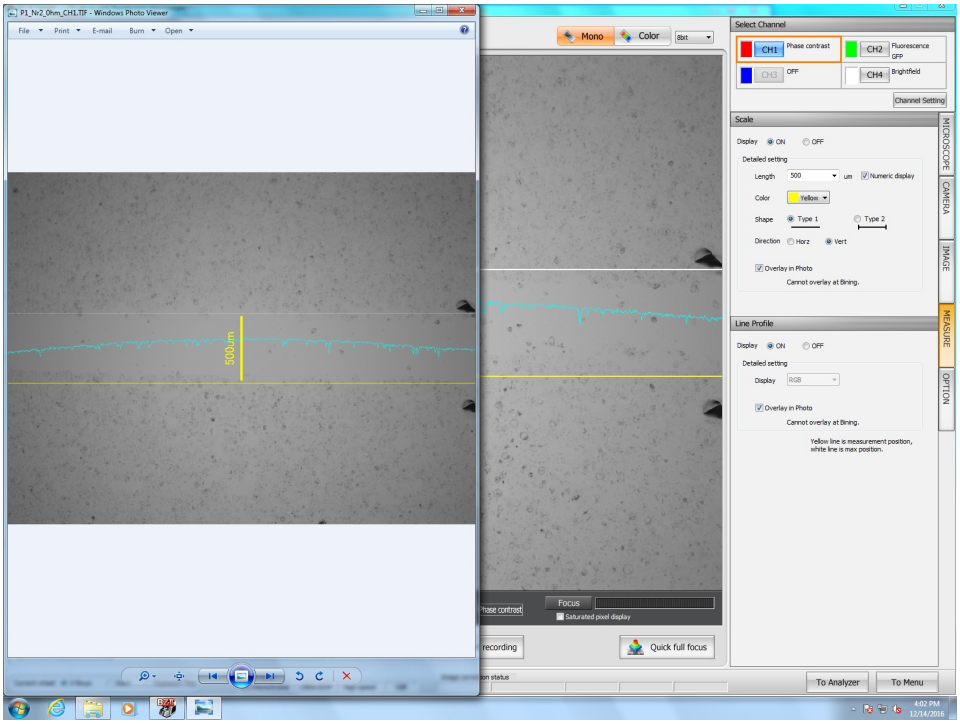

Figure 2.5: MCF-7 cells show complete confluency after 16 hours of observation
This slide shows the 0 Gy subgroup of MCF-7 cells at the initial removal of the silicone insert (left) and at 16 hours after removal (right). Triangular shaped black spots on the right margin of each phase-contrast photo is a marker set using a cannula tip. The yellow baseline simplifies horizontal positioning of each probe.

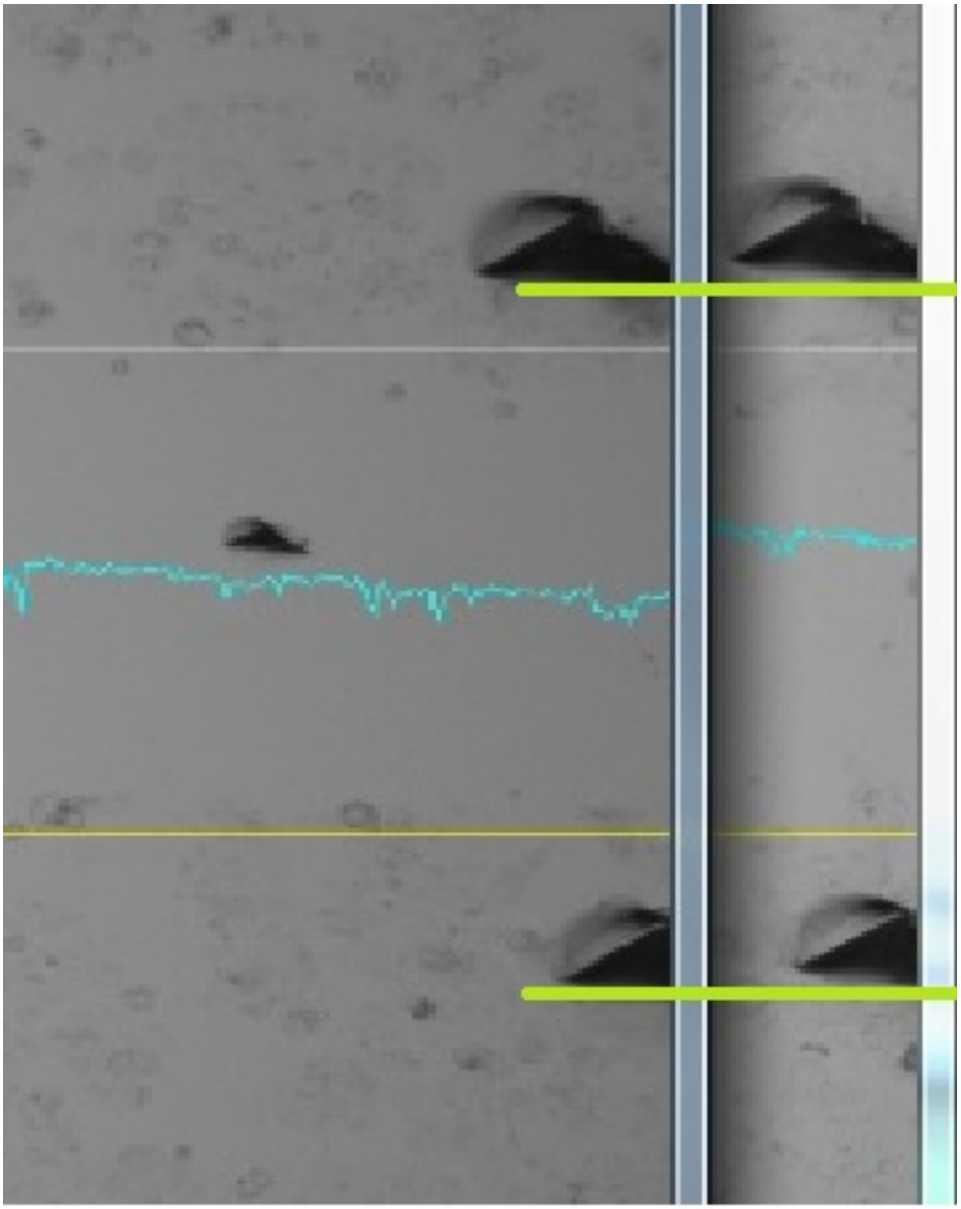

Figure 2.6: Phase contrast microscopy: Positioning needs improvement
This slide shows an enlarged section of the previous images. The added auxiliary green lines help in perceiving the difference in height. The gap has a defined width of 500 µm, the measurement showed that there is a 20 µm deviation to be corrected. Depicted is a sample of MCF-7 cells, the pictures are compared to the initial photo, taken at the 0 hours time point and then adjusted.

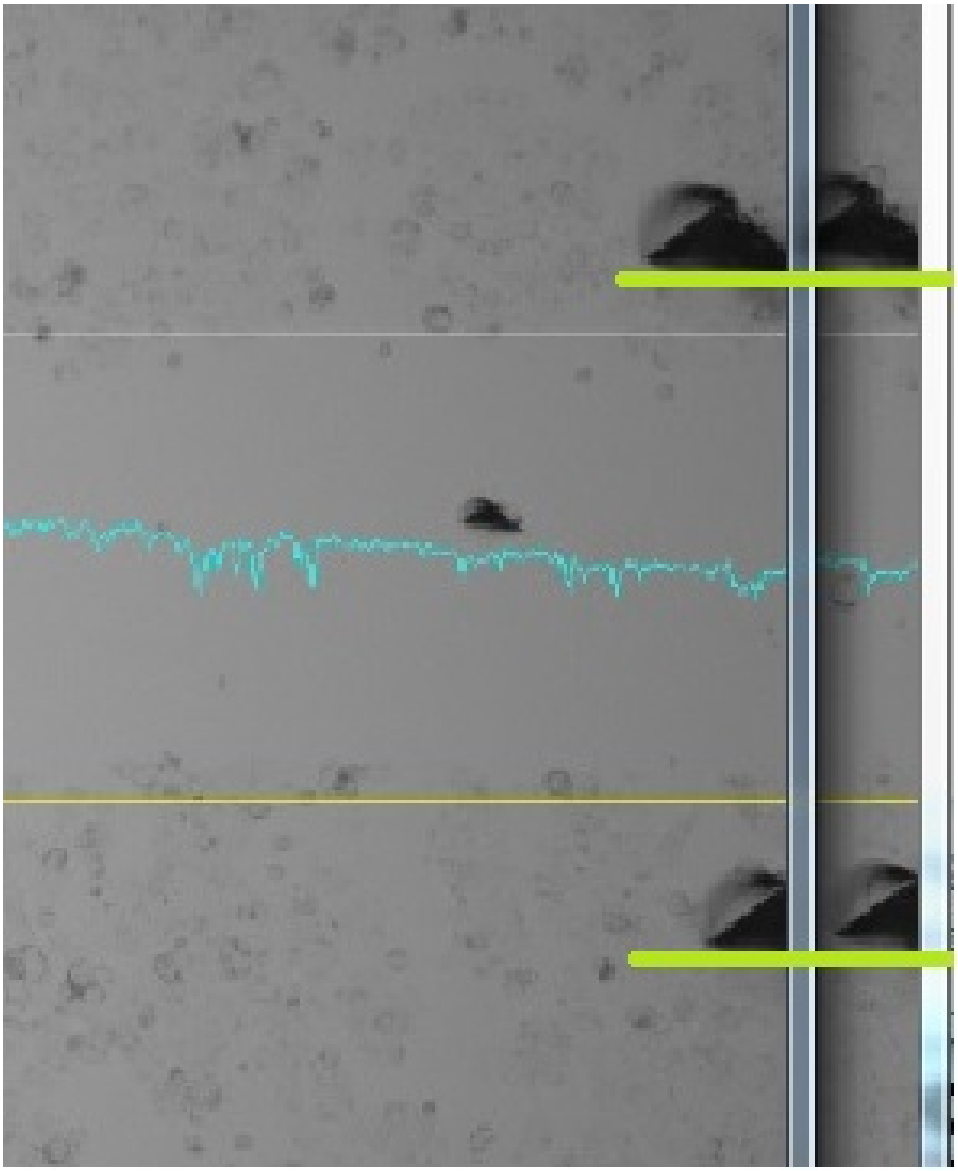

Figure 2.7: Phase contrast microscopy: Positioning improved
This slide shows an enlarged section of the previous images. The added auxiliary green lines help in perceiving the difference in height. The gap has a defined width of 500 µm. The measurement after adjustment of the sample (on the right side) showed, that there remains an estimated 10 µm deviation, that is acceptable. Depicted is a sample of MCF-7 cells, the pictures are compared to the initial photo, taken at the 0 hours time point (depicted left) and then adjusted (on the right).

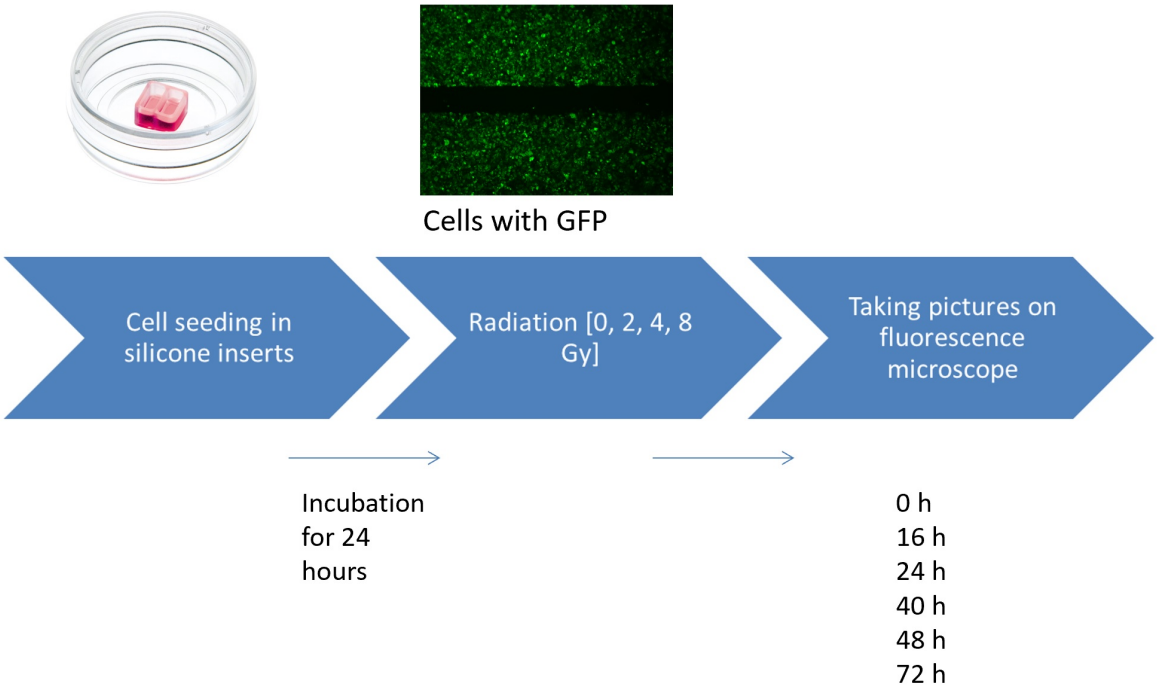

Figure 2.8: Flowchart of the gap closure assay

In the migratory experiments with MCF-7, 27 000 cells were used per well (0.22 cm², equals to 123 000 cells per 1 cm²) to grow to confluency within 24 hours. After the outtaking of the silicone grid insert, the measured time points included 0 hours (directly after irradiation and at starting point of the migratory experiment),16 hours, 24 hours and 48 hours. Four biological replicates with each five technical replicates were performed with full FCS (10%) and scarce FCS medium. (Due to heterogeneity of the data, a fourth biological replicate was created). At each time point I calculated the mean, the standard deviation and performed a t-test. The rough data of green pixels in the 500 µm gap formed by the grids was used in the following way: at each time point, the 0 Gy value was used as 100% migration and was then compared to the values within the 2 Gy, 4 Gy and 8 Gy subgroups.

In the migratory experiments with the SkBr3 cell line, 60 000 cells were used per well (0.22 cm², equals 273 000 cells per 1 cm) in order to grow to confluency within 24 hours after seeding. As the SkBr3 cells are particularly small in size (< 5 µm), they could not be counted with the Coulter Cell counter but had to be counted visually using a glass chamber. In order to maintain exactness multiple rounds of countings were performed. Measuring time points were 0 hours, 24 hours, 48 hours, and 72 hours after irradiation/treatment and removal of the silicone insert. Later in the experimtent, those were reset to 0 hours, 16 hours and 24 hours, as confluency was reached earlier with the smaller silicone inserts. Three biological replicates with each five technical replicates were performed both with full FCS-medium (containing 10% FCS) and scarce medium (containing 1% FCS).

2.2.6 Scratch migration assay

For selecting the method used for gap-closure assay, scratch migration assay was used on the cell lines T47 D and MDA-MB 361. Different pipette tips were used for the creation of a gap in a confluency. Several tips didn't produce sufficiently even borders of the gap and also the width of the gap was not constant enough.

2.2.7 Analysis of data

Analysis of data was performed on fluorescence microscope pictures, by editing them using Adobe Photoshop and the software of Marcus Vetter to count the number of pixels higher than the preset threshold. The raw data was then for each time point and picture a number repesenting the number of pixels. The background pixels already available at the 0 h timepoint were then subtracted from the number of pixels at each later time point (i.e. 24 h, 48 h, 72 h). The mean was calculated from the 5 technical replicates of each subgroup and time point in the experiment. the standard deviation was also calculated within those three to four biological replicates of each experiment. For the migration experiment a one sided t-test was performed between the treatment subgroups and the control group. The mean values for the experiments were calculated using Excel, as well as the standard error of the mean (SEM), which was added to the graphics. For the migratory experiments, the significance was evaluated by a Student's t test (Excel), here a value of ≤ 0.05 was considered as statistically significant.

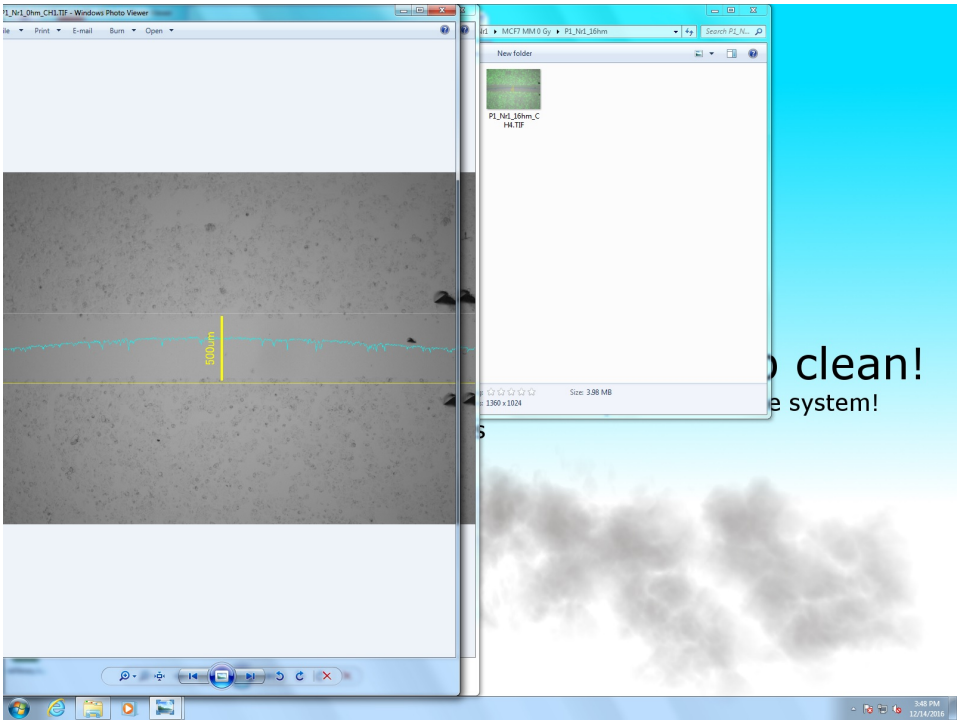

Figure 2.9: Phase contrast microscopy: Positioning adjustment with markers
This slide shows the exemplary positioning of the samples. Displayed are two tif-format photos of MCF-7 cells in the 0 Gy subgroup at the initial removal of the silicone insert (left) and at 16 hours after removal (right). Triangular shaped black spots on the right margin of each phase-contrast photo is a marker set using a cannula tip. The yellow horizontal baseline simplifies horizontal positioning of each probe. Here the positioning is not optimal and requires re-adjustment, so that the exact same sector will be displayed in each photograph taken. The gap between the two confluent layers of cells has a defined width of 500 µm (yellow vertical line in centre).

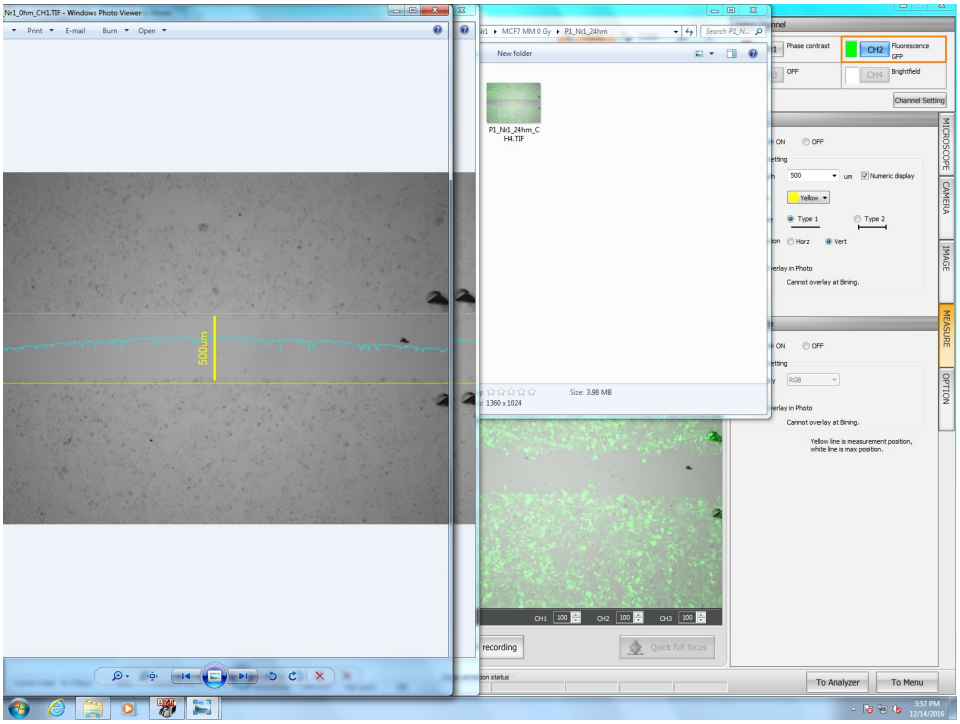

Figure 2.10: Phase contrast microscopy: Positioning well adjusted
This slide shows a good example of exactness in choosing the same sector at each time point for the photographic images on the left half of the figure. The angle and height of the cannula tip markers are approximately the same in the left and right photography. Depicted is a sample of MCF-7 cells, the pictures are compared to the initial photo, taken at the 0 hours time point and then adjusted.

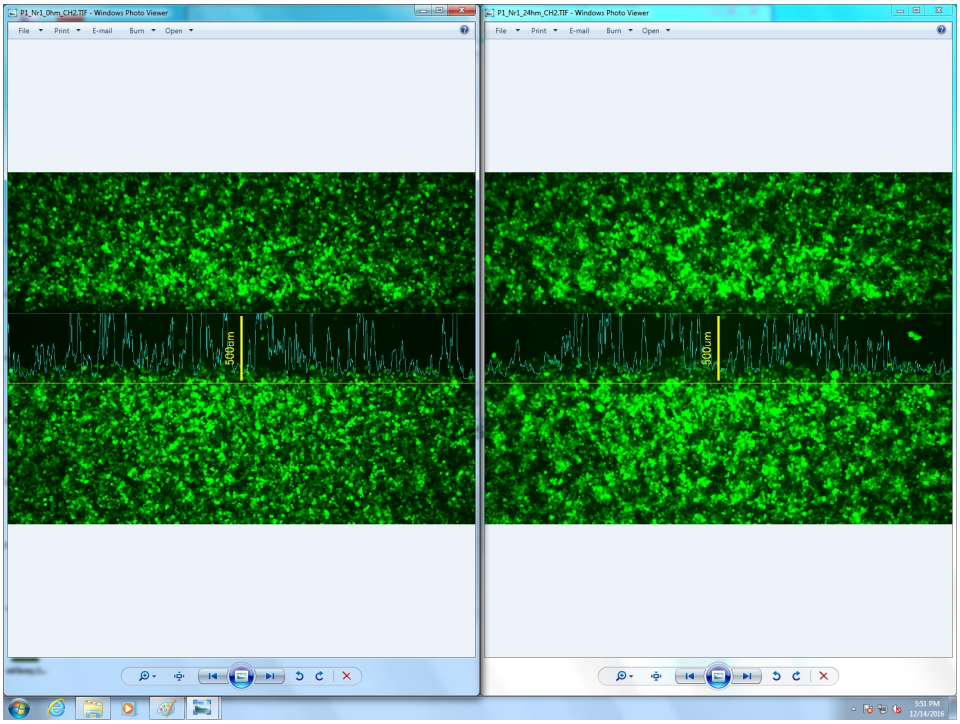

Figure 2.11: Fluorescence microscopy: Evaluation of green pixel values
This slide shows a comparison of the green values of samples of MCF-7 cells in between time values. Adjustment in the fluorescence channel of the microscope is important, as the measurements later depend on green pixel values. The fluorescence channel is then equalized to the samples within the experiment (irradiation doses but also time points), as too light or dark depiction of it could influence the later counted amount of green pixels.

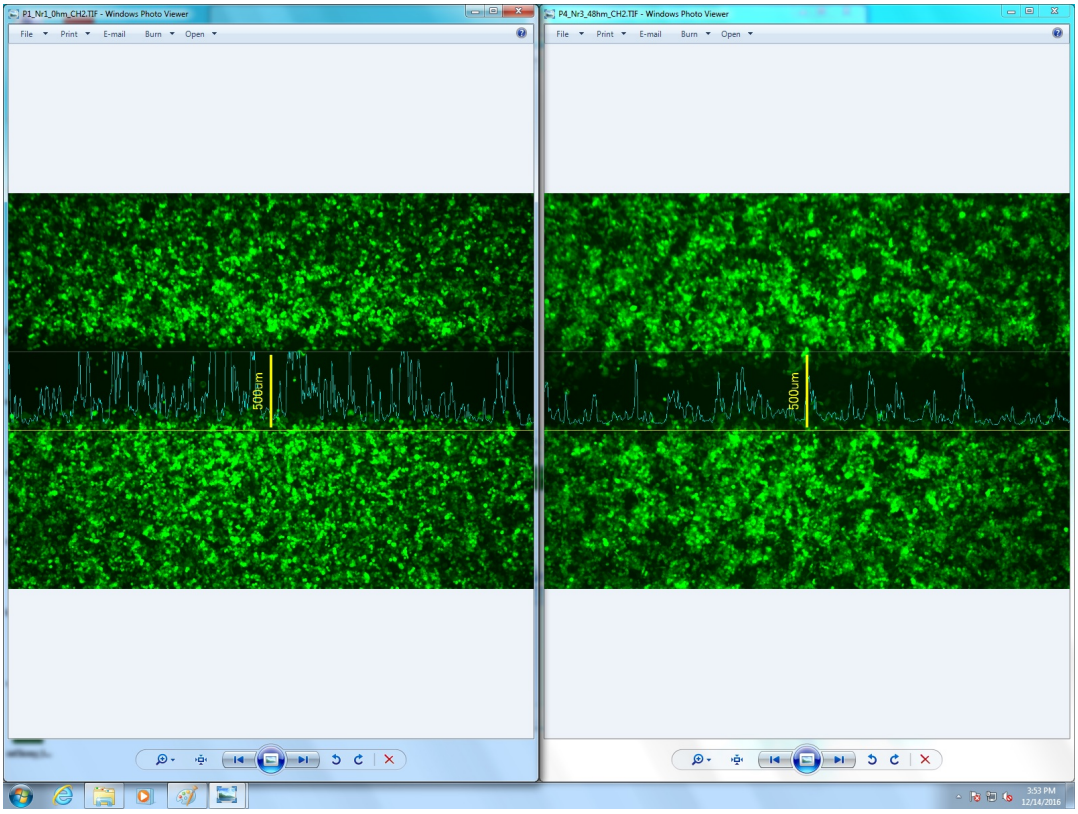

Figure 2.12: Comparison between different irradiation subgroups with MCF-7
MCF-7 cells showed completed confluence and rapid migration into the gap after a 16 h observation period. 27 000 cells were seeded out into each well. After taking out the grid of the silicone insert after 24 hours of incubation photos were taken at the 0 h, 16 h, 24 h and 48 h time point. This slide shows a comparison between different irradiation subgroups, here 0 Gy and 8 Gy, respectively.

3 Results

3.1 Migration experiments

3.1.1 MCF-7 cell line

In the scarce medium branch of the MCF-7 migratory experiment, the value of 0 Gy was set to 1, the 2 Gy group had a value of 1.045 , the 4 Gy group had a value of 1.466, and the 8 Gy group had a value of 1.408 compared to the 0 Gy branch. So at this time point of 16 hours, migration was greater in the 4 and 8 Gy subgroup. The 16 hours time point was chosen because the complete gap was closed at this time point. The following table illustrates this more clearly. It displays that the standard deviation is lowest in the 2 Gy group and highest in the 8 Gy subgroup, with the 4 Gy group ranging in between. In a t-test no values in this particular subtest proved to be statistically significant.

Table 3.1: MCF-7 1% FCS migratory data

Dose	Relative migration	Standard deviation	t-test
0 Gy	1	0	-
2 Gy	1.045	0.125	0.564
4 Gy	1.466	0.497	0.180
8 Gy	1.408	0.866	0.460

The following graph (figure 3.1) displays the migratory behavior in the MCF-7 scarce medium subgroup after 16 hours of observation. It displays the higher rate of migration in the 4 Gy and 8 Gy subgroups, where as the 2 Gy subgroup migrates almost as little as the control group.

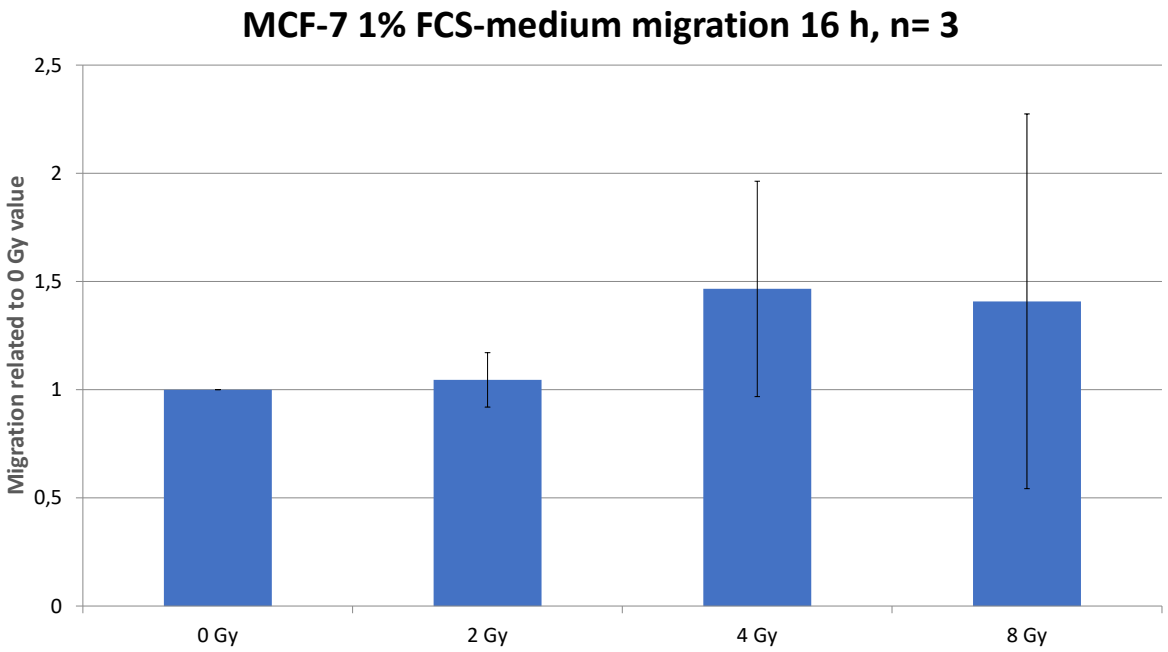

Figure 3.1: Migration MCF-7 cells 1% FCS
Description: MCF-7 cells with scarce medium containing 1% FCS observed for 16 hours: migrational behavior is shown in the 4 Gy and 8 Gy subgroup compared to the sham irradiation subgroup. The 0 Gy subgroup is used as a reference and set to a defined value of 1.

For MCF-7 with complete FCS-medium, the time point of analysis was as well 16 hours after irradiation. Here the following values were measured (analysis with 0 Gy set as 1 and the other energy doses were then compared to this value): 0 Gy: 1; 2 Gy: 1.203; 4 Gy: 1.025; 8 Gy: 1.150.

The following table illustrates these numbers, additionally to the standard deviation and a t-test. The standard deviation is particularly low in the 4 Gy subgroup. It is quite similar in the 2 Gy and 8 Gy subgroup. A t-test revealed no significant results in those differences of migratory behavior after irradiation.

Table 3.2: MCF-7 10% FCS migratory data

Dose	Relative migration	Standard deviation	t-test
0 Gy	1	0	-
2 Gy	1.203	0.410	0.586
4 Gy	1.025	0.050	0.315
8 Gy	1.150	0.309	0.556

The following figure (figure 3.2) shows the four subgroups while examining migratory

behavior after irradiation. The differences in migratory behavior compared to the 0 Gy control group remain small, yet larger in the 2 Gy and 8 Gy subgroups.

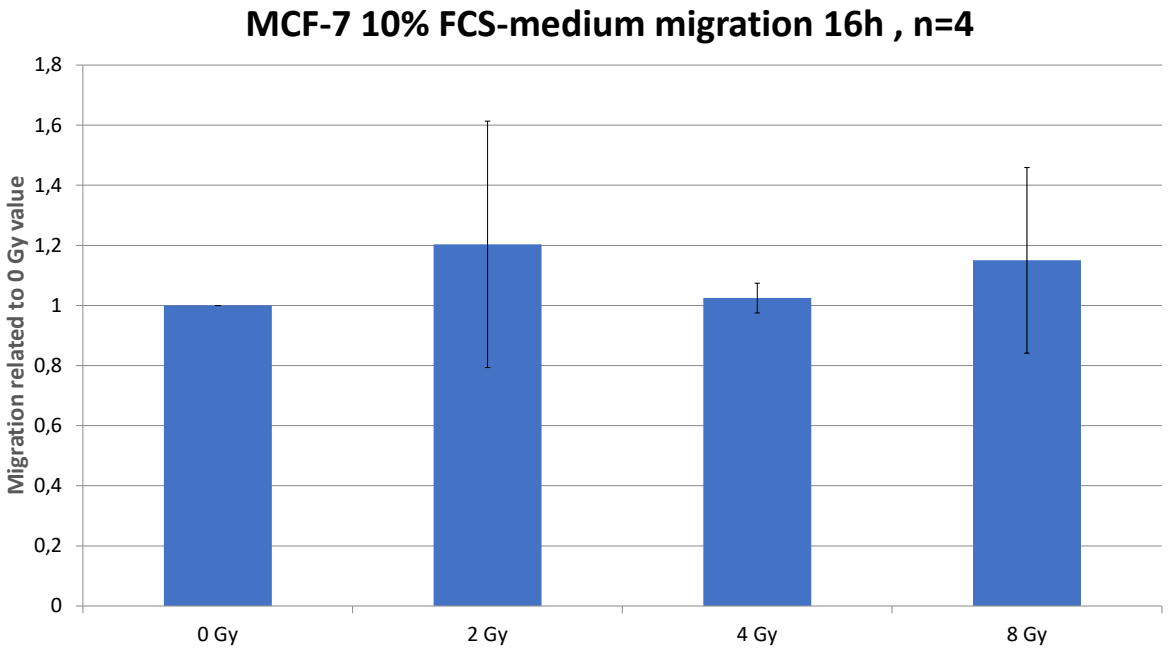

Figure 3.2: Migration MCF-7 cells 10% FCS
Description: MCF-7 cells irradiated and observed for 16 hours while being cultivated with 10% FCS showed increased migratory behavior in the 2 Gy and 8 Gy subgroup. The sham irradiation subgroup is used as a reference and set to a defined value of 1.

A comparison of the scarce and full medium groups puts them here side by side- on the left side of the figure, depicted in blue is the scarce medium group (figure 3.3). Its migratory behavior is more impressive than the compared full medium group in green columns on the right hand side of the diagram. I refer to the discussion chapter for a more detailed review of this graph.

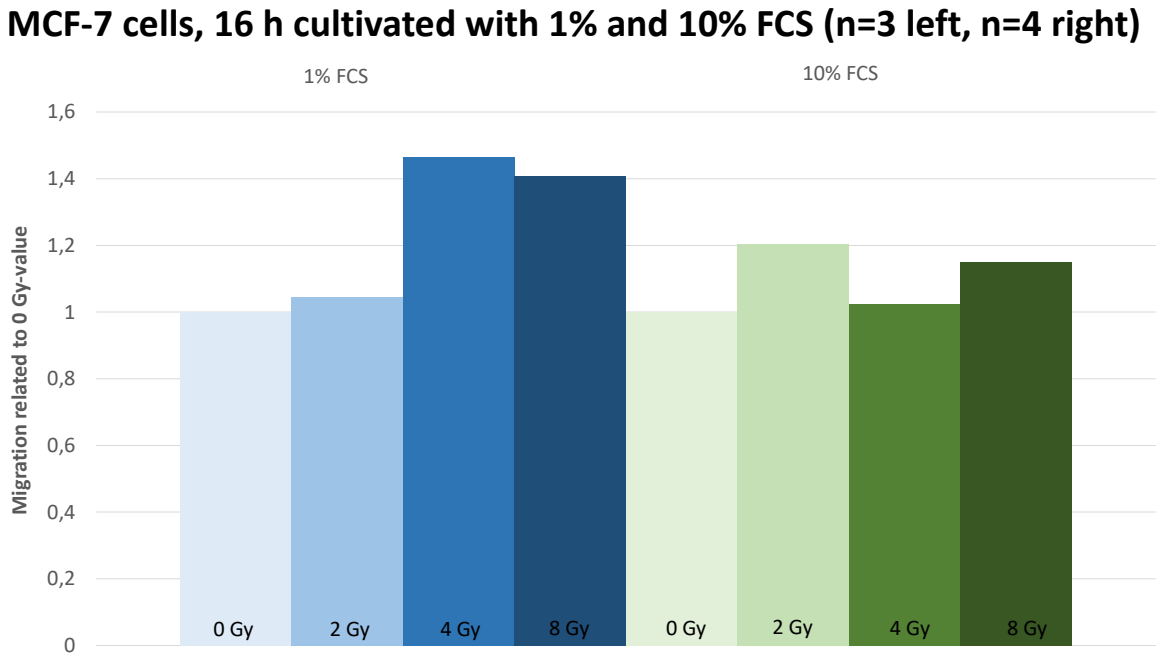

Figure 3.3: Migration comparison of MCF-7 cells
Description: Comparison of MCF-7 cells cultivated with full (10% FCS) and scarce (1% FCS)-medium. The graph shows the 16 hours time point. In scarce medium, the 4 and 8 Gy subgroup showed increased migration in reference to the 0 Gy reference group. In the full medium group, 2 Gy and 8 Gy have an increased migratory behavior compared to the sham irradiation.

As a display of the raw data, this slide (figure 3.4) shows the migratory development during the 48 hours observation period in MCF-7 cells under the fluorescence microscope. It depicts the full closure of the gap as visual to the eye in 48 hours time point in this slide.

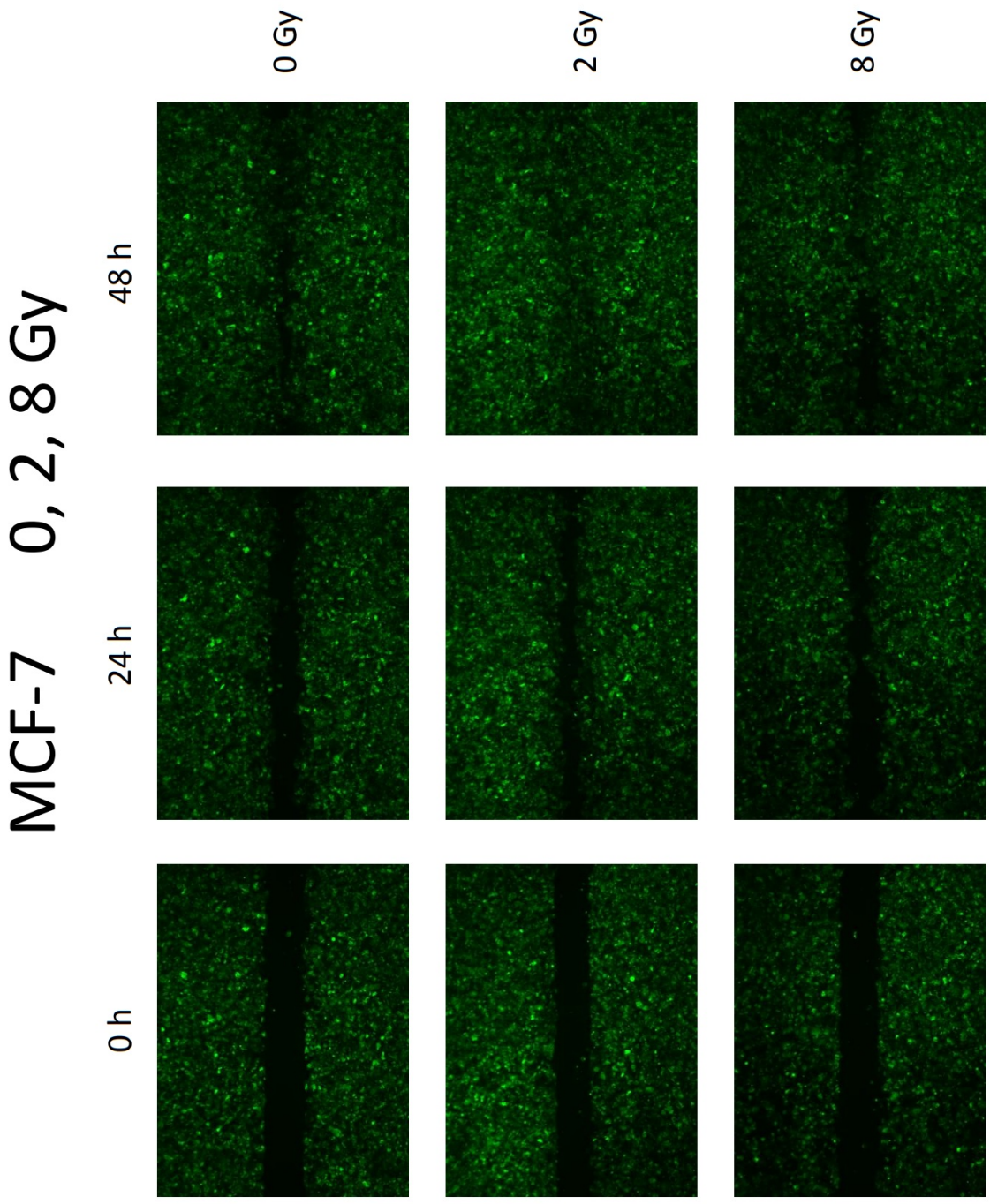

Figure 3.4: Migration of MCF-7 cells at 16 hours
Description: MCF-7 cells overview in the different subgroups at the 16 hours time point.

3.1.2 SkBr3 cell line

For each time point I calculated the mean, standard deviation and did a t-test. As in the previously described experiments with MCF-7 cells, for each time point the 0 Gy control group was set as 100% of migration. Each other value of the treatment groups was compared in reference to this value.

In the 1% scarce medium group, the results were as follows: the 24 hours results were chosen, as they were the closest to the endpoint of the experiment. Migration in the control group (0 Gy) was set to 1, the 2 Gy group showed lesser migration with a value of 0.86 in mean values. The 4 Gy group showed a value of 1.1 with slightly more migration than in the control group. The 8 Gy group showed 1.16 as a slightly higher migration than in the control group. The standard deviation of each group was 0, 0.11 , 0.13 , and 0.18 respectively. A one sided t-test showed no significance for these values (0.095 , 0.266 , 0.213). The following table and figure 3.5 displays the values.

Table 3.3: SkBr3 1% FCS migratory data

Dose	Relative migration	Standard deviation	t-test
0 Gy	1	0	-
2 Gy	0.86	0.11	0.095
4 Gy	1.1	0.13	0.266
8 Gy	1.16	0.18	0.213

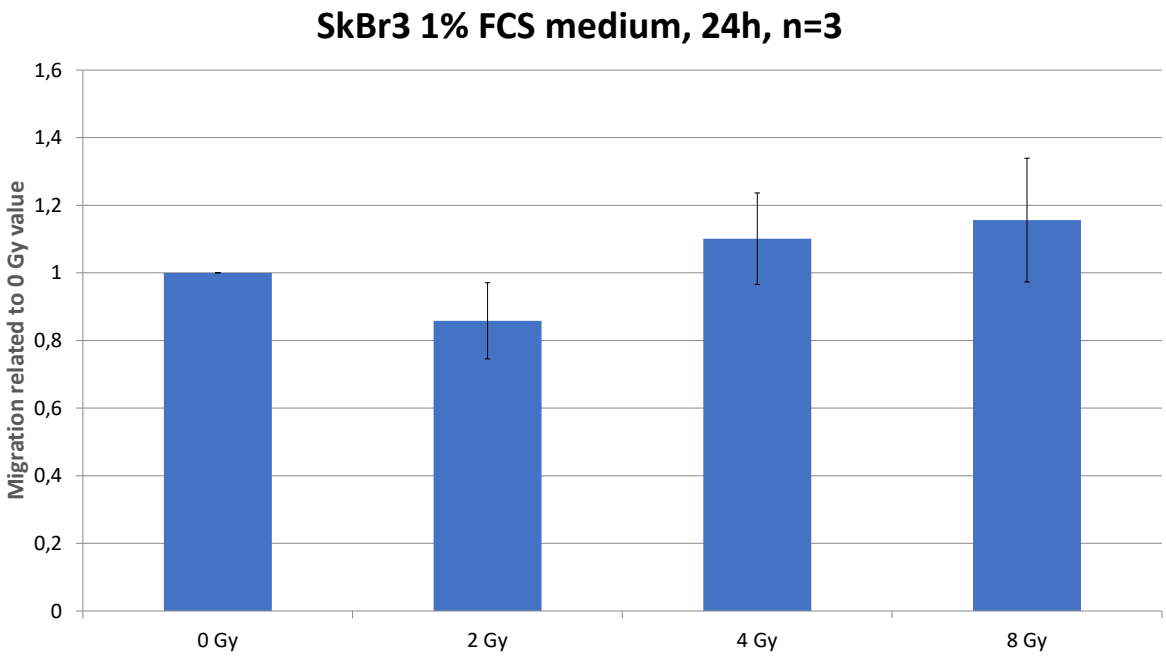

Figure 3.5: Migration of SKBr3 cells after 24 hours, 1% FCS
Description: SkBr3 cells cultivated with 1% FCS showed good confluency and migration into the gap after a 24 h observation period.

For the full medium subgroup, the following results were obtained: With migration in the control group set to 1, the 2 Gy group had a migration of 1.14 being slightly higher than the control group. In the 4 Gy group migration reached 1.24 and in the 8 Gy group it reached 1.23 being both higher values than within the control group. The standard deviation in these groups was 0.11 for the 2 Gy group, 0.13 for the 4 Gy group, and 0.17 for the 8 Gy group. A one sided t-test showed the following values: comparing the 2 Gy group with the sham irradiation the value was 0.084 and was not significant for this group. The value for the 4 Gy subgroup was 0.031 and therefore reached below our border for significance of 0.05. The 8 Gy subgroup showed a value of 0.027 and was also below the defined value, being significant here. So it was shown here that the 4 Gy and 8 Gy subgroup of the full medium SkBr3 cells showed more migration than the control group.

Table 3.4: SkBr3 10% FCS migratory data

Dose	Relative migration	Standard deviation	t-test
0 Gy	1	0	-
2 Gy	1.14	0.11	0.084
4 Gy	1.24	0.13	0.031
8 Gy	1.23	0.17	0.027

The following graph (figure 3.6) displays the SkBr3 cells cultivated with 10% FCS. After taking out the grid of the silicone insert after 24 hours of incubation photos were taken. In this case doses of 0, 2, 4 and 8 Gy irradiation were applied, shown from left to right on the x-axis. Migratory behavior is highest in the 4 and 8 Gy subgroup. This proved to be significant in a one sided t-test compared to the 0 Gy subgroup ($p < 0.05$).

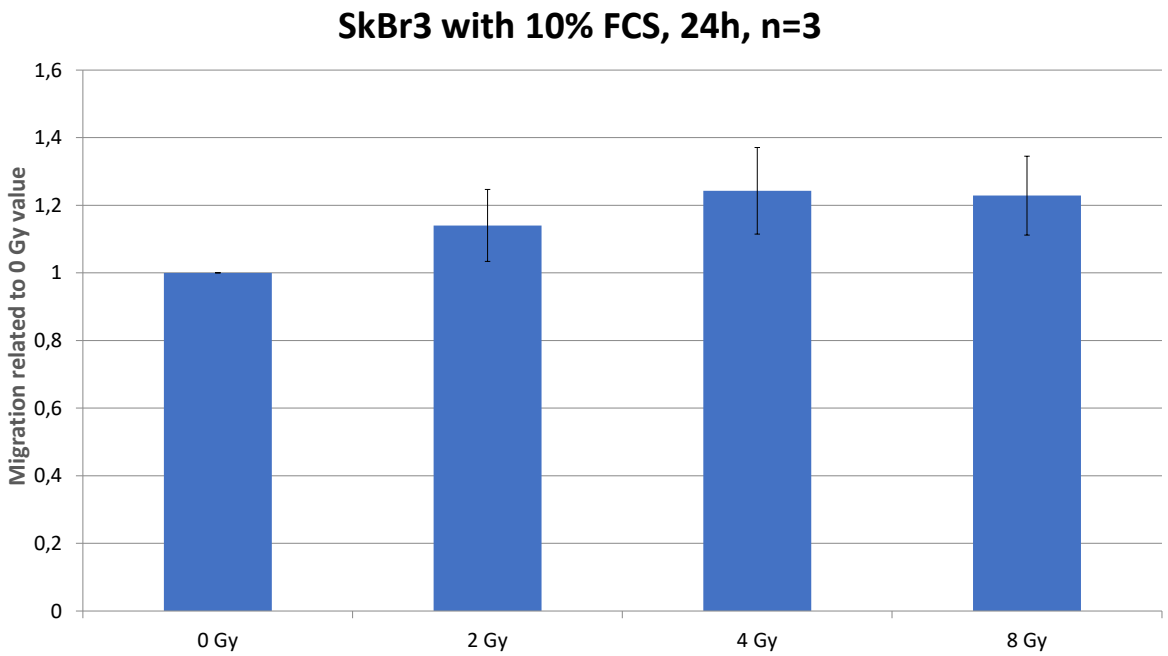

Figure 3.6: Migration of SkBr3 cells after 24 hours, 10% FCS
Discussion: SkBr3 cells cultivated with 10% FCS showed good confluency and migration into the gap after a 24 h observation period. The energy doses are lined up on the x-axis. The y-axis shows the migration related to the 0 Gy value. Migratory behavior is highest in the 4 and 8 Gy subgroup that proved to be significant in a one sided t-test compared to the 0 Gy subgroup defined as a value of 1. $p < 0{,}05$

.

A comparison of the scarce and full medium groups puts them here side by side (figure 3.7). On the left side of the figure, depicted in blue is the scarce medium group. Its migratory behavior is enhanced in the 4 Gy and 8 Gy subgroup in both arms of the experiment. The 2 Gy subgroup performs poorly in the scarce medium group (in blue). I may refer to the discussion chapter for a more detailed review of this graph.

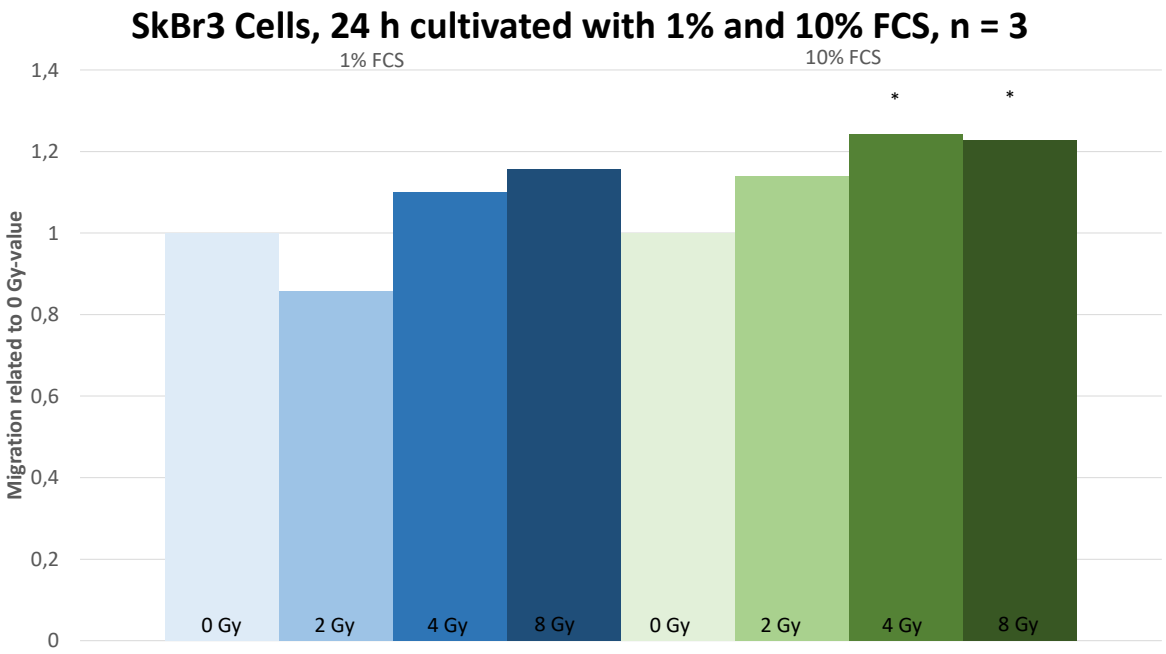

Figure 3.7: Migration of SkBr3 cells cultivated with 1% FCS and 10% FCS after a 24 hours. Description: Migration of SkBr3 cells cultivated with 1% FCS and 10% FCS in comparison after a 24 h observation period. The energy doses are lined up on the x-axis. The y-axis shows the migration related to the 0 Gy value. Migratory behavior is highest in the 4 and 8 Gy subgroup that proved to be significant in a one sided t-test compared to the 0 Gy subgroup defined as a value of 1. $p < 0.05$. The 1% FCS group migrated less than the group of cells receiving full medium. Highest migratory behavior can be seen here at the 4 Gy and 8 Gy subgroup, however without statistical significance.

3.1.3 Cell lines T47D, MDA-MB 361

Migration experiments were first started with four cell lines (T47D, MDA-MB 361, MCF7 and SkBr3) in 2 well silicone inserts (Ibidi 2 well silicone inserts) with a 500 µm gap in between them. T47D cells showed good confluency in the experiments within the wells but did not migrate into the gap. Three biological replicates with five technical replicates were performed with T47 D cells. The following graph illustrates the lack of migration in the gaps.

Table 3.5: T47D and MDA-MB 361 migratory data

Dose	Relative migration	Standard deviation	t-test
0 Gy	1	0	-
2 Gy	approx. 1	-	-
4 Gy	approx. 1	-	-
8 Gy	approx. 1	-	-

The following overview shows T47D cells marked with GFP at different time points. The maximum observation period was here set to 48 hours. Even though the period was long, there was no migration visible into the gap after 24 hours. There is a small changement visible in the gap after 48 hours. This might also be due to proliferation at the borders of the gap. For further details see chapter 4 - discussion.

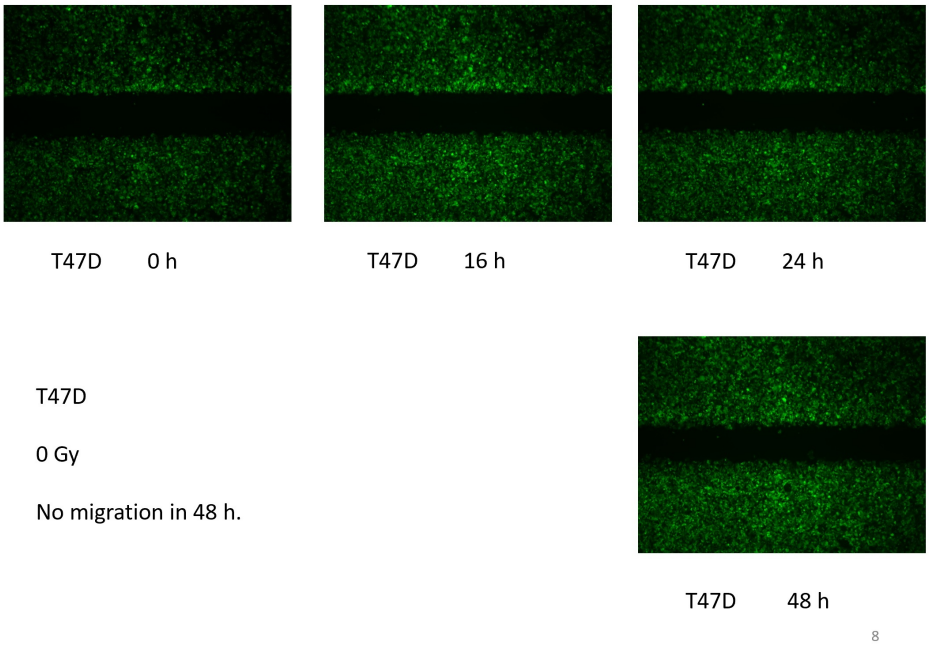

Figure 3.8: No migration in T47D cells
Description: T47D cells showed no migration into the gap after a 48 h time period of surveillance. 51 000 cells were seeded out into each well. After taking out the grid of the silicone insert after 24 hours of incubation photos were taken at the 0 h, 16 h, 24 h and 48 h time point. In this case no irradiation was applied.

The same migratory experiment was performed using MDA-MB 361 cells. The cells showed good confluency but equally lacked migration after 48 hours of observation.

Table 3.6: T47D and MDA-MB 361 migratory data

Dose	Relative migration	Standard deviation	t-test
0 Gy	1	0	-
2 Gy	approx. 1	-	-
4 Gy	approx. 1	-	-
8 Gy	approx. 1	-	-

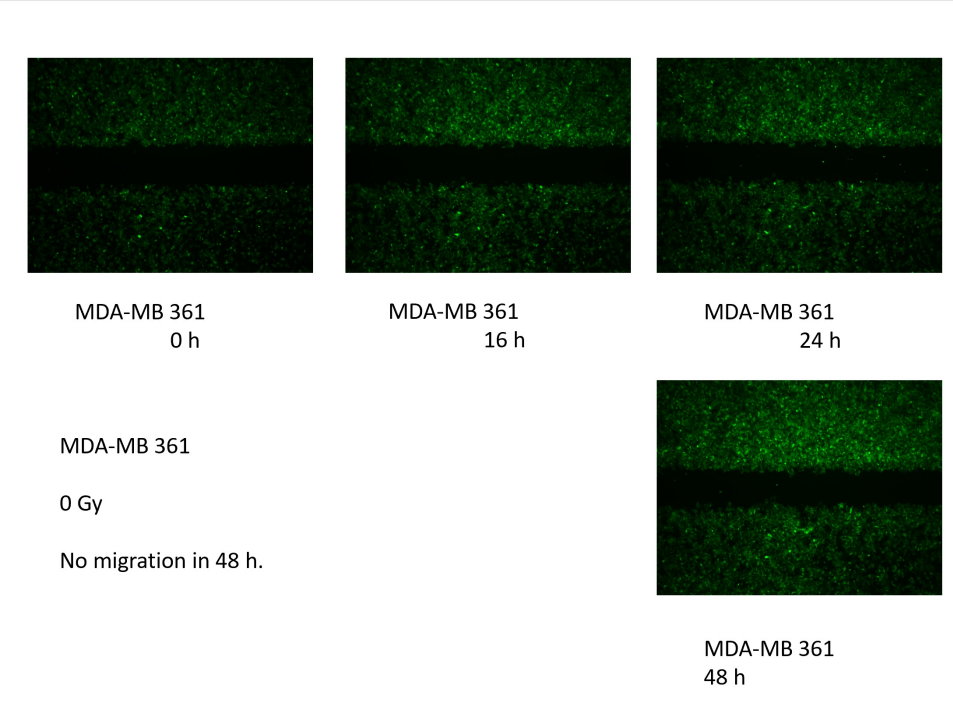

Figure 3.9: No migration in MDA-MB 361 cells
Description: MDA-MB 361 cells showed good confluency but no migration into the gap after a 48 h observation period. 65 000 cells were seeded out into each well. After taking out the grid of the silicone insert after 24 hours of incubation photos were taken at the 0 h, 16 h, 24 h and 48 h time point. In this case no irradiation was applied.

In order to put a migrating cell line exemplary next to a non migrating one, this slide shows on the upper side T47 D initally and after 48 hours. Below, MCF-7 is shown as a miratory cell line. Here, the gap is closed by cells. On the upper line, T47 D cells did not migrate into the gap.

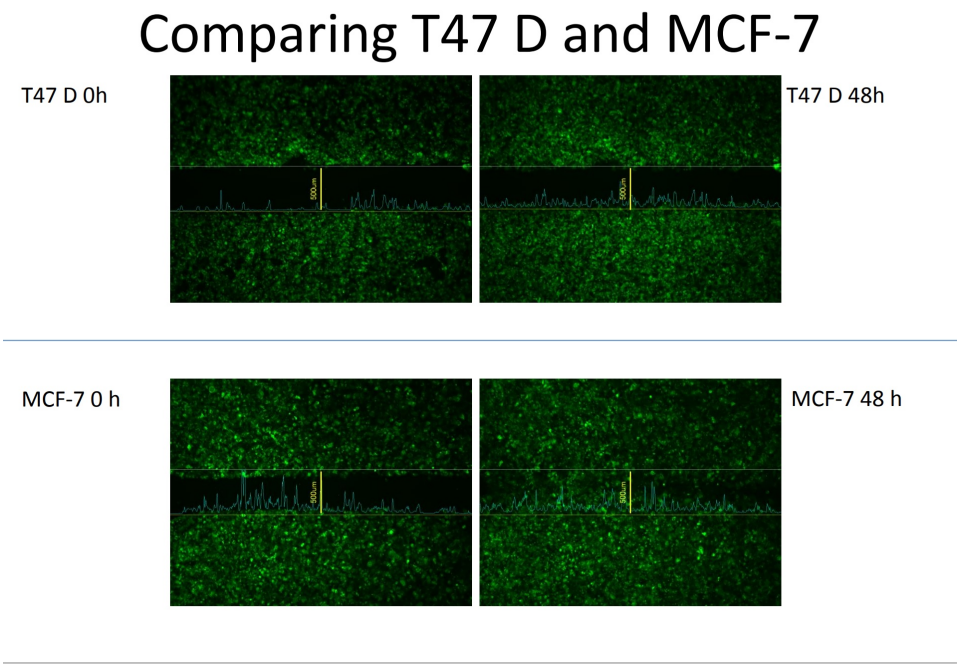

Figure 3.10: Comparison of T47D and MCF-7 migration
Description: T47D cells are shown in this slide sided by MCF-7 cells in order to show the difference in migratory behavior at different time points. In this case, no irradiation was applied. The upper part of the figure shows T47D cells under fluorescence microscope, first at the left side after taking out the grid, then on the right side after 48 hours of observation. No migration took place here. The lower part of the figure shows MCF-7 cells after 0 hours and 48 hours of observation. Here, the gap is closed by migrating cells.

3.2 Cell viability

3.2.1 MCF-7 cells and cell viability

Cell Viability in MCF-7 cells was measured with the Cell Titer Glo-R-kit, measuring metabolic activity of the examined cells and giving an output of luminescence in RLU- relative light units. Time points of measurement were chosen according to the specifities of gap closure paralleled to the main experiment at 24 and 48 hours after irradiation of cells. In figure 3.11, the x axis shows the four subgroups with the 0 Gy group serving as a reference (control group). At the 24 hours time point, the cell viability is lower in the 2 Gy and 4 Gy subgroups with 83% and 86% of viability compared to the control group. In the 8 Gy subgroup viability is slightly higher than in the control group, at a level of 107%.

Table 3.7: Cell viability data of MCF-7, 24 hours

Dose	RLU	Relative signal [%]	Standard deviation [%]	t-test
0 Gy	3194938	100	19	-
2 Gy	2653258	83	17	0.012 *
4 Gy	2774265	86	14	0.089
8 Gy	3415565	107	23	0.733

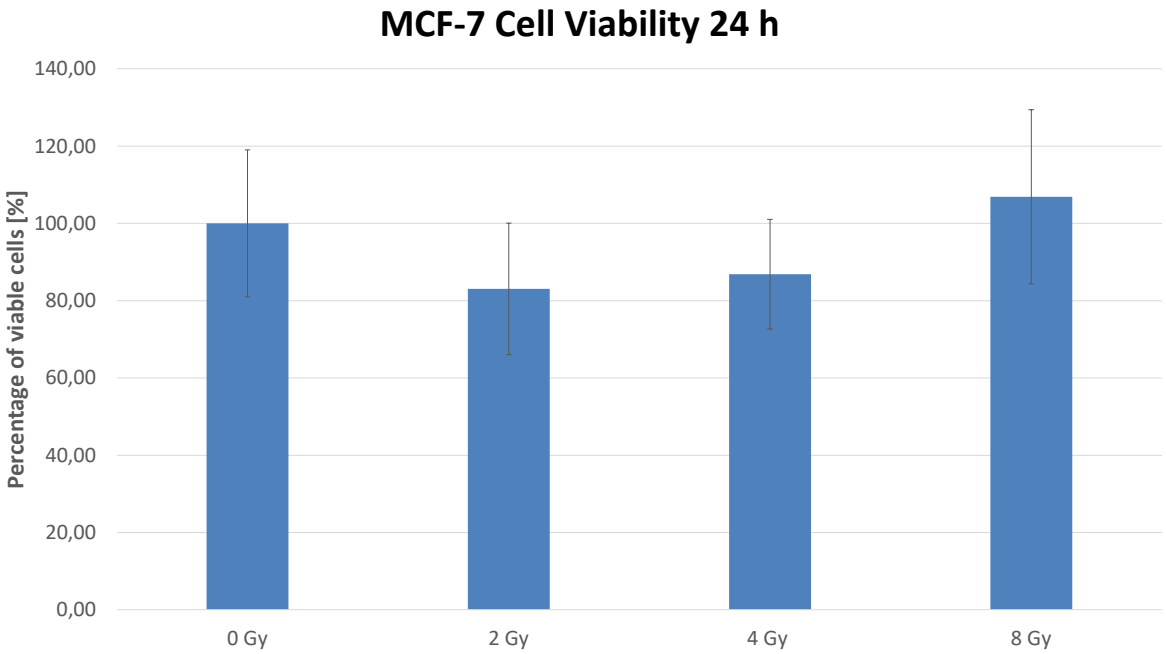

Figure 3.11: Cell viability of MCF-7 cells after 24 hours.
Description: The y-axis shows quantified luminescence in reference to the 0 Gy group set to 100% of cells irradiated with 0 Gy, 2 Gy, 4 Gy, 8 Gy on the x-axis at 24 hours after treatment. Data represent values $\pm$ SEM ($n = 4$) , * $p < 0.05$.

At the 48 hours time point viability stays unchanged of 100%, 94%, 91% respectively (figure 3.12).

Table 3.8: Cell viability data of MCF-7, 48 hours

Dose	RLU	Relative signal [%]	Standard deviation [%]	t-test
0 Gy	3825967	100	6	-
2 Gy	3841164	100	9	0.492
4 Gy	3629028	95	14	0.226
8 Gy	3486231	91	16	0.222

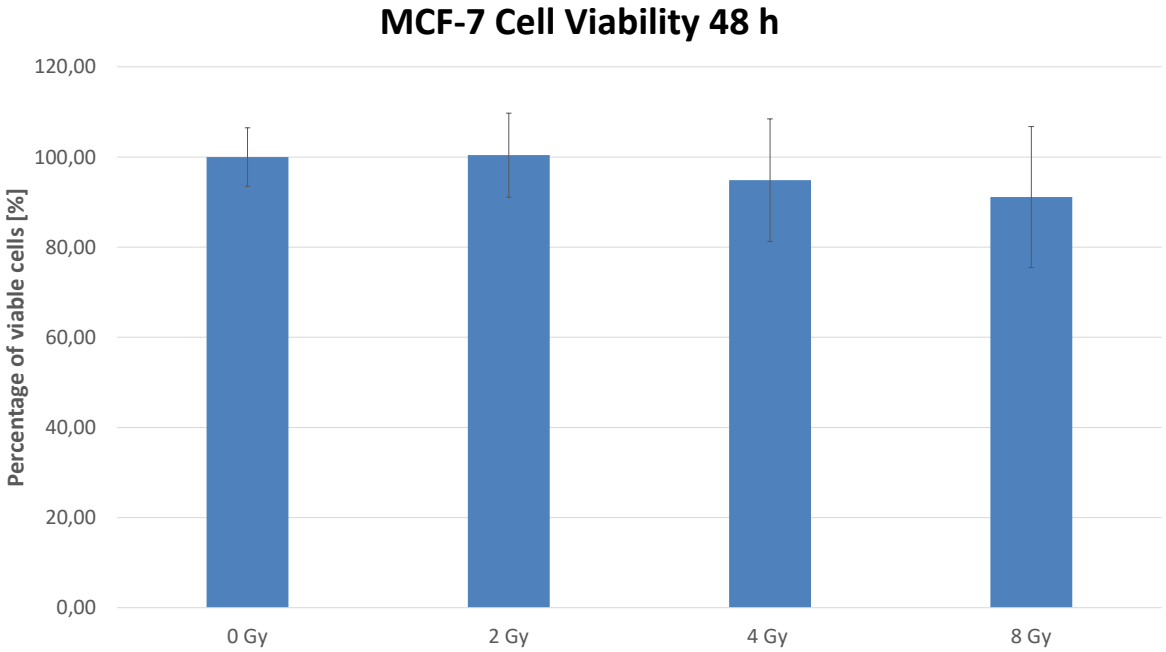

Figure 3.12: Cell viability of MCF-7 cells after 48 hours.
Description: The y-axis shows quantified luminescence in reference to the 0 Gy group set to 100% of cells irradiated with 0 Gy, 2 Gy, 4 Gy, 8 Gy on the x-axis at 24 hours after treatment. Data represent values $\pm$ SEM ($n = 4$) , * $p < 0.05$.

3.2.2 SkBr3 cells and cell viability

The same experiment was performed with SkBr3 cells. The time points were chosen according to the gap-closure assays at 24 hours after irradiation and 48 hours after irradiation (see figure 3.13 and figure 3.14). The x axis shows the four subgroups with the 0 Gy group serving as a reference (control group).
The results in SkBr3-cells at the 24 hours measuring point resulted in no significant change of viability in the different subgroups (0, 2, 4, and 8 Gy respectively). The x-axis shows the subgroups, the y-axis is in percentage and shows the luminescence in relative values. The sham irradiation subgroup was chosen as a reference point to calculate the percentage of

viable cells in the other subgroups. The amount of luminescence emitted by the viable cells in the 0 Gy subgroup was chosen as a reference of 100%. According to this, the amount of luminescence of the other subgroups was compared to this value. Here the 2 Gy subgroup shows only 0.80 viable cells compared to the 0 Gy control group. In the 4 Gy and 8 Gy subgroup this is less evident, with 0.95 and 0.91 respectively. Proliferation cannot be seen here. The viability stays unchanged.

Table 3.9: Cell viability of SkBr3, 24 hours

Dose	RLU	Relative signal [%]	Standard deviation [%]	t-test
0 Gy	3092347	100	8	-
2 Gy	2467441	80	11	0.411
4 Gy	2938560	95	6	0.402
8 Gy	2813802	91	7	0.533

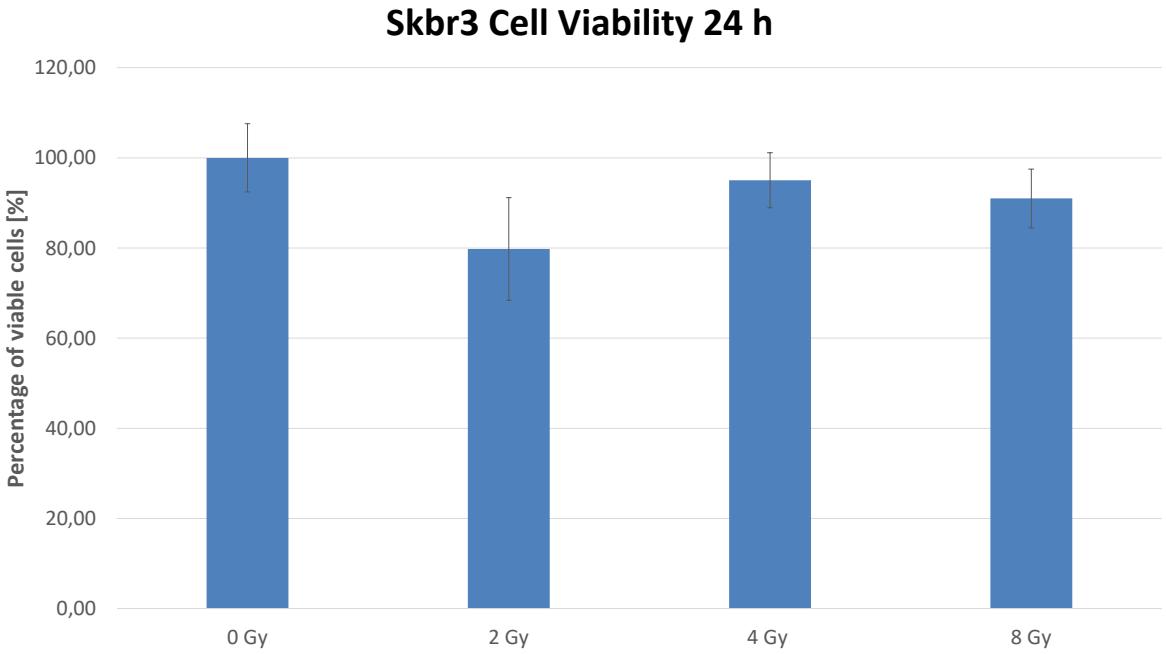

Figure 3.13: Cell viability of SkBr3 cells at 24 hours.
Description: The y-axis shows quantified luminescence in reference to the 0 Gy group set to 100% of cells irradiated with 0 Gy, 2 Gy, 4 Gy, 8 Gy on the x-axis at 24 hours after treatment. Data represent values $\pm$ SEM ($n = 4$) , * $p < 0.05$.

The next time point of measurement was chosen at 48 hours after irradiation (figure 3.14). For analysis and reasons of better comparison, cell viability in the sham irradiation control

group was set to a value of 100%. In the 2 Gy subgroup, there is a value of 1.1 compared to the sham group of viable cells. The 4 Gy and 8 Gy subgroup shows 1.04 and 0.98 of viable cells compared to the sham irradiation subgroup. In total at this 48 hours time point, there is no significant change in viable cells visible. A one sided *t*-test was performed, showing no significance in either of the subgroups. The treatment did not significantly change the viability of cells at either two time points of measurement. So I conclude that there is no significant effect of proliferation interacting with the migration results from the gap closure assay.

Table 3.10: Cell viability of SkBr3, 48 hours

Dose	RLU	Relative signal [%]	Standard deviation [%]	t-test
0 Gy	4744390	100	25	-
2 Gy	5222735	110	14	0.262
4 Gy	4930274	104	23	0.510
8 Gy	4661212	98	14	0.775

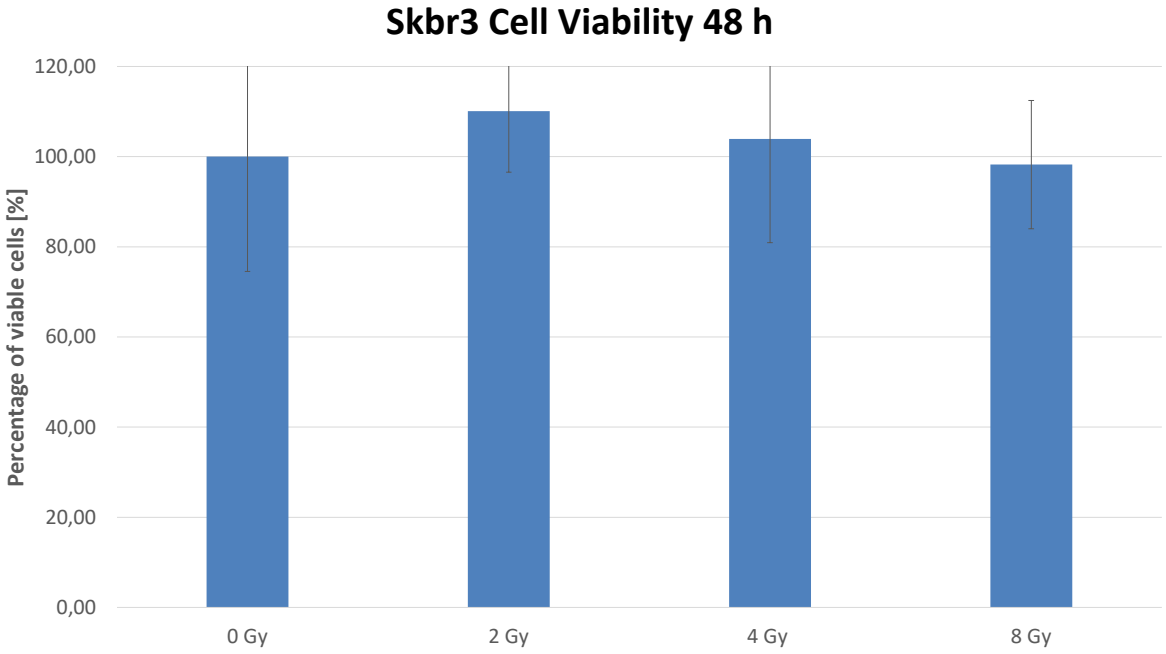

Figure 3.14: Cell viability of SkBr3 cells at 48 hours.
Description: The y-axis shows quantified luminescence in reference to the 0 Gy group set to 100% of cells irradiated with 0 Gy, 2 Gy, 4 Gy, 8 Gy on the x-axis at 48 hours after treatment. Data represent values ± SEM ($n = 4$) , * $p < 0.05$.

3.3 Apoptosis effects

3.3.1 SkBr3 and apoptosis

The effects of apoptosis were measured with the Caspase 3 and 7-kit, produced by Promega. For the cell line SkBr3 the time points were defined at 24 hours and 48 hours after irradiation. The results show a slight rise in apoptosis in higher irradiation doses up to 4 Gy single dose at the 24 hours' time point. Cells irradiated with 8 Gy single dose show about the same signal of luminescence as the 2 Gy group. The following graph shows values of 24 hours observation. The irradiation doses from sham irradiation, 2 Gy, 4 Gy and 8 Gy single dose are displayed on the x axis and the luminescence signal in relation of the Luminescent Units compared to the 0 Gy value in percent on the y-axis (figure 3.15).

Table 3.11: Apoptosis data of SkBr3, 24 hours

Dose	RLU	Relative signal [%]	Standard deviation [%]	t-test
0 Gy	92970	100	21	-
2 Gy	107958	116	23	0.371
4 Gy	112488	121	17	0.340
8 Gy	107120	115	18	0.419

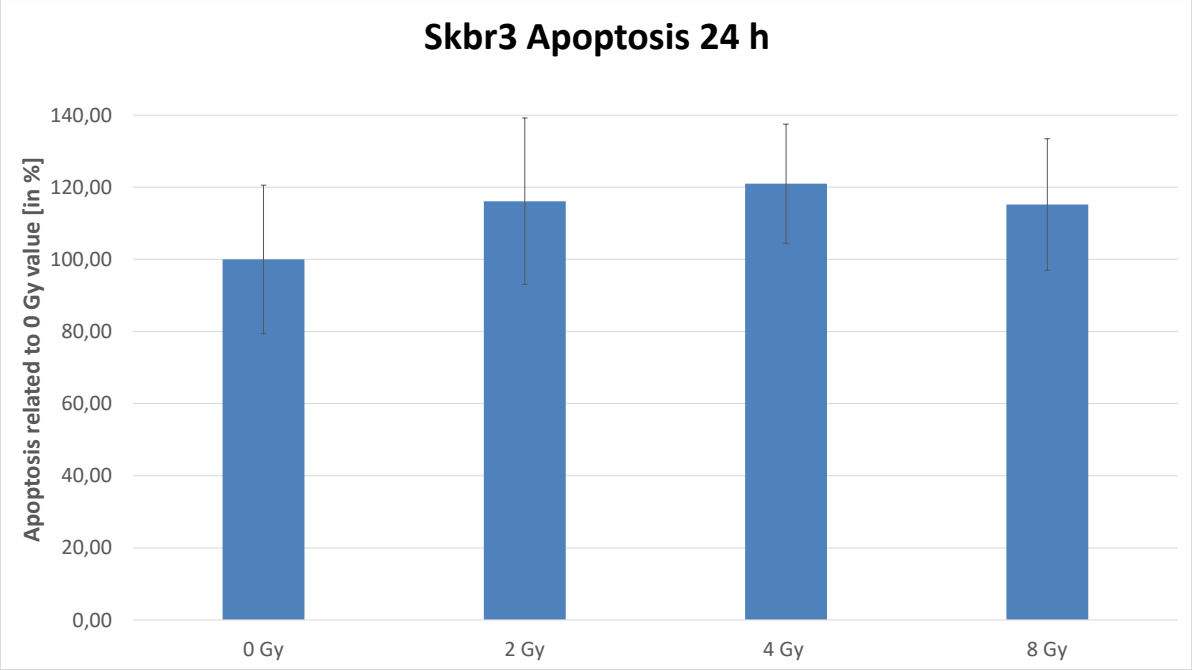

Figure 3.15: Apoptosis of SkBr3 cells at 24 hours.
Description: The apoptosis of SkBr3 cells quantified in luminescence (in relative light units, RLU) of cells irradiated with 0 Gy, 2 Gy, 4 Gy, 8 Gy at 24 hours after treatment. Sham irradiation data set to 100%. Data represent values $\pm$ SEM ($n = 4$) , * p< 0.05

Apoptosis effects after 48 hours are displayed in the graph below (figure 3.16). The results indicate an approximately constant rate of the apoptosis/ luminescence signal. On the x-axis the irradiation doses are displayed, the y-axis shows the luminescence signal in Luminescent units.

Table 3.12: Apoptosis data of SkBr3, 48 hours

Dose	RLU	Relative signal [%]	Standard deviation [%]	t-test
0 Gy	174724	100	19	-
2 Gy	166820	95	28	0.702
4 Gy	146801	84	8	0.418
8 Gy	135263	77	13	0.028 *

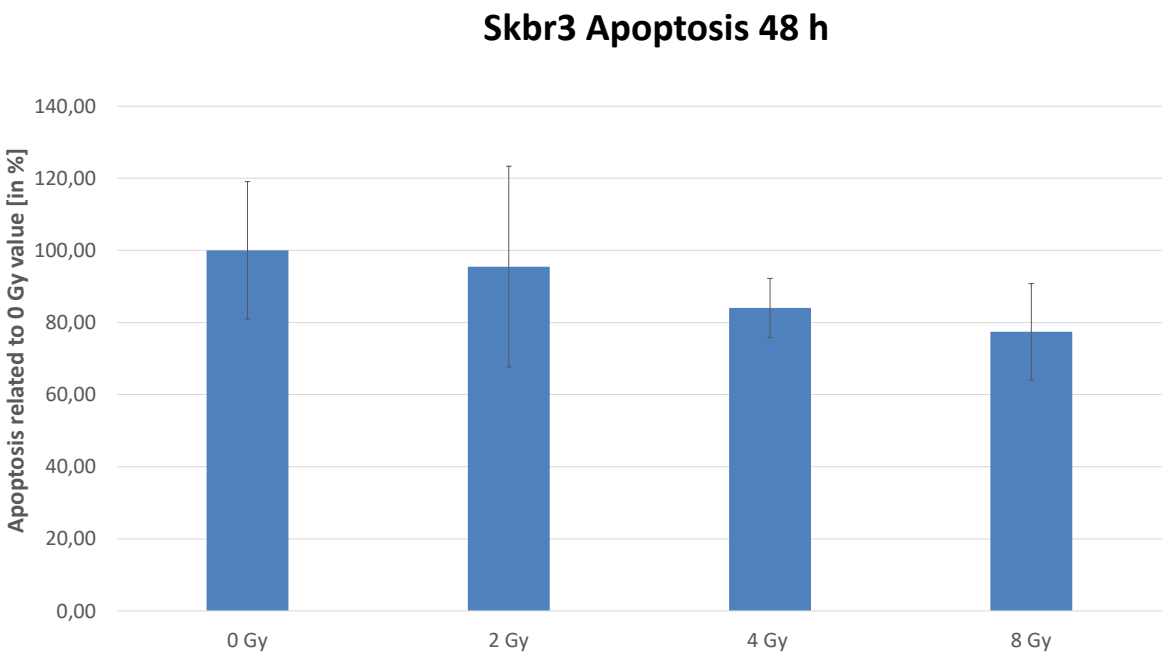

Figure 3.16: Apoptosis of SkBr3 cells at 48 hours.
Description: The apoptosis of SkBr3 cells quantified in luminescence (in relative light units, RLU) of cells irradiated with 0 Gy, 2 Gy, 4 Gy, 8 Gy at 48 hours after treatment. Sham irradiation data set to 100%. Data represent values $\pm$ SEM ($n = 4$) , * $p < 0.05$

To draw a resume out of the data: apoptosis stays at a constant level, no significant changes can be seen at those two time points. As expected, absolute luminescence increases over time in this experiment, as seen in the following graph (figure 3.17).

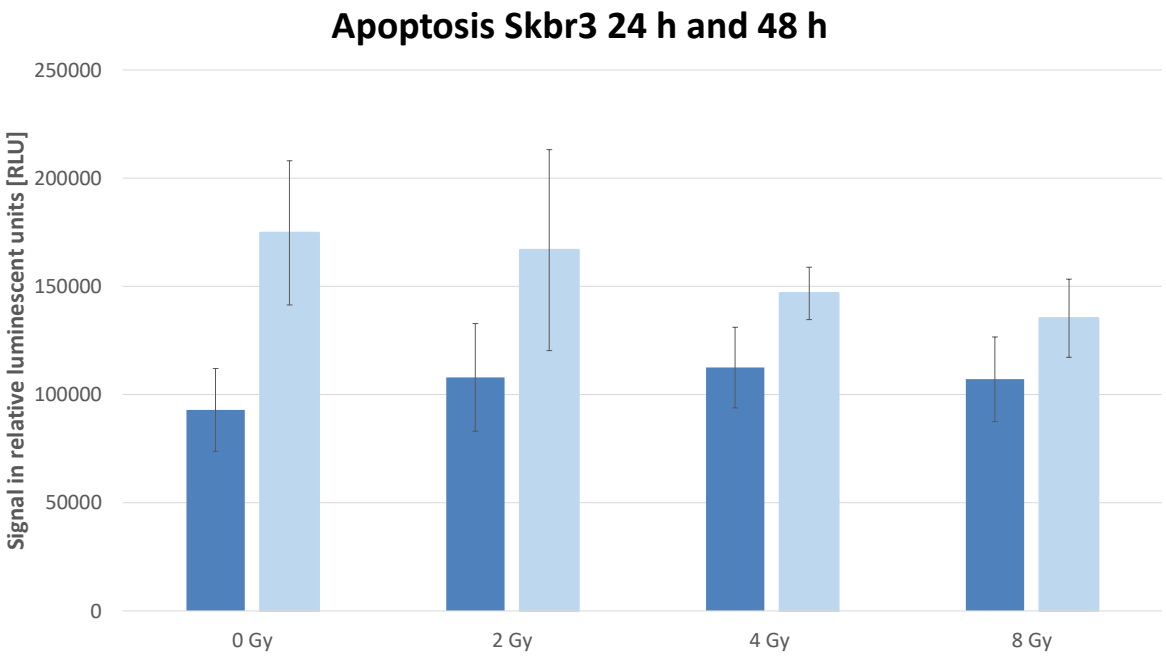

Figure 3.17: Comparison of apoptosis of SkBr3 cells.
Description: The apoptosis of SkBr3 cells quantified in luminescence (in relative light units, RLU) of cells irradiated with 0 Gy, 2 Gy, 4 Gy, 8 Gy at 24 hours (blue column) and 48 hours (green column) after treatment. Data represent values $\pm$ SEM ($n = 4$) , * $p < 0.05$

3.3.2 MCF-7 cells and apoptosis

MCF-7 cells do not express Caspase 3, but they express Caspase 7[106]. They were also examined by using the Caspase 3 and 7 kit by Promega. The following graph shows the irradiation dose on the x-axis and the luminescence on the y-axis in RLUs (figure 3.18). The luminescence signal, meant the apoptosis levels stay steady after 24 hours. There is a slight downbreak in signal in the 8 Gy subgroup.

Table 3.13: Apoptosis data of MCF-7, 24 hours

Dose	RLU	Relative signal [%]	Standard deviation [%]	t-test
0 Gy	118224	100	22	-
2 Gy	127365	108	33	0.810
4 Gy	121039	102	22	0.523
8 Gy	106738	90	29	0.577

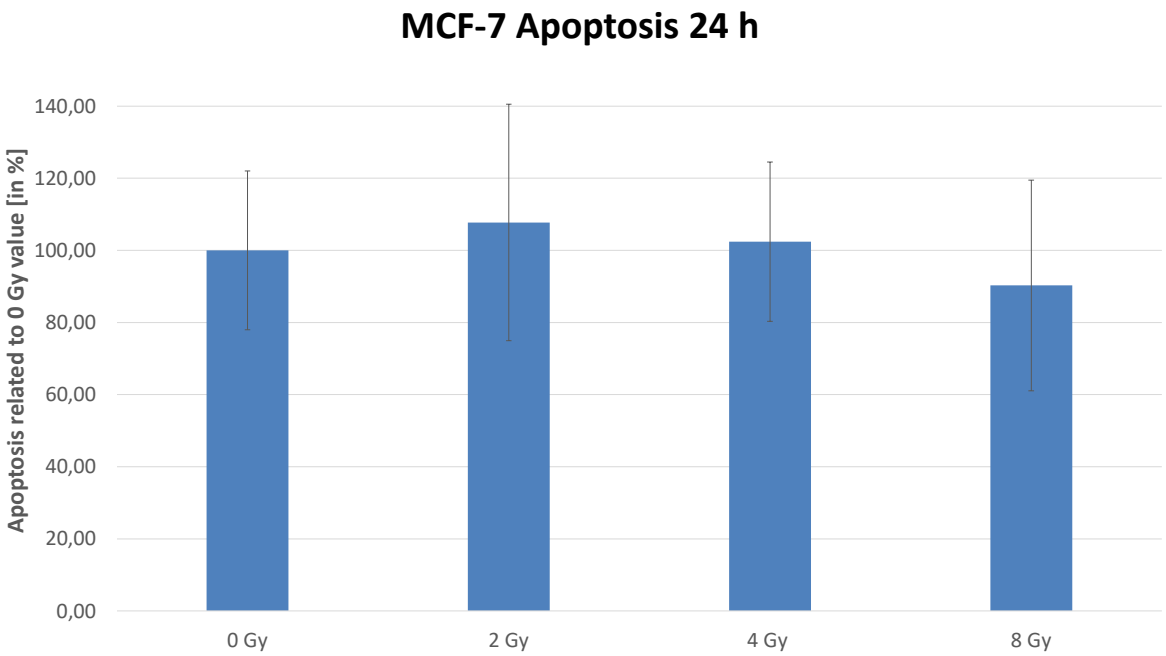

Figure 3.18: Apoptosis of MCF-7 cells at 24 hours.
Description: The apoptosis of MCF-7 cells quantified in luminescence (in relative light units, RLU) of cells irradiated with 0 Gy, 2 Gy, 4 Gy, 8 Gy at 24 hours after treatment. Sham irradiation data set to 100%. Data represent values ± SEM ($n = 4$) , * $p < 0.05$

The following graph shows MCF-7 cells' apoptosis signal after 48 hours of observation (figure 3.19). The x-axis again shows the irradiation doses and the y-axis indicates the luminescence signal. This time the apoptosis signal remains unchanged in the sham irradiation subgroup. Toward higher doses of irradiation apoptosis is declining.

Table 3.14: Apoptosis data of MCF-7, 48 hours

Dose	RLU	Relative signal [%]	Standard deviation [%]	t-test
0 Gy	288266	100	39	-
2 Gy	265900	92	33	0.656
4 Gy	181283	63	30	0.008 *
8 Gy	136999	48	24	0.041 *

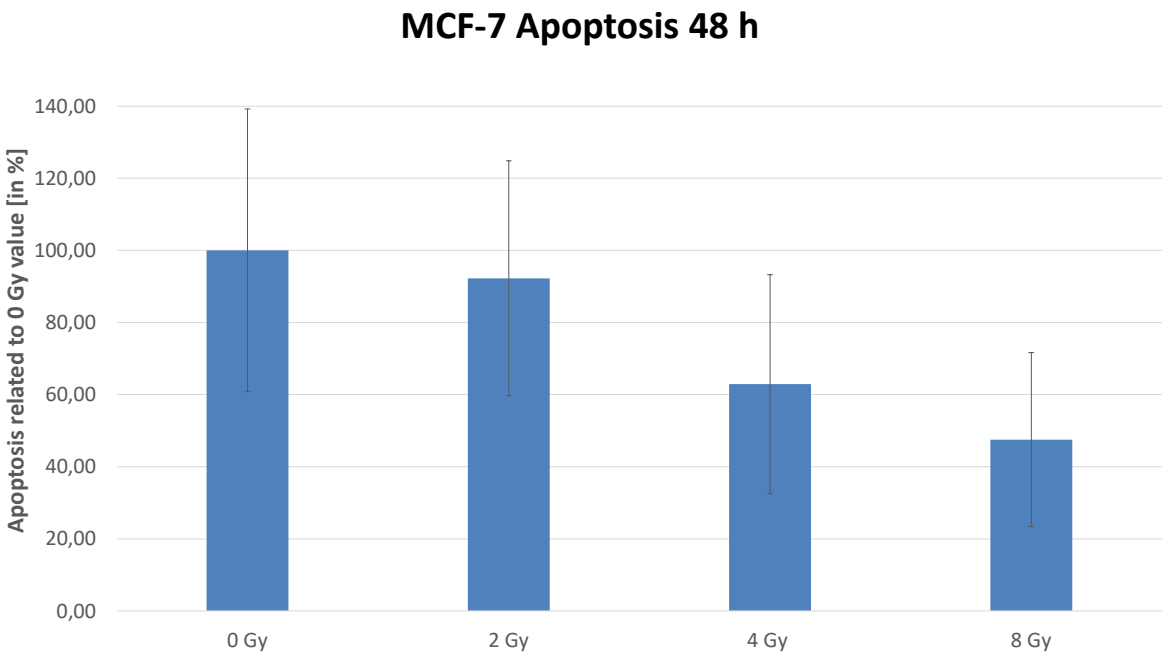

Figure 3.19: Apoptosis of MCF-7 cells at 48 hours.
Description: The apoptosis of MCF-7 cells quantified in luminescence (in relative light units, RLU) of cells irradiated with 0 Gy, 2 Gy, 4 Gy, 8 Gy at 48 hours after treatment. Sham irradiation data set to 100%. Data represent values $\pm$ SEM ($n = 4$) , * $p < 0.05$

The following graph (figure 3.20) shows absolute luminescence on the y-axis and the samples after 24 hours (depicted in blue) and 48 hours (depicted in green) on the x-axis. As expected, absolute luminescence increases over time within the samples in this experiment.

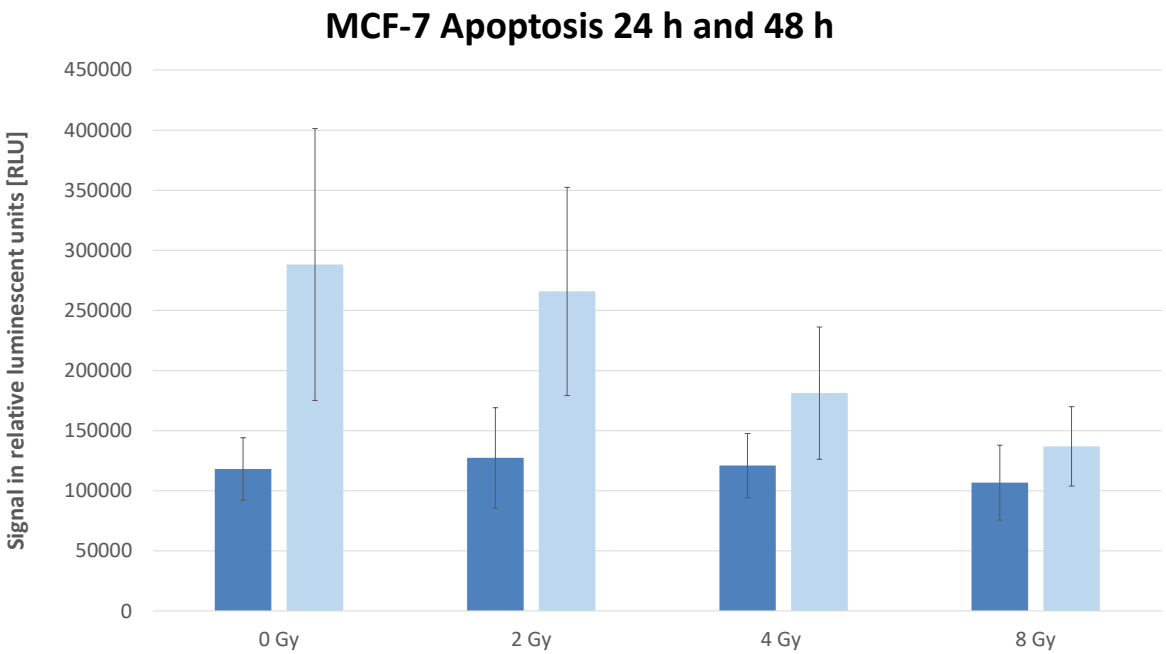

Figure 3.20: Comparison of apoptosis of MCF-7 cells.
Description: The apoptosis of MCF-7 cells quantified in luminescence (in relative light units, RLU) of cells irradiated with 0 Gy, 2 Gy, 4 Gy, 8 Gy at 24 hours (blue column) and 48 hours (green column) after treatment. Data represent values $\pm$ SEM ($n = 4$) , * $p < 0.05$.

4 Discussion

4.1 Migration experiments

A literature research showed in chapter 2, that usually a specific gene or protein is analyzed rather than sole migration effects on the whole cell. This makes comparability more challenging. In the following, I will interpret the results for each cell line.

The first trials were still performed using the breast cancer cell lines T47D and MDA-MB 361. These showed no significant migrational behavior in my pre-exams and were hence excluded. Literature makes heterogeneous statements about this behavior. T47D and MBA-MB 361 are predominantly adherent cells that have little tendency to migrate. However, some sources state that T47D migrate, depending on the cell passage. In addition,the generations of cell lines that show different phenotypes should usually be regularly sequenced. A valid argument is, that certainly other phenotypes of these cell lines migrate, as shown in the literature. The here used phenotypes, hence did not. Sources stating T47D and MDA-MB 361 as migrational exist. But those stating T47D as migrational after irradiation are scarce. They mostly refer to a pre-treatment [43], [110]. Ko et al. created radio-resistant cells in their experiment by using a common fractionation scheme of adjuvant treatment after breast-conserving therapy in vitro. The so-called RT-R-breast cancer cells showed an increased cell viability and were more resistible against radiation compared to the untreated breast cancer cells. Compared to my results, the T47 D cells were pre-treated here. Mikalsen et al. used low dose irradiation to target hypoxia in the breast cancer cell T47D, containing different amounts of DNA. There was no difference in migrational behavior in any subgroups. The irradiation dose in my experimental design was different, but similarly, T47D showed no migration at all, also in the 0 Gy control group.

Concerning the cell line MDA-MB 361, works involving irradiation and migration analysis were also scarce. Here I would like to mention the following works, although they do not involve irradiation: Mishra et al. [111] used this cell line among others to examine a reactive oxygen species-induced prodrug on breast cancer cell lines. Here, the ROS-activated prodrug inhibited migration, when combined with doxorubicin. This experiment lacked irradiation in its design, and is therefore hardly comparable, but despite all - one of few sources examining migration of MDA-MB 361 cells. Kulmany et al. [112] examined the effects of a single drug (an androstadiene-derivant) on migration and invasion in four breast cancer cell lines and fibroblasts. Here, the drug had an inhibiting effect mainly on MCF-7 and MDA-MB 231, not on MDA-MB 361. Both papers used Boyden chambers for measuring migration, making the design of the experiments differ from mine. Additionally, the design of the experiment lacked irradiation. Additionally to these mentioned above, I would like to refer to many sources

stating, that they also decided against using T47D and MDA-MB-361 in their design due to lack of migration [94].

The following paragraphs focus on the cell lines MCF-7 and SkBr3. These were used in the main experiments.

In a short resumee of the results with MCF-7: MCF-7 cells cultivated with a scarce medium showed most migration in the 4 Gy and 8 Gy subgroup (1.466 resp. 1.408 relative migration compared to the control group). However, this result was not statistically significant. This might result from the scarce medium starving the cells, or, due to the higher irradiation dose. It could be that higher irradiation doses under starvation medium lead to an alteration in migration. MCF-7 cultivated in the full medium (10% FCS) migrated most in the 2 Gy, then 8 Gy subgroup (1.203 resp. 1.105). It was also not statistically significant.

Comparing high with low levels of FCS in absolute numbers of luminescent units is rather difficult, as each experiment has to be calibrated according to the background scattering. Only this ensures a constant signal and adequate signal output for each biological replicate of the assays. When comparing relative levels of migration, the starvation medium led to more migration with the MCF-7 cells. On the contrary, literature rather indicates, that higher levels of glucose in the medium lead to increase in migration and invasion [113]. Here, cells adapted after a three hour time period to the altered levels in glucose. It finally lead, among other effects, to epithelial to mesenchymal transition in higher glucose levels.

Could it be a dose-dependent effect? In my experiments with MCF-7 cells, no linear effect of more migration with higher doses could be seen. Higher doses of irradiation, such as 10 Gy and above showed migration and invasion induction by EMT in other publications. Radioresistance and metastasis are results of the EMT. Tripathy et al. [114] showed that irradiation induces EMT in MCF-7 cells and this effect can be inverted by pre-treatment with a lipoic acid. Kantapan et al. [115] presented similar results using a different radiosensitizer. Young et al. stated that intermediate doses, such as 2.3 Gy can induce migration in certain cell lines (MDA-MB 231, but not MCF-7), but not invasion [116]. In their experiment, irradiation with 2.3 Gy could not induce migration in MCF-7 cells. At least, in my experiments, 2 Gy irradiation dose lead to migration higher than the control group in full medium. Pan et al. [117] examined MCF-7 Cells and intrabeam-irradiation doses of 0 Gy to 16 Gy, as well as apoptosis and migration in a wound healing assay. In their experiment, a scratch gap assay was used. The results showed equal levels of migration after irradiation with doses of 2 Gy and 4 Gy. Migration decreased largely over 6 Gy. The aim of the study was to examine effects of intraoperative irradiation on breast cancer cell lines. This study design differs from my experiment, but shares some certain proportions. It remains unsure, if higher doses of irradiation clearly lead to a plus in migration. Also low doses of irradiation seem to be able to induce this effect. Zhang et al. proved that already such low doses of irradiation can induce EMT in MCF-7 Cells, leading to invasiveness [94]. In this setting, the group used matrigel coated transwell chambers for evaluation invasion. To document the transformation,

mesenchymal markers were measured, as well as vimentin and E-cadherin. The dosage was 20 Gy, administered in 1 Gy and 2 Gy single fractions. However, different publications state the opposite: Kaushik et al. observed lesser migration after low dose irradiation. In this case, the dosage was defined as 0.1 Gy, administered in 10 fractions of 0.01 Gy [118]. In a subpopulation, CSC of MDA-MB 231, the low dose irradiation reduced EMT by down-regulating the JAK/STAT-pathway. MCF-7 cells were used in a subpart of the experiment in spheroids. Equally, this publication can not be fully compared to my work, as the dosage of 0.01 Gy as single faction is way below my 2 Gy fractionation. Additionally, cancer stem cells are examined in the subpopulation. They show a different behavior than usual cancer cells. Mei et al. [119] examined a spheroid co-culture of breast cancer cell lines, among them MCF-7 and fibroblasts to determine invasion after 5 Gy irradiation. In their study, irradiation did not lead to higher levels of invasion. Despite this, this experiment design is a very promising one as it represents the tumor microenvironment and tumor stroma more likely than plain 2 D cell culture - though technically more difficult to perform. Differing from my experiments it examines invasion. It is therefore not suitable for a direct comparison. Al-Abedi et al. [120] stated that invasiveness and migration can be exosome-mediated. Exosomes harvested from irradiated MCF-7 cells induced invasion in non-irradiated cells, when exposed with the exosomes. Doses of 2 Gy were sufficient for producing this effect. Similar results are available for many cancer entities, such as in HNSCC [121]. It is a clear example of irradiation mediated migration on MCF-7 cells, that also works indirect through proteins. Proteins, such as Micro-RNAs can influence many cellular actions. Yoo et al. describe that miR-181b-3p regulates EMT. Adding a specific inhibitor to MCF-7 cells led to a reduction of the invasiveness and migratory behavior in the cells as well as to a reduction of mesenchymal marker expression. Theys et al. examined several cell lines, among them, MCF-7. Under Hypoxia, EMT was promoted. It also lead to radioresistance. This was tested with the clonogenic survival [122]. A dose-dependent change of migration could not be seen in my experiments. An effect of irradiation on migration could clearly be seen with the MCF-7 cells. However, it did not reach levels of statistical significance.

Now, I would like to discuss the results for the SkBr3 cells. The 24 hours time point was chosen here to observe the results, differing from the 16 hours with MCF-7 cells. This cell line showed very little difference in the scarce medium branch of the experiment. The 2 Gy subgroup showed lesser migration than the 0 Gy control group. The 4 Gy and 8 Gy subgroups showed 1.10 and 1.16 fold more migration than the 0 Gy control group. In general, it was not significantly different. The 10 % FCS-full Medium branch of the migration experiment with SkBr3 showed significantly more migration in the 4 Gy and 8 Gy subgroup, proven by a one sided t-test. To discuss involvement of the full medium, two arms of the experiment were performed, as well as an analysis of proliferation and apoptosis. Regarding Cell viability after 24 hours with SkBr3 cells, 0 Gy, showed almost equal viability as 4 Gy and 8 Gy. Whereas the 2 Gy subgroup showed lesser viable cells, with only 80%. Here, I assume that more biological and technical replicates could be useful for determining the outcome of these aspects more clearly, especially in the case of these deviating results for the 2 Gy subgroup, that have no

specific explanation.

Regarding Apoptosis with SkBr3, after 24 hours of observation, there was only little difference between the irradiation subgroups. Irradiated groups showed more apoptosis than sham irradiation, as expected. It was the highest in the 4 Gy subgroup. 2 Gy and 8 Gy ware almost on a similar level. So, apoptosis and proliferation effects can be ruled out in this case. Regarding the 2 Gy subgroup, it can be possible to think that with lesser viable cells, generally lesser migrating potential is available.

In general, research about Skbr3 cells and migration combined with irradiation is scarce. A Pubmed search displayed 13 results for a time span of 1992 to 2022. Actual usable publications were limited to three results. Parts of the data of this work were used in further experiments on micro-RNA 221. Its use leads to reduction in migration of SKBr3 cells when combined with the MEK-Inhibitor [96]. Yu et al. examined the influence of microRNA 144 on breast cancer cells. They examined MDA-MB-231 and SKBR3 cells. Overexpression of miR-144 leads to proliferation, migration and invasion [123]. Here, transwell migration and matrigel invasion was measured. These methods differ from mine. Mir-144 turned SkBr3 cells more radioresistant. Changes of migration after irradiation - as in my work- were not directly examinded. Olivares-Urbano et al. investigated the influence of radiation on Matrix metalloproteases (as well as TIMPs and HDACs) in the cancer cell lines MCF-7, SKBr3 and MDA-MB 231 [124]. They reported differences in their analysis of markers of cancer stem cells in 2D and 3D cell culture. They state that irradiation may lead to the creation of very radio-resistant cancer stem cells. These were characterized by using markers (CD44+ and ALDH1) after irradiation with 2 Gy and 6 Gy doses. Especially CD44+ is associated with Epithelial to mesenchymal transition, as the start of migration [124]. Still, these findings can not be directly compared to my work, as methods and the objective of these studies differ.

When examining the impact of irradiation on the migrational behavior, I experienced heterogeneous outcomes. This is due to the many possible influencing aspect. These can be partly ruled out by strictly standardizing the experiments and use of good cell culture practice (use of batches of an early passage-number, mycoplasma-testing and genetic analysis of the cell lines). All these precautions were followed in this work.

Literature research also confirms that migration is highly heterogeneous in vitro since many aspects are involved. These are i.e. differences between passages of cell lines [106], biological and technical replicates. All of these lead to changes in the microenvironment. In general, migration of cells is a phenotypical phenomenon. As such it is highly influenced by the aforementioned microenvironment and variable between cell lines, cancer entities. It also differs in between the specific biological replicates and passages of cell lines. Between those passages, cells may gain or lose mutations. For metastasis, the cancer cells need to detach themselves from their formation and float with the blood flow or in lymphatic vessels. Arrived at a distant distinct other point in the body, they need to attach themselves to a blood vessel wall and finally invade it in order to reach other organs. This whole process can naturally not be completely depicted in 2D in vitro experiments. Additionally, it comprises too many factors and cannot be this simplified. Possible improvements are made by using 3D cell culture, such as organoids. Another option is using animal models. A possible future

aspect would be high-output experiments (automatized) using AI to recognize migrational patterns of singular cells, or also to determine further influences we might not realize with our manual approach.

4.2 Gap migration evaluation

Another aspect of the work was to establish a reproducible migration assay: The migration experiment in this work consists of a semi-automatised assay for measuring migration, as stated in previous chapters. It uses silicone inserts to grow a cell layer to confluence and of the same size, standardized amounts of cells for each replicate, taking the photo in the fluorescent microscope at the same time point and same sector each time using markings, as shown in chapter 3.1. All this is a standardized approach, especially with markings used for displaying the exact same position of the cell layer at each observation point. Additionally GFP-labelled cells facilitate the later analysis, see chapter methods, materials - software.

In general, this approach is a large improvement to the scratch-pipette method. Because of its unreliable size of the gap and unwanted lesions in the cell layer, this experiment is out-dated and rarely used nowadays. When comparing it to the usual use of migration assays using silicone insert, this method has two main advantages. Usually the cell number seeded out is standardized, but the GFP-labelled cells facilitate the observation by far. An additional advantage is, that we can reliably evaluate migration by calculating the exact sections, occupied by the cells on their migrational trail. Finally, we can indicate with precision how the migration behavior of the cells develops. Utilizing fluorescent marked cell lines and analysing it with a pixel counting software is also very reliable and reproducible. Its reliability is due to the selected cell lines, the careful selection of the number of seeded cells and the reproducability with marks that ensure a correct position of the gap under the fluorescence microscope.

All materials used here are affordable. Apart from a fluorescence microscope all other materials are usually available in a cell culture laboratory. This makes the assay flexible. Different parts of it can be used in other experiments and are not restricted to the observation of migration, as automatised commercial versions might be. Automatised assays may have higher precision and can analyse at a higher output (more cell lines and subsets in a shorter time span). However the high costs of such devices (acquisition and maintenance cost) restrict it to industrial uses.

I showed that the improved migratory assay using silicone inserts and analysis-software proved to be highly accurate and technically reproducible. It demonstrated several advantages compared to the widely used scraping method using a pipette tip as being more exact causing lesser harm within the cell layer. Commercial options for migratory experiments are available, these proved to be highly exact and easy to perform. They provide a heated chamber with a build on camera fixed to a microscope. It enables observing migration over a longer period of time without moving the samples. Which is the most exact way of measuring migration. It also enables observation of 3D-culture. The downsides of this machine or technical equipment are the huge acquisition costs and less flexibility compared to using a fluorescence microscope

and conventional cell culture.

4.3 Apoptosis and cell viability

The results from the apoptosis and cell viability experiments demonstrated that there is no or just a slight difference in the treatment and control group. In migration assays, a critical point is to outrule possible implications of proliferation and apoptosis at the chosen time points. Overall, the results from my experiments proved that migration was not influenced by apoptosis or proliferation.

The cell viability assay with MCF-7 showed the number of viable cells to be equal between the irradiation subgroups at a 48 hours time point. At the 24 hours observation point, a two sided t-test showed a significant difference between the 0 Gy group and the 2 Gy group (0.012 with a p-value defined as 0.05). The 4 Gy group did not show a statistically significant difference (0.089 with a p-value of 0.05), but was showing a slight difference.

SkBr3 cells in the cell viability assay showed no significant difference between the control group with 0 Gy and the trial groups. This was the same for the 24 hours time point as it was for the 48 hours time point.

A possible explanation why differences occur in the MCF-7 24 hours 2 Gy subgroup might be that due to the relatively low number of samples (n=4) there may be a variety inbetween the different samples. The standard deviation is within the expected range and gives no indicator of a faulty arm of the experiment.

The apoptosis results showed constant levels of apoptosis in the MCF-7 24 hours measurement. There was no significant difference between the arms of the assay. My results show similarity to the literature [125]. Wendt et al. experienced similar results when irradiating MCF-7 cells and measuring apoptosis vs. G2 checkpoint arrest. Other publications use longer time periods, when measuring apoptosis [126]. Here, X-ray irradiation inhibited proliferation in MCF-7 cells, and induced apoptosis.

The 48 hours time point shows a decline in apoptosis, this effect increases with increasing irradiation dose. The parallel experiment with MCF-7 cells measuring viability also shows a decline in living cells the higher the irradiation dose at the same time point.

SkBr3 cells in the apoptosis assay showed a relatively constant level in the 24 hours observation point. After 48 hours, apoptosis declines the higher the irradiation dose is chosen. The comparison between the time points shows a increase in apoptosis, which was expected in both cell lines.

Possible explanations why proliferation and apoptosis do not differ significantly are that apoptosis reactions are often visible at a 48 hours or later time point. It is likely that the time points chosen here were too early to detect apoptosis. The same applies to proliferation. With the doubling time of MCF-7 and SkBr3 known, I can rule out large proliferation effects at the time points of 16 hours and 24 hours.

It is vital to ensure that the experiments securely measure migration. Distinguishing cell proliferation from migration is difficult to detect visually. To determine if a measured effect is influenced by motility or proliferation, usually an additional examination is needed.

Here, the number of cells was detected using a Cell viability kit. It determines if a cell is viable or dead. The cell titer glo-assay has proven to be reliable and reproducible. Within the measuring points of my experiment I did not measure any higher amount of proliferation other than expected. This means that my results are not due to cell layers stacking over one another and finally filling up the gap, but migrating cells.

Analyzing the expression of E-cadherin and N-cadherin could be important in future work. Changes in the expression of these would show EMT-transfer and activation of migration. It could be an important aspect to consider in further studies on migration, in order to show active migrational processes. Other possible options would be to detect changes in expression of vimentin and fibronectin. Another option could be to observe the decline in occludin. These last listed options are related to EMT but less specific than the E to N-cadherin switch. Other options may be to observe a smaller number of samples with a constant time lapse microscope to directly depict migrational lanes.

However, migratory experiments after irradiation proved to be heterogeneous. Several sources stated previously that within technical and biological replicates lies a huge variety and volatility within migration. Apoptosis and cell viability proved to be relatively stable over the short period of observation (24 hours). There were no major changes in apoptosis and cell viability within the 24-hours of the observation. This was to be expected as apoptotic induction after irradiation needs time and would more likely be occurring after 48 hours and a longer period of time. Previous works examining apoptosis after irradiation usually use a 48 hours time period when observing apoptosis [126]. Cell viability also did not prove to show a huge difference between the observation points and the different irradiation subgroups (0,2,4,8 Gy). This shows that I did not measure proliferation effects on my results.

4.4 Conclusion

The future of medicine in first world countries will be dominated by the use of artificial intelligence for therapy and diagnostics. Huge datasets can be analyzed by deep learning methods and lead to machine-learning approaches to medicine using algorithms. As the analysis of vast datasets can be used for selecting benefiting subgroups. This will lead to more detailed and specified decision making as well personalized therapy approaches for each patient. Another vital aspect in future medicine is budgeting in the health system and the economization of medicine. Spending in the health care system rises constantly and the german society is increasingly aging. With age being the main risk factor for many diseases (cardiovascular, arthritic, dementia and cancer), further expenses are to be foreseen. The close consideration of financial funds and corresponding allocation within the health system and more evidence based medicine will be an important topic in the future.

Returning to future advances in the field of cancer research, the introduction of diverse immunotherapies (monoclonal antibodies, CAR T-cells and tumor vaccines) progresses. An extended analysis of the field of the tumor microenvironment will lead to targeting cancer stem cells as well as micro-RNAs (diagnostics and therapy). Further basic research is vital for understanding metastasis formation. In the example of breast cancer, most women

are successfully treated for their primary tumor, but still too many suffer from late onset metastasis, that then leads to fatality. Our aim in the future must be to target CSC in order to break the pre-metastatic niche. Another option is to target metastasis in a way to endure stable disease.

Considerations for the future of oncology and radiation oncology will be the use of artificial intelligence and algorithms, as well as -omics for the analysis of big data. Current developments in AI and machine learning is auto-contouring in radiation therapy, and auto-diagnostics, i.e. for diagnosing lung metastasis. These may bring better results in a combination of the experienced physician with the algorithm than an algorithm alone or even a stressed physician [127]. Some parts of diagnostics and radiation oncology planning could be completely supported by well-trained algorithms in common stages of frequent diseases.

Last, I would like to discuss the promising options of micro-RNAs in metastatic breast cancer.

A possible option for targeting the tumor microenvironment in breast cancer would be to observe signalling molecules and tiny protein particles [128]. Exosomes contain signalling molecules and micro-RNA. They are a promising field of research for theranostics [129]. Among the most frequently addressed microRNAs in cancer is the mir221 and mir21. The upregulation of microRNA 21 in cancers leads to more epithelial-mesenchymal transition by targeting the tumor suppressorgene Pten. Several microRNAs have been reported to be overexpressed in breast cancer. They stimulate migration and invasion in vitro and in vivo. This observation makes them interesting for metastasis research.

There are so called prometastatic microRNAs such as miRNA 10b and microRNA 373 and 520 C. There are two possible ways of alteration of microRNAs and the subsequent development of breast cancer. It is either possible by a loss of a tumorsuppressor microRNA or by the overexpression of so-called oncomiRNAs that activate oncogenetic transcription factors [130]. The expression profiles of microRNAs offer the possibility of distinguishing the molecular subtype of the breast cancer. The families of tumor-suppressing microRNAs in breast cancer are known [88]. Their knowledge is vital for choosing a potential candidate for therapeutic use. Several microRNAs are in discussion for targeted therapies, hormone therapies or as sensitizers for chemotherapeutic agents [131], [87]. Among those for hormonal therapies are the specimens 221 and 222. These are highly homologous and they were found to be regulators of the EMT through the RAS RAF MEK signalling pathway [132]. The microRNA21 is a rather proproliferative and prometastatic microRNA which has several important roles in development, morphogenesis and differentiation. It is usually overexpressed in breast cancer and is positively associated with the tumor size, stage and grade. Overexpression in breast cancer is associated with a high invasiveness and metastatic potential. It is often overexpressed in ER- her2neu positive cancer cells. It also regulates EMT and inhibits tumor suppressor proteins for instance. The idea of targeting microRNA21 is to restore the expression of genes. For instance, proliferation and growth of MCF-7 cells is slowed down by a Knockdown of microRNA21. It is also reported that in in vivo experiments it reduced the invasion and metastasis of MDA-MB 231 cells. So, choosing micro-RNAs for further molecular classification of breast cancer and later therapeutic intervention could be a

promising field, worth examining.

Abbreviations

AI	Artificial intelligence
AKT	Protein kinase B (PKB)
ATCC	American Type Culture Collection
ATM	Ataxia-telangiectasia mutated gene
AREG	Amphiregulin, part of EGFR-family
APBI	Accelerated partial breast irradiation
BRCA	BRCA-tumor suppressor gene
CHEK2	Checkpoint kinase 2 tumorsuppressor gene
CCNU	Lomustine, Chlorethyl-Cyclohexyl-Nitroso-Urea
CSC	Cancer stem cells
CTC	Circulating tumor cells
CUP	Cancer of unknown primary
Cs137	Cesium 137
CXCL12	CXC motif chemokine ligand 12
DMEM	Dulbecco's Modified Eagle's Medium
DMSO	Dimethyl sulfoxide
DCIS	Ductal carcinoma in situ
Dmean	Mean Dose
ECM	Extracellular matrix
EC-scheme	Epirubicin and cyclophosphamide chemotherapy
EMT	Epithelial-mesenchymal transition
EORTC	European organisation for research and treatment of cancer
ERBB2	Erythroblastic oncogene B
FCS	Fetal calf serum
G-CSF	Granulocyte colony stimulating factor
GFP	green fluorescent protein
Hedgehog	Signaling pathway
Her2neu	Human epidermal growth factor receptor 2
HIF-1	Hypoxia-inducible factors, transcription factor
IMRT	Intensity modulated radiation therapy
IGRT	Image guided radiation therapy
IL-1 beta	Interleukin-1 beta cytokine
LAD	Left anterior descending artery

MAPK	Mitogen-activated protein kinases
MDSC	Myeloid derived suppressor cells
MET	Mesenchymal-epithelial transition
MiR	Micro-RNA
MMP	Matrix metalloprotease
NEAA	Non essential amino acids
Notch	Neurogenic locus notch homolog protein
OS	Overall survival
PALB2	Partner and localizer of BRCA2 gene
PARP-inhibitor	inhibitor of the enzyme poly ADP ribose polymerase
PBS	Phosphate-buffered saline
PDL1	Programmed cell death ligand 1
PIK3CA	Phosphatidylinositol-4,5-Bisphosphate 3-Kinase Catalytic Subunit Alpha
PTEN	Phosphatase and Tensin homolog, tumorsuppressor gene
R0/R1	Resection margin
R0	No cancer cells seen microscopically at the primary tumor site.
R1	Cancer cells present microscopically at the primary tumor site.
ROS	Reactive oxygen species
RLU	Relative light unit
RPMI	Roswell Park Memorial Institute 1640 medium
SEM	Standard error of the mean
Snail	Zinc finger protein SNAI1 transcription factor
Stat3	Signal transducer and activator of transcription 3 transcription factor
TAM	Tumor associated macrophages
TGF-beta	Transforming growth factor β cytokine
TNBC	Triple negative breast cancer
TNM	Tumor (T), Nodes (N), Metastasis (M)
TP53	Tumor protein p53, tumor suppressor gene
TREG	Regulatory T-cells
TTF	Tumor treating fields
UICC	Union internationale contre le cancer
V20	lung volume receiving $\geq$ 20 Gy
VEGF	Vascular Endothelial Growth Factor
Wnt	Wingless and Int-1-signal transduction pathway
XCL1	X-C motif chemokine ligand 1
ZEB1	Zinc-finger E-box binding protein 1

List of Figures

List of Tables

Bibliography

[1] M. M.-T. Mattila, J. K. Ruohola, T. Karpanen, D. G. Jackson, K. Alitalo, and P. L. Härkönen. "VEGF-C induced lymphangiogenesis is associated with lymph node metastasis in orthotopic MCF-7 tumors". In: *International journal of cancer* 98.6 (2002), pp. 946–951.

[2] T. J. Key, P. K. Verkasalo, and E. Banks. "Epidemiology of breast cancer". In: *The Lancet Oncology* 2.3 (2001), pp. 133–140. ISSN: 1470-2045. DOI: https://doi.org/10.1016/S1470-2045(00)00254-0. URL: http://www.sciencedirect.com/science/article/pii/S1470204500002540.

[3] B. Barnes, K. Kraywinkel, E. Nowossadeck, I. Schönfeld, A. Starker, A. Wienecke, and U. Wolf. *Bericht zum Krebsgeschehen in Deutschland 2016*. 2016. DOI: 10.17886/rkipubl-2016-014.

[4] R. K.-I. (Hrsg). "Krebs in Deutschland für 2015/2016. 12. Ausgabe." In: *die Gesellschaft der epidemiologischen Krebsregister in Deutschland e.V. (Hrsg)* (2019).

[5] S. H. Giordano. "Breast cancer in men". In: *New England Journal of Medicine* 378.24 (2018), pp. 2311–2320.

[6] D. Héquet, C. Huchon, A.-L. Soilly, B. Asselain, H. Berseneff, C. Trichot, A. Combes, K. Alves, T. Nguyen, R. Rouzier, et al. "Direct medical and non-medical costs of a one-year care pathway for early operable breast cancer: Results of a French multicenter prospective study". In: *PloS one* 14.7 (2019), e0210917.

[7] S. Capri and A. Russo. "Cost of breast cancer based on real-world data: a cancer registry study in Italy". In: *BMC health services research* 17.1 (2017), pp. 1–10.

[8] A. Gogate, J. S. Rotter, J. G. Trogdon, K. Meng, C. D. Baggett, K. E. Reeder-Hayes, and S. B. Wheeler. "An updated systematic review of the cost-effectiveness of therapies for metastatic breast cancer". In: *Breast cancer research and treatment* 174.2 (2019), pp. 343–355.

[9] J. Raphael, J. Helou, K. Pritchard, and D. Naimark. "Palbociclib in hormone receptor positive advanced breast cancer: a cost-utility analysis". In: *European Journal of Cancer* 85 (2017), pp. 146–154.

[10] U. Sabale, M. Ekman, D. Thunström, C. Telford, and C. Livings. "Economic evaluation of fulvestrant 500 mg compared to generic aromatase inhibitors in patients with advanced breast cancer in Sweden". In: *PharmacoEconomics-open* 1.4 (2017), pp. 279–290.

[11] several. "Arbeitsgemeinschaft Gynäkologische Onkologie: Diagnostik und Therapie primärer und metastasierter Mammakarzinome: Neoadjuvante (Primäre) systemische Therapie,2020." In: *journal* (2020).

[12] C. Vrieling, E. van Werkhoven, P. Maingon, P. Poortmans, C. Weltens, A. Fourquet, D. Schinagl, B. Oei, C. C. Rodenhuis, J.-C. Horiot, et al. "Prognostic factors for local control in breast cancer after long-term follow-up in the EORTC boost vs no boost trial: a randomized clinical trial". In: *JAMA oncology* 3.1 (2017), pp. 42–48.

[13] V. Strnad, O. J. Ott, G. Hildebrandt, D. Kauer-Dorner, H. Knauerhase, T. Major, J. Lyczek, J. L. Guinot, J. Dunst, C. G. Miguelez, et al. "5-year results of accelerated partial breast irradiation using sole interstitial multicatheter brachytherapy versus whole-breast irradiation with boost after breast-conserving surgery for low-risk invasive and in-situ carcinoma of the female breast: a randomised, phase 3, non-inferiority trial". In: *The Lancet* 387.10015 (2016), pp. 229–238.

[14] O. J. Ott, V. Strnad, W. Stillkrieg, W. Uter, M. W. Beckmann, and R. Fietkau. "Accelerated partial breast irradiation with external beam radiotherapy". In: *Strahlentherapie und Onkologie* 193.1 (2017), pp. 55–61.

[15] M. Becker-Schiebe, N. Bogdanova, M. Bremer, F. Bruns, H. Christiansen, C. Henkenberens, R. M. Hermann, H. John, R. Merten, A. Meyer, et al. "Strahlentherapie und Radioonkologie aus interdisziplinärer Sicht". In: ().

[16] M. D. Piroth, R. Baumann, W. Budach, J. Dunst, P. Feyer, R. Fietkau, W. Haase, W. Harms, T. Hehr, D. Krug, et al. "Heart toxicity from breast cancer radiotherapy". In: *Strahlentherapie und Onkologie* 195.1 (2019), pp. 1–12.

[17] O. Schmidt-Kittler, T. Ragg, A. Daskalakis, M. Granzow, A. Ahr, T. J. F. Blankenstein, M. Kaufmann, J. Diebold, H. Arnholdt, P. Müller, J. Bischoff, D. Harich, G. Schlimok, G. Riethmüller, R. Eils, and C. A. Klein. "From latent disseminated cells to overt metastasis: Genetic analysis of systemic breast cancer progression". In: *Proceedings of the National Academy of Sciences* 100.13 (2003), pp. 7737–7742. ISSN: 0027-8424. DOI: 10.1073/pnas.1331931100. eprint: https://www.pnas.org/content/100/13/7737.full.pdf. URL: https://www.pnas.org/content/100/13/7737.

[18] E. Chow, Y. M. van der Linden, D. Roos, W. F. Hartsell, P. Hoskin, J. S. Wu, M. D. Brundage, A. Nabid, C. J. Tissing-Tan, B. Oei, et al. "Single versus multiple fractions of repeat radiation for painful bone metastases: a randomised, controlled, non-inferiority trial". In: *The Lancet Oncology* 15.2 (2014), pp. 164–171.

[19] J. J. Meeuse, Y. M. van der Linden, G. van Tienhoven, R. O. Gans, J. W. H. Leer, and A. K. Reyners. "Efficacy of radiotherapy for painful bone metastases during the last 12 weeks of life: results from the Dutch Bone Metastasis Study". In: *Cancer: Interdisciplinary International Journal of the American Cancer Society* 116.11 (2010), pp. 2716–2725.

[20] R. A. Patchell, P. A. Tibbs, W. F. Regine, R. Payne, S. Saris, R. J. Kryscio, M. Mohiuddin, and B. Young. "Direct decompressive surgical resection in the treatment of spinal cord compression caused by metastatic cancer: a randomised trial". In: *The Lancet* 366.9486 (2005), pp. 643–648.

[21] P. J. Hoskin, K. Hopkins, V. Misra, T. Holt, R. McMenemin, D. Dubois, F. McKinna, B. Foran, K. Madhavan, C. MacGregor, et al. "Effect of single-fraction vs multifraction radiotherapy on ambulatory status among patients with spinal canal compression from metastatic cancer: the SCORAD randomized clinical trial". In: *Jama* 322.21 (2019), pp. 2084–2094.

[22] D. Rades, A. J. Conde-Moreno, J. Cacicedo, T. Veninga, B. Segedin, K. Stanic, V. Rudat, and S. E. Schild. "1x8 Gy versus 5x4 Gy for metastatic epidural spinal cord compression: a matched-pair study of three prognostic patient subgroups". In: *Radiation Oncology* 13.1 (2018), pp. 1–7.

[23] D. Rades, B. Šegedin, A. J. Conde-Moreno, R. Garcia, A. Perpar, M. Metz, H. Badakhshi, A. Schreiber, M. Nitsche, P. Hipp, et al. "Radiotherapy with 4 Gy$\times$ 5 versus 3 Gy$\times$ 10 for metastatic epidural spinal cord compression: Final results of the SCORE-2 trial (ARO 2009/01)". In: *Journal of Clinical Oncology* 34.6 (2016), pp. 597–602.

[24] B. Pereira, S.-F. Chin, O. M. Rueda, H.-K. M. Vollan, E. Provenzano, H. A. Bardwell, M. Pugh, L. Jones, R. Russell, S.-J. Sammut, et al. "The somatic mutation profiles of 2,433 breast cancers refine their genomic and transcriptomic landscapes". In: *Nature communications* 7.1 (2016), pp. 1–16.

[25] B. Chen, G. Zhang, X. Li, C. Ren, Y. Wang, K. Li, H. Mok, L. Cao, L. Wen, M. Jia, et al. "Comparison of BRCA versus non-BRCA germline mutations and associated somatic mutation profiles in patients with unselected breast cancer". In: *Aging (Albany NY)* 12.4 (2020), p. 3140.

[26] J. Lebert, R. Lester, E. Powell, M. Seal, and J. McCarthy. "Advances in the systemic treatment of triple-negative breast cancer". In: *Current oncology* 25.s1 (2018), pp. 142–150.

[27] Z. Baretta, S. Mocellin, E. Goldin, O. I. Olopade, and D. Huo. "Effect of BRCA germline mutations on breast cancer prognosis: A systematic review and meta-analysis". In: *Medicine* 95.40 (2016).

[28] N. Rodríguez de Dios, F. Couñago, M. Murcia-Mejía, M. Rico-Oses, P. Calvo-Crespo, P. Samper, C. Vallejo, J. Luna, I. Trueba, A. Sotoca, et al. "Randomized phase III trial of prophylactic cranial irradiation with or without hippocampal avoidance for small-cell lung cancer (PREMER): a GICOR-GOECP-SEOR study". In: *Journal of Clinical Oncology* 39.28 (2021), pp. 3118–3127.

[29] M. A. Vogelbaum, P. D. Brown, H. Messersmith, P. K. Brastianos, S. Burri, D. Cahill, I. F. Dunn, L. E. Gaspar, N. T. N. Gatson, V. Gondi, et al. *Treatment for brain metastases: ASCO-SNO-ASTRO guideline*. 2022.

[30] I. Popp, A. Rau, E. Kellner, M. Reisert, J. T. Fennell, T. Rothe, C. Nieder, H. Urbach, K. Egger, A. L. Grosu, et al. "Hippocampus-avoidance whole-brain radiation therapy is efficient in the long-term preservation of hippocampal volume". In: *Frontiers in Oncology* 11 (2021), p. 714709.

[31] W. Ngwa, O. C. Irabor, J. D. Schoenfeld, J. Hesser, S. Demaria, and S. C. Formenti. "Using immunotherapy to boost the abscopal effect". In: *Nature Reviews Cancer* 18.5 (2018), pp. 313–322.

[32] E. G. Nesbit, E. D. Donnelly, and J. B. Strauss. "Treatment strategies for oligometastatic breast cancer". In: *Current treatment options in oncology* 22.10 (2021), pp. 1–18.

[33] R. R. Weichselbaum and S. Hellman. "Oligometastases revisited". In: *Nature reviews Clinical oncology* 8.6 (2011), pp. 378–382.

[34] M. Guckenberger, Y. Lievens, A. B. Bouma, L. Collette, A. Dekker, M. d. Nandita, A.-M. C. Dingemans, B. Fournier, C. Hurkmans, F. E. Lecouvet, et al. "Characterisation and classification of oligometastatic disease: a European Society for Radiotherapy and Oncology and European Organisation for Research and Treatment of Cancer consensus recommendation". In: *The Lancet Oncology* 21.1 (2020), e18–e28.

[35] S. Acharyya, T. Oskarsson, S. Vanharanta, S. Malladi, J. Kim, P. G. Morris, K. Manova-Todorova, M. Leversha, N. Hogg, V. E. Seshan, et al. "A CXCL1 paracrine network links cancer chemoresistance and metastasis". In: *Cell* 150.1 (2012), pp. 165–178.

[36] F. Andre and C. Zielinski. "Optimal strategies for the treatment of metastatic triple-negative breast cancer with currently approved agents". In: *Annals of oncology* 23.suppl_6 (2012), pp. vi46–vi51.

[37] X. Li, J. Yang, L. Peng, A. A. Sahin, L. Huo, K. C. Ward, R. O'Regan, M. A. Torres, and J. L. Meisel. "Triple-negative breast cancer has worse overall survival and cause-specific survival than non-triple-negative breast cancer". In: *Breast cancer research and treatment* 161.2 (2017), pp. 279–287.

[38] A. B. Krøigård, M. J. Larsen, C. Brasch-Andersen, A.-V. Lænkholm, A. S. Knoop, J. D. Jensen, M. Bak, J. Mollenhauer, M. Thomassen, and T. A. Kruse. "Genomic analyses of breast cancer progression reveal distinct routes of metastasis emergence". In: *Scientific Reports* 7.1 (2017), p. 43813.

[39] K. Hunter, N. Crawford, and J. Alsarraj. "Mechanisms of metastasis." In: *Breast Cancer Res.* (2008). DOI: https://10.1186/bcr1988.PMID:19091006. URL: https://breast-cancer-research.biomedcentral.com/articles/10.1186/bcr1988.

[40] T. P. Butler and P. M. Gullino. "Quantitation of cell shedding into efferent blood of mammary adenocarcinoma". In: *Cancer research* 35.3 (1975), pp. 512–516.

[41] M. Najafi, K. Mortezaee, and J. Majidpoor. "Cancer stem cell (CSC) resistance drivers". In: *Life sciences* 234 (2019), p. 116781.

[42] V. Catalano, A. Turdo, S. Di Franco, F. Dieli, M. Todaro, and G. Stassi. "Tumor and its microenvironment: a synergistic interplay". In: *Seminars in cancer biology*. Vol. 23. 6. Elsevier. 2013, pp. 522–532.

[43] Y. Ko, H. Jin, Y. Joo, J. Lee, S. Park, K. Chang, K. Kang, B. Jeong, and H. Kim. "Radioresistant breast cancer cells derived from highly metastatic breast cancer cells exhibit increased resistance to chemotherapy, enhanced invasive properties and premetastatic niche formation due to cancer stem cells". In: *Oncol. Rep* 40 (2018), pp. 3752–3762.

[44] D. Nassar and C. Blanpain. "Cancer stem cells: basic concepts and therapeutic implications". In: *Annual Review of Pathology: Mechanisms of Disease* 11 (2016), pp. 47–76.

[45] X. Shi, Y. Zhang, J. Zheng, and J. Pan. "Reactive oxygen species in cancer stem cells". In: *Antioxidants & redox signaling* 16.11 (2012), pp. 1215–1228.

[46] U. Lendeckel and C. Wolke. "Redox-Regulation in Cancer Stem Cells". In: *Biomedicines* 10.10 (2022), p. 2413.

[47] J. Fares, M. Y. Fares, H. H. Khachfe, H. A. Salhab, and Y. Fares. "Molecular principles of metastasis: a hallmark of cancer revisited". In: *Signal transduction and targeted therapy* 5.1 (2020), pp. 1–17.

[48] A. J. Minn, Y. Kang, I. Serganova, G. P. Gupta, D. D. Giri, M. Doubrovin, V. Ponomarev, W. L. Gerald, R. Blasberg, J. Massagué, et al. "Distinct organ-specific metastatic potential of individual breast cancer cells and primary tumors". In: *The Journal of clinical investigation* 115.1 (2005), pp. 44–55.

[49] F. Dong, A. S. Budhu, and X. W. Wang. "Translating the metastasis paradigm from scientific theory to clinical oncology". In: *Clinical Cancer Research* 15.8 (2009), pp. 2588–2593.

[50] I. Bross, E. Viadana, and J. Pickren. "The metastatic spread of myeloma and leukemias in men". In: *Virchows Archiv A* 365.2 (1975), pp. 91–101.

[51] G. Riethmüller and C. A. Klein. "Early cancer cell dissemination and late metastatic relapse: clinical reflections and biological approaches to the dormancy problem in patients". In: *Seminars in cancer biology*. Vol. 11. 4. Elsevier. 2001, pp. 307–311.

[52] A. Ring, M. Spataro, A. Wicki, and N. Aceto. "Clinical and Biological Aspects of Disseminated Tumor Cells and Dormancy in Breast Cancer". In: *Frontiers in Cell and Developmental Biology* 10 (2022).

[53] S. Meng, D. Tripathy, E. P. Frenkel, S. Shete, E. Z. Naftalis, J. F. Huth, P. D. Beitsch, M. Leitch, S. Hoover, D. Euhus, et al. "Circulating tumor cells in patients with breast cancer dormancy". In: *Clinical cancer research* 10.24 (2004), pp. 8152–8162.

[54] S. Paget. "The distribution of secondary growths in cancer of the breast." In: *The Lancet* 133.3421 (1889), pp. 571–573.

[55] P. C. Nowell. "The Clonal Evolution of Tumor Cell Populations: Acquired genetic lability permits stepwise selection of variant sublines and underlies tumor progression." In: *Science* 194.4260 (1976), pp. 23–28.

[56] L. Weiss. "Metastatic inefficiency". In: *Advances in cancer research* 54 (1990), pp. 159–211.

[57] J. M. Pawelek. "Tumour-cell fusion as a source of myeloid traits in cancer". In: *The lancet oncology* 6.12 (2005), pp. 988–993.

[58] D. GARCÍA-OLMO and D. C. GARCÍA-OLMO. "Functionality of circulating DNA: the hypothesis of genometastasis". In: *Annals of the New York Academy of Sciences* 945.1 (2001), pp. 265–275.

[59] L. Mutschelknaus. "Functional analysis of head and neck cancer exosomes released in response to ionizing radiation". Dissertation. München: Technische Universität München, 2018.

[60] P. A. Konstantinopoulos, M. V. Karamouzis, A. G. Papatsoris, and A. G. Papavassiliou. "Matrix metalloproteinase inhibitors as anticancer agents". In: *The International Journal of Biochemistry & Cell Biology* 40.6 (2008). Directed Issue: Proteases and Antiproteases in Development, Homeostasis and Disease, pp. 1156–1168. ISSN: 1357-2725. DOI: https://doi.org/10.1016/j.biocel.2007.11.007. URL: https://www.sciencedirect.com/science/article/pii/S1357272507003895.

[61] T. G. Simonsen, J.-V. Gaustad, and E. K. Rofstad. "Intracranial Tumor Cell Migration and the Development of Multiple Brain Metastases in Malignant Melanoma". In: *Translational Oncology* 9.3 (2016), pp. 211–218. ISSN: 1936-5233. DOI: https://doi.org/10.1016/j.tranon.2016.04.003. URL: https://www.sciencedirect.com/science/article/pii/S1936523316300109.

[62] A. T. Beliën, P. A. Paganetti, and M. E. Schwab. "Membrane-type 1 matrix metalloprotease (MT1-MMP) enables invasive migration of glioma cells in central nervous system white matter". In: *The Journal of cell biology* 144.2 (1999), pp. 373–384.

[63] S. Y. Lee, E. K. Jeong, M. K. Ju, H. M. Jeon, M. Y. Kim, C. H. Kim, H. G. Park, S. I. Han, and H. S. Kang. "Induction of metastasis, cancer stem cell phenotype, and oncogenic metabolism in cancer cells by ionizing radiation". In: *Molecular cancer* 16.1 (2017), pp. 1–25.

[64] M. Fujita, S. Yamada, and T. Imai. "Irradiation induces diverse changes in invasive potential in cancer cell lines". In: *Seminars in Cancer Biology* 35 (2015). Complexity in Cancer Biology, pp. 45–52. ISSN: 1044-579X. DOI: https://doi.org/10.1016/j.semcancer.2015.09.003. URL: http://www.sciencedirect.com/science/article/pii/S1044579X1500084X.

[65] C. Moncharmont, A. Levy, J.-B. Guy, A. T. Falk, M. Guilbert, J.-C. Trone, G. Alphonse, M. Gilormini, D. Ardail, R.-A. Toillon, C. Rodriguez-Lafrasse, and N. Magné. "Radiation-enhanced cell migration/invasion process: A review". In: *Critical Reviews in Oncology/Hematology* 92.2 (2014), pp. 133–142. ISSN: 1040-8428. DOI: https://doi.org/10.

1016/j.critrevonc.2014.05.006. URL: https://www.sciencedirect.com/science/article/pii/S1040842814000857.

[66] R. Stupp, W. P. Mason, M. J. van den Bent, M. Weller, B. Fisher, M. J. Taphoorn, K. Belanger, A. A. Brandes, C. Marosi, U. Bogdahn, J. Curschmann, R. C. Janzer, S. K. Ludwin, T. Gorlia, A. Allgeier, D. Lacombe, J. G. Cairncross, E. Eisenhauer, and R. O. Mirimanoff. "Radiotherapy plus Concomitant and Adjuvant Temozolomide for Glioblastoma". In: *New England Journal of Medicine* 352.10 (2005). PMID: 15758009, pp. 987–996. DOI: 10.1056/NEJMoa043330. eprint: https://doi.org/10.1056/NEJMoa043330. URL: https://doi.org/10.1056/NEJMoa043330.

[67] S. Rieken, J. Rieber, S. Brons, D. Habermehl, H. Rief, L. Orschiedt, K. Lindel, K. J. Weber, J. Debus, and S. E. Combs. "Radiation-induced motility alterations in medulloblastoma cells". In: *Journal of radiation research* 56.3 (2015), pp. 430–436.

[68] M. Wank, D. Schilling, T. E. Schmid, B. Meyer, J. Gempt, M. Barz, J. Schlegel, F. Liesche, K. A. Kessel, B. Wiestler, et al. "Human glioma migration and infiltration properties as a target for personalized radiation medicine". In: *Cancers* 10.11 (2018), p. 456.

[69] J. E. Baulch, E. Geidzinski, K. K. Tran, L. Yu, Y.-H. Zhou, and C. L. Limoli. "Irradiation of primary human gliomas triggers dynamic and aggressive survival responses involving microvesicle signaling". In: *Environmental and molecular mutagenesis* 57.5 (2016), pp. 405–415.

[70] C.-M. Park, M.-J. Park, H.-J. Kwak, H.-C. Lee, M.-S. Kim, S.-H. Lee, I.-C. Park, C. H. Rhee, and S.-I. Hong. "Ionizing radiation enhances matrix metalloproteinase-2 secretion and invasion of glioma cells through Src/epidermal growth factor receptor–mediated p38/Akt and phosphatidylinositol 3-kinase/Akt signaling pathways". In: *Cancer research* 66.17 (2006), pp. 8511–8519.

[71] N. Cordes, B. Hansmeier, C. Beinke, V. Meineke, and D. Van Beuningen. "Irradiation differentially affects substratum-dependent survival, adhesion, and invasion of glioblastoma cell lines". In: *British journal of cancer* 89.11 (2003), pp. 2122–2132.

[72] D. Hanahan and R. A. Weinberg. "Hallmarks of cancer: the next generation". In: *cell* 144.5 (2011), pp. 646–674.

[73] F. Simon, J.-O. Dittmar, S. Brons, L. Orschiedt, S. Urbschat, K.-J. Weber, J. Debus, S. E. Combs, and S. Rieken. "Integrin-based meningioma cell migration is promoted by photon but not by carbon-ion irradiation". In: *Strahlentherapie und Onkologie* 191.4 (2015), pp. 347–355.

[74] S. Rieken, D. Habermehl, A. Mohr, L. Wuerth, K. Lindel, K. Weber, J. Debus, and S. E. Combs. "Targeting $\alpha v\beta 3$ and $\alpha v\beta 5$ inhibits photon-induced hypermigration of malignant glioma cells". In: *Radiation Oncology* 6.1 (2011), pp. 1–7.

[75] S. Rieken, D. Habermehl, L. Wuerth, S. Brons, A. Mohr, K. Lindel, K. Weber, T. Haberer, J. Debus, and S. E. Combs. "Carbon ion irradiation inhibits glioma cell migration through downregulation of integrin expression". In: *International Journal of Radiation Oncology* Biology* Physics* 83.1 (2012), pp. 394–399.

[76] S. Rieken, F. Simon, D. Habermehl, J. O. Dittmar, S. E. Combs, K. Weber, J. Debus, and K. Lindel. "Photon-induced cell migration and integrin expression promoted by DNA integration of HPV16 genome". In: *Strahlentherapie und Onkologie* 190.10 (2014), pp. 944–949.

[77] T. Ogata, T. Teshima, K. Kagawa, Y. Hishikawa, Y. Takahashi, A. Kawaguchi, Y. Suzumoto, K. Nojima, Y. Furusawa, and N. Matsuura. "Particle irradiation suppresses metastatic potential of cancer cells". In: *Cancer research* 65.1 (2005), pp. 113–120.

[78] M. Merrick, M. J. Mimlitz, C. Weeder, H. Akhter, A. Bray, A. Walther, C. Nwakama, J. Bamesberger, H. Djam, K. Abid, et al. "In vitro radiotherapy and chemotherapy alter migration of brain cancer cells before cell death". In: *Biochemistry and biophysics reports* 27 (2021), p. 101071.

[79] C. Wild-Bode, M. Weller, A. Rimner, J. Dichgans, and W. Wick. "Sublethal Irradiation Promotes Migration and Invasiveness of Glioma Cells". In: *Cancer Research* 61.6 (2001), pp. 2744–2750. ISSN: 0008-5472. eprint: https://cancerres.aacrjournals.org/content/61/6/2744.full.pdf. URL: https://cancerres.aacrjournals.org/content/61/6/2744.

[80] P. Nguemgo Kouam, G. A. Rezniczek, A. Kochanneck, B. Priesch-Grzeszkowiak, T. Hero, I. A. Adamietz, and H. Bühler. "Robo1 and vimentin regulate radiation-induced motility of human glioblastoma cells". In: *PLOS ONE* 13.6 (June 2018), pp. 1–18. DOI: 10.1371/journal.pone.0198508. URL: https://doi.org/10.1371/journal.pone.0198508.

[81] C. Stahler, J. Roth, N. Cordes, G. Taucher-Scholz, and W. Mueller-Klieser. "Impact of carbon ion irradiation on epidermal growth factor receptor signaling and glioma cell migration in comparison to conventional photon irradiation". In: *International Journal of Radiation Biology* 89.6 (2013), pp. 454–461. DOI: 10.3109/09553002.2013.766769. eprint: https://doi.org/10.3109/09553002.2013.766769. URL: https://doi.org/10.3109/09553002.2013.766769.

[82] I. Eke, K. Storch, I. Kästner, A. Vehlow, C. Faethe, W. Mueller-Klieser, G. Taucher-Scholz, A. Temme, G. Schackert, and N. Cordes. "Three-dimensional Invasion of Human Glioblastoma Cells Remains Unchanged by X-ray and Carbon Ion Irradiation In Vitro". In: *International Journal of Radiation Oncology*Biology*Physics* 84.4 (2012), e515–e523. ISSN: 0360-3016. DOI: https://doi.org/10.1016/j.ijrobp.2012.06.012. URL: http://www.sciencedirect.com/science/article/pii/S0360301612008061.

[83] M. Steinle, D. Palme, M. Misovic, J. Rudner, K. Dittmann, R. Lukowski, P. Ruth, and S. M. Huber. "Ionizing radiation induces migration of glioblastoma cells by activating BK K+ channels". In: *Radiotherapy and Oncology* 101.1 (2011), pp. 122–126. ISSN: 0167-8140. DOI: https://doi.org/10.1016/j.radonc.2011.05.069. URL: http://www.sciencedirect.com/science/article/pii/S0167814011002787.

[84] D. A. Ferraro, F. Patella, S. Zanivan, C. Donato, N. Aceto, M. Giannotta, E. Dejana, M. Diepenbruck, G. Christofori, and M. Buess. "Endothelial cell-derived nidogen-1 inhibits migration of SK-BR-3 breast cancer cells". In: *BMC cancer* 19.1 (2019), p. 312.

[85] H. Schmucker, W. M. Blanding, J. M. Mook, J. F. Wade, J. P. Park, K. Kwist, H. Shah, and B. W. Booth. "Amphiregulin regulates proliferation and migration of HER2-positive breast cancer cells". In: *Cellular Oncology* 41.2 (2018), pp. 159–168.

[86] H. T. T. Do and J. Cho. "Involvement of the ERK/HIF-1α/EMT Pathway in XCL1-Induced Migration of MDA-MB-231 and SK-BR-3 Breast Cancer Cells". In: *International Journal of Molecular Sciences* 22.1 (2021), p. 89.

[87] H. Liu, X. Huang, and T. Ye. "MiR-22 down-regulates the proto-oncogene ATP citrate lyase to inhibit the growth and metastasis of breast cancer". In: *American journal of translational research* 10.3 (2018), p. 659.

[88] V. Radulovic. "Role of miR-21 in determining sensitivity of mammary epithelial cells to radiation treatment". Dissertation. München: Technische Universität München, 2017.

[89] P.-W. Tsai, S.-G. Shiah, M.-T. Lin, C.-W. Wu, and M.-L. Kuo. "Up-regulation of vascular endothelial growth factor C in breast cancer cells by heregulin-β1 a critical role of p38/nuclear factor-κb signaling pathway". In: *Journal of Biological Chemistry* 278.8 (2003), pp. 5750–5759.

[90] C. Gest, U. Joimel, L. Huang, L.-L. Pritchard, A. Petit, C. Dulong, C. Buquet, C.-Q. Hu, P. Mirshahi, M. Laurent, et al. "Rac3 induces a molecular pathway triggering breast cancer cell aggressiveness: differences in MDA-MB-231 and MCF-7 breast cancer cell lines". In: *BMC cancer* 13.1 (2013), pp. 1–14.

[91] E. A. Pérez-Yépez, J.-T. Ayala-Sumuano, A. M. Reveles-Espinoza, and I. Meza. "Selection of a MCF-7 breast cancer cell subpopulation with high sensitivity to IL-1β: characterization of and correlation between morphological and molecular changes leading to increased invasiveness". In: *International journal of breast cancer* 2012 (2012).

[92] F. De Bacco, P. Luraghi, E. Medico, G. Reato, F. Girolami, T. Perera, P. Gabriele, P. M. Comoglio, and C. Boccaccio. "Induction of MET by ionizing radiation and its role in radioresistance and invasive growth of cancer". In: *JNCI: Journal of the National Cancer Institute* 103.8 (2011), pp. 645–661.

[93] A. Kawamoto, T. Yokoe, K. Tanaka, S. Saigusa, Y. Toiyama, H. Yasuda, Y. Inoue, C. Miki, and M. Kusunoki. "Radiation induces epithelial-mesenchymal transition in colorectal cancer cells". In: *Oncology reports* 27.1 (2012), pp. 51–57.

[94] X. Zhang, X. Li, N. Zhang, Q. Yang, and M. S. Moran. "Low doses ionizing radiation enhances the invasiveness of breast cancer cells by inducing epithelial–mesenchymal transition". In: *Biochemical and biophysical research communications* 412.1 (2011), pp. 188–192.

[95] J. K. Park, S. J. Jang, S. W. Kang, S. Park, S.-G. Hwang, W.-J. Kim, J. H. Kang, and H.-D. Um. "Establishment of animal model for the analysis of cancer cell metastasis during radiotherapy". In: *Radiation oncology* 7.1 (2012), pp. 1–11.

[96] N. Anastasov, I. Höfig, V. Radulović, S. Ströbel, M. Salomon, J. Lichtenberg, I. Rothenaigner, K. Hadian, J. M. Kelm, C. Thirion, et al. "A 3D-microtissue-based phenotypic screening of radiation resistant tumor cells with synchronized chemotherapeutic treatment". In: *BMC cancer* 15.1 (2015), p. 466.

[97] I. Keydar, L. Chen, S. Karby, F. Weiss, J. Delarea, M. Radu, S. Chaitcik, and H. Brenner. "Establishment and characterization of a cell line of human breast carcinoma origin". In: *European Journal of Cancer (1965)* 15.5 (1979), pp. 659–670.

[98] ATCC. *ATCC-T47D*. URL: `https://www.lgcstandards-atcc.org/products/all/HTB-133.aspx?geo_country=de#generalinformation`.

[99] ATCC. *ATCC-MDAMB361*. URL: `https://www.lgcstandards-atcc.org/products/all/HTB-27.aspx?geo_country=de`.

[100] R. Cailleau, R. Young, M. Olive, and W. Reeves Jr. "Breast tumor cell lines from pleural effusions". In: *Journal of the National Cancer Institute* 53.3 (1974), pp. 661–674.

[101] C. R. Tate, L. V. Rhodes, H. C. Segar, J. L. Driver, F. N. Pounder, M. E. Burow, and B. M. Collins-Burow. "Targeting triple-negative breast cancer cells with the histone deacetylase inhibitor panobinostat". In: *Breast Cancer Research* 14.3 (2012), pp. 1–15.

[102] K. S. Wilson, H. Roberts, R. Leek, A. L. Harris, and J. Geradts. "Differential gene expression patterns in HER2/neu-positive and-negative breast cancer cell lines and tissues". In: *The American journal of pathology* 161.4 (2002), pp. 1171–1185.

[103] G. Trempe. "Human breast cancer in culture". In: *Breast Cancer*. Springer, 1976, pp. 33–41.

[104] H. Soule, J. Vazquez, A. Long, S. Albert, and M. Brennan. "A human cell line from a pleural effusion derived from a breast carcinoma". In: *Journal of the national cancer institute* 51.5 (1973), pp. 1409–1416.

[105] F. H. Shirazi, A. Zarghi, A. Ashtarinezhad, F. Kobarfard, M. Nakhjavani, N. Anjidani, R. Zendehdel, S. Arfaiee, S. Shoeibi, S. Mohebi, et al. *Remarks in successful cellular investigations for fighting breast cancer using novel synthetic compounds*. INTECH Open Access Publisher Croatia, 2011.

[106] Ş. Comşa, A. M. Cimpean, and M. Raica. "The story of MCF-7 breast cancer cell line: 40 years of experience in research". In: *Anticancer research* 35.6 (2015), pp. 3147–3154.

[107] M. Perrot-Applanat and M. Di Benedetto. "Autocrine functions of VEGF in breast tumor cells: adhesion, survival, migration and invasion". In: *Cell adhesion & migration* 6.6 (2012), pp. 547–553.

[108] Promega. "TECHNICAL BULLETIN,CellTiter-Glo® Luminescent Cell Viability Assay Instructions for Use of Products G7570, G7571, G7572 and G7573". In: *journal* (2015).

[109] Promega. "TECHNICAL BULLETIN, Caspase-Glo® 3/7 AssayInstructions for Use of Products G8090, G8091, G8092 and G8093". In: *journal* (2019).

[110] S. G. Mikalsen, N. Jeppesen Edin, J. A. Sandvik, and E. O. Pettersen. "Separation of two sub-groups with different DNA content after treatment of T-47D breast cancer cells with low dose-rate irradiation and intermittent hypoxia". In: *Acta Radiologica* 59.1 (2018), pp. 26–33.

[111] R. Mishra, L. Yuan, H. Patel, A. S. Karve, H. Zhu, A. White, S. Alanazi, P. Desai, E. J. Merino, and J. T. Garrett. "Phosphoinositide 3-Kinase (PI3K) Reactive Oxygen Species (ROS)-Activated Prodrug in Combination with Anthracycline Impairs PI3K Signaling, Increases DNA Damage Response and Reduces Breast Cancer Cell Growth". In: *International Journal of Molecular Sciences* 22.4 (2021), p. 2088.

[112] Á. E. Kulmány, É. Frank, D. Kovács, K. Kirisits, G. Krupitza, P. Neuperger, R. Alföldi, L. G. Puskás, G. J. Szebeni, and I. Zupkó. "Antiproliferative and antimetastatic characterization of an exo-heterocyclic androstane derivative against human breast cancer cell lines". In: *Biomedicine & Pharmacotherapy* 140 (2021), p. 111728.

[113] S. Aftab and A. R. Shakoori. "Glucose Stress Induces Early Onset of Metastasis in Hormone-Sensitive Breast Cancer Cells". In: *Critical Reviews™ in Eukaryotic Gene Expression* 31.6 (2021).

[114] J. Tripathy, A. R. Chowdhury, M. Prusty, K. Muduli, N. Priyadarshini, K. S. Reddy, B. Banerjee, and S. Elangovan. "α-Lipoic acid prevents the ionizing radiation-induced epithelial-mesenchymal transition and enhances the radiosensitivity in breast cancer cells". In: *European Journal of Pharmacology* 871 (2020), p. 172938.

[115] J. Kantapan, S. Paksee, A. Duangya, P. Sangthong, S. Roytrakul, S. Krobthong, W. Suttana, and N. Dechsupa. "A radiosensitizer, gallotannin-rich extract from Bouea macrophylla seeds, inhibits radiation-induced epithelial-mesenchymal transition in breast cancer cells". In: *BMC complementary medicine and therapies* 21.1 (2021), pp. 1–19.

[116] A. G. Young and K. L. Bennewith. "Ionizing radiation enhances breast tumor cell migration in vitro". In: *Radiation Research* 188.4 (2017), pp. 381–391.

[117] L. Pan, M. Wan, W. Zheng, R. Wu, W. Tang, X. Zhang, T. Yang, and C. Ye. "Intrabeam radiation inhibits proliferation, migration, and invasiveness and promotes apoptosis of MCF-7 breast cancer cells". In: *Technology in Cancer Research & Treatment* 18 (2019), p. 1533033819840706.

[118] N. Kaushik, M.-J. Kim, R.-K. Kim, N. Kumar Kaushik, K. M. Seong, S.-Y. Nam, and S.-J. Lee. "Low-dose radiation decreases tumor progression via the inhibition of the JAK1/STAT3 signaling axis in breast cancer cell lines". In: *Scientific reports* 7.1 (2017), pp. 1–9.

[119] J. Mei, C. Böhland, A. Geiger, I. Baur, K. Berner, S. Heuer, X. Liu, L. Mataite, M. Melo-Narváez, E. Özkaya, et al. "Development of a model for fibroblast-led collective migration from breast cancer cell spheroids to study radiation effects on invasiveness". In: *Radiation Oncology* 16.1 (2021), pp. 1–14.

[120] R. Al-Abedi, S. Tuncay Cagatay, A. Mayah, S. A. Brooks, and M. Kadhim. "Ionising Radiation Promotes Invasive Potential of Breast Cancer Cells: The Role of Exosomes in the Process". In: *International Journal of Molecular Sciences* 22.21 (2021), p. 11570.

[121] L. Mutschelknaus, O. Azimzadeh, T. Heider, K. Winkler, M. Vetter, R. Kell, S. Tapio, J. Merl-Pham, S. M. Huber, L. Edalat, et al. "Radiation alters the cargo of exosomes released from squamous head and neck cancer cells to promote migration of recipient cells". In: *Scientific reports* 7.1 (2017), pp. 1–13.

[122] J. Theys, B. Jutten, R. Habets, K. Paesmans, A. J. Groot, P. Lambin, B. G. Wouters, G. Lammering, and M. Vooijs. "E-Cadherin loss associated with EMT promotes radioresistance in human tumor cells". In: *Radiotherapy and oncology* 99.3 (2011), pp. 392–397.

[123] L. Yu, Y. Yang, J. Hou, C. Zhai, Y. Song, Z. Zhang, L. Qiu, and X. Jia. "MicroRNA-144 affects radiotherapy sensitivity by promoting proliferation, migration and invasion of breast cancer cells". In: *Oncology reports* 34.4 (2015), pp. 1845–1852.

[124] M. A. Olivares-Urbano, C. Griñán-Lisón, S. Ríos-Arrabal, F. Artacho-Cordón, A. I. Torralbo, E. López-Ruiz, J. A. Marchal, and M. I. Núñez. "Radiation and stemness phenotype may influence individual breast cancer outcomes: the crucial role of mmps and microenvironment". In: *Cancers* 11.11 (2019), p. 1781.

[125] J. Wendt, S. Radetzki, C. Von Haefen, P. Hemmati, D. Güner, K. Schulze-Osthoff, B. Dörken, and P. Daniel. "Induction of p21CIP/WAF-1 and G2 arrest by ionizing irradiation impedes caspase-3-mediated apoptosis in human carcinoma cells". In: *Oncogene* 25.7 (2006), pp. 972–980.

[126] D.-L. Li, L. Wei, X.-M. Wen, H. Song, Q. Li, J.-W. Lv, C.-C. Kuang, Z.-Z. Wei, and J.-W. Zhang. "The effects of X-ray irradiation on the proliferation and apoptosis of MCF-7 breast cancer cells". In: *Ultrastructural pathology* 38.3 (2014), pp. 211–216.

[127] B. E. Bejnordi, M. Veta, P. J. Van Diest, B. Van Ginneken, N. Karssemeijer, G. Litjens, J. A. Van Der Laak, M. Hermsen, Q. F. Manson, M. Balkenhol, et al. "Diagnostic assessment of deep learning algorithms for detection of lymph node metastases in women with breast cancer". In: *Jama* 318.22 (2017), pp. 2199–2210.

[128] S.-S. Yang, S. Ma, H. Dou, F. Liu, S.-Y. Zhang, C. Jiang, M. Xiao, and Y.-X. Huang. "Breast cancer-derived exosomes regulate cell invasion and metastasis in breast cancer via miR-146a to activate cancer associated fibroblasts in tumor microenvironment". In: *Experimental cell research* 391.2 (2020), p. 111983.

[129] J. S. Wong and Y. K. Cheah. "Potential miRNAs for miRNA-Based Therapeutics in Breast Cancer". In: *Non-coding RNA* 6.3 (2020), p. 29.

[130] B. Wu, G. Liu, Y. Jin, T. Yang, D. Zhang, L. Ding, F. Zhou, Y. Pan, and Y. Wei. "miR-15b-5p Promotes Growth and Metastasis in Breast Cancer by Targeting HPSE2". In: *Frontiers in Oncology* 10 (2020), p. 108.

[131] X. Wang, H. Qiu, R. Tang, H. Song, H. Pan, Z. Feng, and L. Chen. "miR-30a inhibits epithelial-mesenchymal transition and metastasis in triple-negative breast cancer by targeting ROR1". In: *Oncology Reports* 39.6 (2018), pp. 2635–2643.

[132] Y.-J. Liang, Q.-Y. Wang, C.-X. Zhou, Q.-Q. Yin, M. He, X.-T. Yu, D.-X. Cao, G.-Q. Chen, J.-R. He, and Q. Zhao. "MiR-124 targets Slug to regulate epithelial–mesenchymal transition and metastasis of breast cancer". In: *Carcinogenesis* 34.3 (2013), pp. 713–722.

Acknowledgements

I would like to express my deepest appreciation and gratitude for the opportunity to write my doctoral thesis and continuous support throughout the process to:

Prof. Stephanie Combs for providing the topic and the opportunity to write my doctoral thesis at the clinic for radiation oncology and her continuous support over the years.

Prof. Thomas Schmid for the invaluable patience and feedback, especially during the writing process.

PD Dr. Simone Mörtl: A major thanks for the on-site support in cell culture and while performing the experiments, as well as providing new ideas for additional testing.

Dr. Lisa Mutschelknaus: I am extremely grateful for the guidance and on-site support in cell culture and during the experiments.

In memoriam of PD Dr. Nataša Anastasov who contributed greatly to the topic and provided invaluable support. Moreover, she supplied major cell lines and contributed greatly with her vast experience.